Interscience Research Network

Interscience Research Network

Conference Proceedings - Full Volumes | IRNet Conference Proceedings

8-19-2012

# Proceedings of International Conference on Computational Vision And Robotics

Prof.Srikanta Patnaik Mentor
*IRNet India*, patnaik_srikanta@yahoo.co.in

Follow this and additional works at: https://www.interscience.in/conf_proc_volumes

 Part of the Computer and Systems Architecture Commons, Data Storage Systems Commons, Digital Circuits Commons, Digital Communications and Networking Commons, Hardware Systems Commons, Robotics Commons, and the Systems and Communications Commons

## Recommended Citation

Patnaik, Prof.Srikanta Mentor, "Proceedings of International Conference on Computational Vision And Robotics" (2012). *Conference Proceedings - Full Volumes*. 58.
https://www.interscience.in/conf_proc_volumes/58

This Book is brought to you for free and open access by the IRNet Conference Proceedings at Interscience Research Network. It has been accepted for inclusion in Conference Proceedings - Full Volumes by an authorized administrator of Interscience Research Network. For more information, please contact sritampatnaik@gmail.com.

*Proceedings of International Conference on*

# Computational Vision And Robotics

(ICCVR-2012)
19th August, 2012
BHUBANESWAR, India

Interscience Research Network (IRNet)
Bhubaneswar, India

# International Conference
# On
# Computational Vision and Robotics

**ICCVR-2012**

**Bhubaneswar, 19th August, 2012**

## CONTENTS:

# Editorial

Computer Vision and Robotic is one of the most challenging areas of 21st century. Its application ranges from Humanoid to Man-less-plant, Deep-sea-application to Space application, and Agriculture to Medicine, House hold good to Industries. Today's technologies demand to produce intelligent machine, which are enabling applications in various domains and services. Robotics is one such area which encompasses number of technology in it and its application is wide spread. Computational or machine vision is the most challenging tool for the robot to make it intelligent. To perceive the real world scenario which is 3D in nature from the normal camera which takes images in 2D plane is the most challenging job for the researchers who are working in this area.

For many people it is a machine that imitates a human—like the androids in Star Wars, Terminator and Star Trek: The Next Generation. However much these robots capture our imagination, such robots still only inhabit Science Fiction. People still haven't been able to give a robot enough 'common sense' to reliably interact with a dynamic world. However, Rodney and his team at MIT Artificial Intelligence Lab are working on creating such humanoid robots. Robotics had become a craze nowadays. The type of robots that you will encounter most frequently are robots that do work that is too dangerous, boring, onerous, or just plain nasty. Most of the robots in the world are of this type. They can be found in auto, medical, manufacturing and space industries. In fact, there are over a million of these type of robots working for us today.

Some robots like the Mars Rover Sojourner and the upcoming Mars Exploration Rover, or the underwater robot Caribou help us learn about places that are too dangerous for us to go. While other types of robots are just plain fun for kids of all ages. Popular toys such as Techno, Polly or AIBO ERS-220 seem to hit the store shelves every year around Christmas time.

And as much fun as robots are to play with, robots are even much more fun to build. In Being Digital, Nicholas Negroponte tells a wonderful story about an eight year old, pressed during a televised premier of MIT Media Lab's LEGO/Logo work at Hennigan School. A zealous anchor, looking for a cute sound bite, kept asking the child if he was having fun playing with LEGO/Logo. Clearly exasperated, but not wishing to offend, the child first tried to put her off. After her third attempt to get him to talk about fun, the child, sweating under the hot television lights, plaintively looked into the camera and answered, ***"Yes it is fun, but it's hard fun."***

**Chief Mentor**
**Prof. (Dr.) Srikanta Patnaik**

# IMAGE PROCESSING BASED NAVIGATION ROBOT AN APPLICATION OF COMPUTER VISION

**ANKIT JAIN & MILKY SAHU**

Department of Electronics and Telecommunication Engineering , S.G.S.I.T.S, Indore

**Abstract**- In this paper we propose a technique for providing vision to robot based on images acquired by an active stereo camera system. We propose the implementation of this method on a computer assisted robot as part of a multi-modal environment-machine interaction system: detecting the environment or surroundings, the robot can take an appropriate decision and follow a path.

## I. INTRODUCTION

Human-computer interaction (HCI) and artificial intelligence (AI) share a long history of research. Concepts such as problem spaces, goals and operators, rationality, and computational models of cognitive have significantly influenced research directions in both fields. Recently the concept of agents has sparked a common interest among AI and HCI researchers.

### *A. Why Robot Vision?*

1. Defined as the process of acquiring and extracting information from the images of 3D world.
2. Most powerful sensor, which can equip a robot with large variety of sensory information.

A vision system comprises hardware and software for performing the functions of sensing and processing the image and utilizing the results to command the robot.

### *B. Areas of Robot Vision:*

1. Robot Vision: System to capture and process image.
2. Robot Learning: For robot manipulation.
3. Robot Navigation: For tracking.

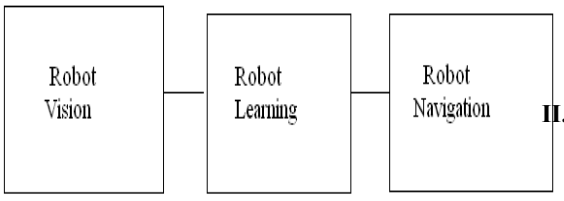


Fig.1.1 Areas of Robot Vision

The idea is to utilize a simple system which processes the camera output and implements a control scheme which can quickly and accurately control the vehicle. The self-localization of the robot is done with a model-based vision system, and a non-stop navigation is realized by a retroactive position correction system.

The end product of the design project is an intelligent vehicle that is able to follow an emulated high-way automatically. A camera with embedded color tracking capabilities is included in the project. The objective for building the intelligent vehicle is to design an intelligent controller for path taking tasks.

The important function of vision-based processing in this case consists of 'self-localization'. In a different approach, a robot is provided with a sequence of images of the interior space. By comparing these prerecorded images with the camera images taken during navigation, the robot is able to determine its location.

To satisfy above aim, several objectives have been identified:

1. Carry out a comprehensive review of current vision based methodologies to establish the current state of the art.
2. Design camera based autonomous mobile robot system.
3. Design and Implement of the software and control architecture of the desired system.
4. Implement a powerful image processing and computer visual library for object recognition and feature tracking tasks.

## II. SYSTEM DESCRIPTION

The system consists of:

1. Image acquisition setup: It consists of a video camera, web camera, or an analogue camera with suitable interface for connecting it to processor.

2. Processor**:** It consists of a personal computer or a dedicated image processing unit.
3. Image analysis**:** Certain tools are used to analyze the content in the image captured and device conclusions e.g detecting a color.

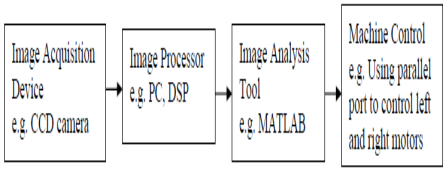


Fig.2.1 System Description

*A. Block Diagram:*

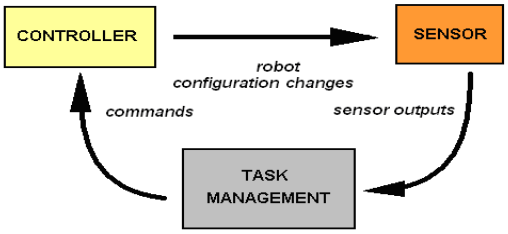


Fig 2.2

- First of all, sensor captures the input and transfers it to the task management bloc which in turn will give appropriate commands to the controller as a result of which robot configuration changes.
- Here image acquisition device like CCD Camera captures the image. This captured image will be the input to the image processor. Image processor can be a PC or a digital signal processor.
- Image analysis tool is required to extract the information from the image. MATLAB performs the task of image processing. Then decisions are taken accordingly and are transferred to the motors through serial or parallel communication as a result of which robot moves in the required direction. This whole working can be shown with the help of a block diagram given below.

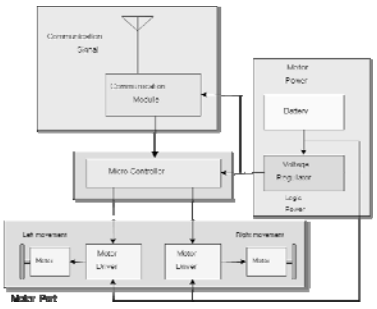

Fig 2.3

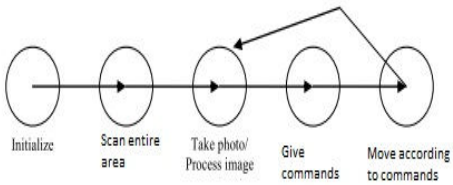


**Chart flow for the robot tracking algorithm**

Fig 2.4

## III. SNAPSHOTS

*Fig 3.1 Working of proposed idea*

## IV. MICROCONTROLLER PROGRAMMING

Program for the application is built in the C language to support the simple and fast execution of instruction and to avoid long and complex jumping instructions. The C for microcontrollers and the standard C syntax and semantics a slightly die rent. The former is aimed at the general purpose programming paradigm whereas the latter is for a specific target microcontroller such as 8051. The underlying fact is that everything will be ultimately mapped into the micro controller machine code. If a certain feature such as indirect access to I/O registers is inhibited in the target microcontroller, the compiler will also restrict the same at higher level.

```
#include<reg51.h>

sfr motor = 0xa0;        %redefining the address

void forw();     % defining functions for movement of robot
in void reverse();          different directions
void left();
void right();
void recv();
void compare(unsigned char,unsigned char);
void delay(unsigned int);
```

```
unsigned char d,step;

void main()
{

  delay(1);              % introducing delay in execution of
serial
 TMOD = 0X20;    communication
  SCON = 0X50;
  TH1 = 0XFD;
  TL1 = 0XFD;
  TR1 = 1;
  while(1)
               {
                while(RI==0);
                recv();    %calling 'receive' function for
initiating                  compare(d,step);        serial
communication
               }
}

void recv()           %declaring 'receive' function
{
 unsigned char r;
  while(RI==0);
  RI = 0;
  r = SBUF;
  if(r=='*')
    {
                while(RI==0);
                d = SBUF;
                RI = 0;
                while(RI==0);
                step = SBUF;
                RI = 0;
              }
}

void compare(unsigned char c,unsigned char s )   {
%declaring  compare function to
compare the variables to decide the direction of motion.
unsigned char i;
 if (c=='f')
   {
                for(i=0;i<s;i++)
                  {
                              forw();
                            }
   }
else if (c=='b')
  {
              for(i=0;i<s;i++)
                 {
                              reverse();
                            }
  }
else if (c=='l')
  {
              for(i=0;i<s;i++)
                 {
                              left();
                            }

  }
else if (c=='r')
  {
              for(i=0;i<s;i++)
                                  {
                                              right();
                                            }
  }
}

void forw() % defining functions for movement of robot in
{                 different directions
 motor = 0x06;
 delay(20);
 motor = 0x00;
}

void reverse()
{
 motor = 0x09;
 delay(20);
 motor = 0x00;
}

void left()
{
 motor = 0x0a;
 delay(20);
 motor = 0x00;
}

void right()
{
 motor = 0x05;
 delay(20);
 motor = 0x00;
}

void delay(unsigned int t)
{
  unsigned int i,j;
  for(i=0;i<t;i++)
    for(j=0;j<144;j++);              //  1ms
}
```

## V. MATLAB PROGRAMMING

To start the camera

```
vid = videoinput('winvideo',2,'YUY2_160x120');
triggerconfig(vid,'manual');
set(vid,'framesPerTrigger',1);
set(vid,'TriggerRepeat',Inf);
set(vid,'ReturnedColorSpace','RGB');
start(vid);
```

To convert the image into black & white

```
snap;
gray=rgb2gray(im);
%l=0.50;
%bw=im2bw(gray,l);
cr=imcrop(gray,[1,170,320,240]);
figure(1),imshow(cr);
```

To detect the turn

```
t=0;
flag=0;
for i = 70:-1:1
for  j = 80: 220
if cr(i,j)>230
flag=1;
for k = i:-1:10
if cr(k,j-50)>225
t = 'l_turn';
break;
end
end
for k = i:-1:10
if cr(k,j+55)>225
t = 'r_turn';
break;
end
end
break;
end
end
if flag==1
break;
end
end
disp(t);
%disp([i,j]);
```

To detect the road

```
clear t left_flag right_flag wh wl tol direction k flag
lo i j s
 trff=0;
 Intcty =100;
 bnw;
 turntrial;
 if(t==0)
left_flag=0;
right_flag=0;
wh=256;
wl=200;
tol=4;
direction = 0;
k=1;
flag=0;
lo=1;
i=1;
s1=0;
while(i<70)
for i=lo:70
for j=160:220
if cr(i,j)>Intcty
s1(k) = j;
flag=1;
break;
 end
 end
 if flag==1
 break;
 end
 end
 lo=i+1;
 k = k+1;
 end
 k=1;
 flag=0;
 lo=1;
 i=1;
 s2=0;
 while(i<70)
 for i=lo:70
 for j=160:-1:90
   if cr(i,j)>Intcty
   s2(k) = j;
   flag=1;
   break;
   end
   end
   if flag==1
   break;
   end
   end
   lo=i+1;
   k = k+1;
   end
   size(s2)
   size(s1)
   if (size(s1,2)-size(s2,2)<10 && size(s1,2)-
size(s2,2)>=0 ) || (size(s2,2)- size(s1,2)<10 && size(s2,2)-
size(s1,2)>=0 )
  direction = 's'
   send('f',20,ser);
   pause(1)
   end
   if size(s1,2)-size(s2,2)>10
   direction = 'r'
   send('r',5,ser);
   pause(0.5)
   end
   if size(s2,2)-size(s1,2)>10
   direction = 'l'
   send('l',5,ser);
    pause(0.5);
    end
   disp(direction)
   else
   if strcmp(t,'l_turn')
   left_turn(ser);
   else
   if strcmp(t,'r_turn')
```

```
right_turn(ser);
end
pause(1);
end
```

For left turning

```
function left_turn(ser)
disp('turning.....')
send('r',1,ser);
pause(1);
send('f',130,ser);
pause(4);
send('l',65,ser)
pause(2);
end
```

For right turning

```
function right_turn(ser)
disp('turning.....')
send('l',1,ser);
pause(1)
send('f',130,ser);
pause(4);
send('r',65,ser)
pause(2)
end
```

For detecting traffic light

```
function c = trafficdetect(im)
rcount=0;
gcount=0;
rrh=255;
rrl=200;
rgh=120;
rgl=50;
rbh=130;
rbl=70;
%grh=
%grl=
%ggh=
%ggl=
%gbh=
%gbl=
%gth=
%rth=
for i=1:240
for j=1:150
if im(i,j,1)<=rrh && im(i,j,1)>=rrl && im(i,j,2)<=rgh &&
im(i,j,1)>=rgl && im(i,j,3)<=rbh

&& im(i,j,3)>=rbl
rcount=rcount+1;
end
end
end
disp(rcount);
if rcount>400
c=1;
else
c=0;
end
%for i=1:240
%for j=1:320
%if im(i,j,1)<rrh && im(i,j,1)>rrl && im(i,j,2)<rgh &&
im(i,j,1)>rgl && im(i,j,3)<rbh &&

im(i,j,3)>rbl
%gcount=gcount+1;
%end
% end
%end

%if(rcount>rth)
%   rflag=1;
%end
%if(gcount>gth)
%   gflag=1;
%disp(rcount);
%end
```

For sending data serially

```
tic
ser = serial('COM9','BaudRate',9600,'DataBits',8);
toc
```

Main function

```
snap;
for i=1:30
rd_detect1
trff = trafficdetect(im);
while trff==1
snap;
trff = trafficdetect(im)
disp('Red Light');
end
end
```

For taking a snap

```
trigger(vid);
im = getdata(vid,1);
%imtool(im);
```

## VI. CONCLUSION AND FUTURE ENHANCEMENTS

We have presented a basic concept for a vision based interactive robot control as a part of multi-modal man-machine interaction system.

Visual sensing will be essential for mobile robots to progress in the direction of increased robustness, reduced cost, and reduced power consumption. Moreover, if robots can make use of computationally efficient algorithms and off-the-shelf cameras with minimal setup (e.g., no calibration), then the opportunity exists for robots to be widely deployed (e.g., multiple inexpensive coordinating robots). A novel visual based navigation system will be an important step in this direction. The road recognition system can use more efficient camera for better navigation. Also the

detection of road and traffic light can be done efficiently by minimizing the scan area of the image processor for the pixel count.

Thereby the information regarding road recognition and traffic light detection is extracted very robustly. By using multiple channels of information, the whole

system is able to overcome ambiguities and the robot can react in an adequate matter.

For the future we plan to extend the multi-modal environment-machine interaction system by integrating shape recognition and obstacle avoidance .

## REFERENCES

[1] The documentation and demos provided in the Help section of MATALB
[2] www.iitk.ac.in
[3] http://www.hometoys.com/htinews/aug00/articles/metricom/mathieu.html
[4] http://www.massmind.org/images/www/hobby_elec/e_pic6_6.html
[5] http://www.ee.latrobe.edu.au/~djc/UltraSonics/Ultrasonics.html

◈◈◈

# GPS-GSM NAVIGATION & POSITION LOCATOR ROBOT WITH GOOGLE EARTH TRACKING

**FOWAD AHMAD**

Department of Computer Science & Engineering, Integral University, Lucknow

**Abstract**: An integrated GPS-GSM navigation system is developed & it can be tracked using Google Earth application. The remote module has a GPS mounted on the moving vehicle to identify its current position, and to be transferred by GSM with other parameters acquired by the automobile's data port as an SMS to a recipient station. The received GPS coordinates are filtered using a Kalman filter to enhance the accuracy of measured position. After data processing, Google Earth application is used to view the current location and status of the robot. The goal of this system is to enable remote navigation of a robot just like human by programming the robot with GPS coordinates of the destination location, control & monitor the navigation of the robot via GSM module, manage fleet, police automobiles distribution and car theft cautions.

## 1. INTRODUCTION

The ability to accurately navigate & detect the robot's location and its status is the main goal of this automobile robot navigation & trajectory monitoring systems. These systems are implemented using several hybrid techniques that include: wireless communication, geographical positioning and embedded applications. The robotic vehicle & tracking systems are designed to assist corporations with large number of remotely controlled navigation and several usage purposes. A Fleet management system can minimize the cost and effort of employees to finish road assignments within a minimal time. Besides, assignments can be scheduled in advanced based on current automobiles location. Therefore, central fleet management is essential to large enterprises to meet the varying requirements of customers and to improve the productivity [1].In the GPS Position Locator & navigation system we have presented the solution of cost & data support problem and we can know the position, latitude & longitude, course angle, speed, altitude & other satellite data. To implement just the working model, I ATmega 8535 microcontroller is used that is serially interfaced with sensors, actuators & GPS module & LCD to display real-time GPS NMEA data. To support better analysis of GPS NMEA string data & know more of the navigation of the kit a software application is developed which would extract information from the NMEA string & display GPS data like latitude, longitude, satellite information etc. & with the use of Google Earth & KML Generator; we could get better information of the GPS data & navigation. The GPS navigation of the system is enabled by chassis & wheel driven by the DC motor, the DC motor is controlled by the GPS data like longitude & latitude. The system is enabled with Line following & obstacle avoider capabilities. But the functionality of the system can be increased modularly by interfacing the microcontroller with sensors & modules like GSM & internet module to provide tracking & data transfer capabilities.

GPS Position Locator system would work using the GPS satellites information & without internet. This would first make this device work in any remote area without internet & secondly it will reduce the cost of programming the system with an embedded real-time system. We will program the system with Embedded C codes, multiple codes can be burned & can be called specifically using switches. Normally most the generic vendor specific GPS devices cost to around 15000 INR. This system is vendor independent GPS devices costing just 5000 INR of acceptable performance & features. Moreover, any user of our GPS system with good knowledge of Embedded C can customize the working of the GPS system according to his/her need. Upgrading or customizing the features of this GPS system is very easy, while such luxury is not available with vendor specific GPS systems.

## 2. RELATED WORK

Many researchers have proposed the use of cutting edge technologies to serve the target of vehicle tracking. These technologies include: Communication, GPS, GIS, Remote Control, server systems and others.

The proposed tracking system in this paper is designed to enable the navigation of the robot &track and monitor robot' status that are used by certain party for particular purposes, this system is an integration of several modern embedded and communication technologies [2]-[6]. To provide location and time information anywhere on earth, Global Positioning System (GPS) is commonly used as a space-based global navigation satellite system [2]. The location information provided by GPS systems can be visualized using Google Earth [3].

In wireless data transporting, Global System of Mobile (GSM) and Short Message Service (SMS) technology is a common feature with all mobile network service providers [4, 5]. Utilization of SMS technology has become popular because it is an inexpensive, convenient and accessible way of transferring and receiving data with high reliability

[6].As shown in figure (1), the proposed system consists of: in-vehicle GPS receiver, GSM modems (stationary and in-vehicle), and embedded controller [7]. The users of this application can monitor the location graphically on Google Earth; they also can view other relevant information of the robot & it can remotely monitor & controlled [8, 9].

**Figure 1. Block Diagram of the System**

The implemented GPS navigation & position locator robotic system can be used to monitor various parameters related to navigation ,area exploration, safety, emergency services and engine stall [10]. The paper shows an implementation of several modern technologies to achieve a desirable goal of remote robot navigation via GPS & fleet monitoring and management via GSM.


## 3. SYSTEM OVERVIEW

The system has two main modules, as shown in figure (2). The first module is the navigation & tracking device which is attached to the moving robotic system. This module composes of: a GPS receiver, Microcontroller and a GSM Modem. The GPS Receiver retrieves the location information from satellites in the form of latitude and longitude real-time readings & navigate accordingly keeping the goal of reaching the destination. The Microcontroller has three main tasks: to read certain robotic parameters from data port (OBD-II), to processes the GPS information to extract desired values and to transmit this data to the server using GSM modem by SMS. The chosen engine parameters are: RPM, engine coolant temperature, vehicle speed, percent throttle. The system is implemented with accelerometer, line follower, edge avoider, water phobic, fire phobic & bump resistant using specific sensors.

The second module consists of a recipient GSM modem and workstation PC. The modem receives the SMS that includes GPS coordinates and engine parameters. This text is processed using a Visual Basic program to obtain the numeric parameters, which are saved as a Microsoft Office Excel file. The received reading of the GPS is further corrected by Kalman filter. To transfer this information to Google Earth, the Excel file is converted to KML (Keyhole Markup Language) format. Google Earth interprets KML file and shows automobile's location and engine parameters on the map. The system's efficiency is dependable on the sufficiency of the used communication network.

ATMEL ATmega8535 microcontroller is used for interfacing to various hardware peripherals. The current design is an embedded application, which will continuously monitor a system and report the status of the system on demand. For doing so an ATMEL ATmega8535 microcontroller is interfaced serially to a GPS Receiver/Transmitter & GSM module.

The GPS modem will continuously give the data i.e. the latitude and longitude indicating the position of the vehicle. The GPS modem gives many parameters as the output, but only the NMEA data coming out is read and displayed on to the LCD.An EEPROM is used to store the locations & parameters with results.

The GPS navigation of the system is enabled by chassis & wheel driven by the DC motor, the DC motor is controlled by the GPS data like longitude & latitude. The system is enabled with Line following & obstacle avoider capabilities. But the functionality of the system can be increased modularly by interfacing the microcontroller with sensors & modules like GSM & internet module to provide tracking & data transfer capabilities.

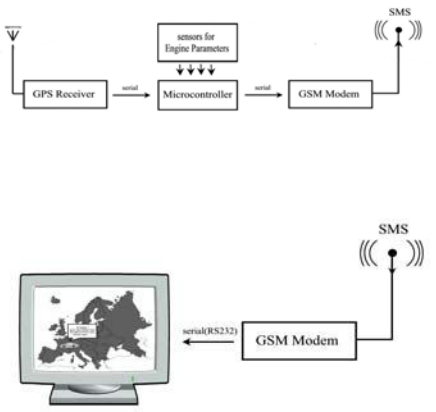


**Figure 2. The system architecture**

The NMEA String can be logged by connecting the GPS module via UART to PC & using NMEA Data Extractor & HyperTerminal to record the journey GPS NMEA strings & simulate it on Google Earth & KML Generator Pro to acquire geographical & statistical data about the journey, path & locations.

The NMEA 0813 standard for interfacing marine electronics devices specifies the NMEA data

sentence structure as well as general definitions of approved sentences. However, the specification does not cover implementation and design. I will hopefully clarify some of the design tasks needed to parse through NMEA sentences robustly. It will try to show techniques in parsing and data integrity checking. I will reference the NMEA 0183 specification and it is recommended that the NMEA 0813 specification be available as a reference.

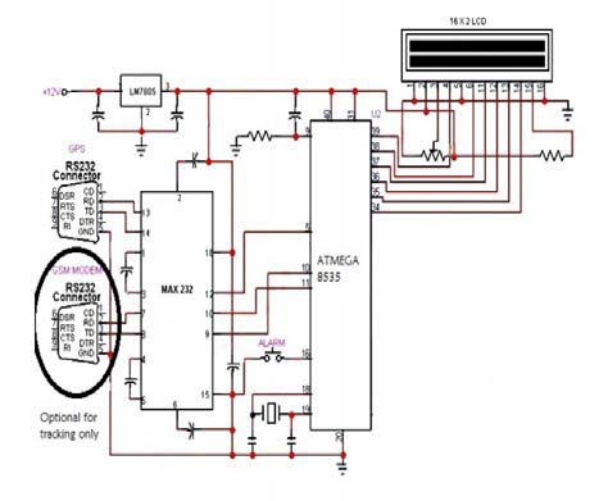


**Figure 3. Circuit Diagram of the system**

## 4. HARDWARE SPECIFICATIONS

The robot, as shown in figure (2), consists of two main inputs: The first received input is the GPS output, which has a sentence based on NMEA 0183 standard. The other input is obtained by the port, version II (OBD-II). The unit send an SMS using Hayes command (AT Command).

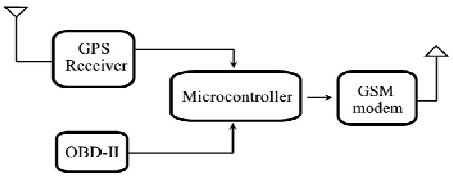


**Figure 4. Hardware Block Diagram**

On-Board Diagnostics port (OBD-II) is a universal automotive protocol supported by modern automobiles to retrieve diagnostic errors over a Controller Area Network (CAN) bus of the microcontroller (MCU) [11].The used GSM module is of type SIM900D, this module supports standard AT command and compatible with several GSM networks. Transmission parameters are set to: Baud rate is set at 19200 bps, the data is 8N1 format, and flow control is set to none. For this study, we chose certain parameters to show the status of the engine: RPM, engine coolant temperature, vehicle speed and percent throttle.

The GPS receiver is a GTop A20. The GPS module supports up to a 10Hz update rate. The microcontroller Atmel ATmega 8535 is the main operational unit of the robot. The GPS receiver collects the latitude, longitude and speed information and forwards them to the microcontroller [12]. The GSM module communicates with the microcontroller to send the information package to another GSM Module at the recipient station, all information appears on Google Earth after processing [13]. The robot is designed to be powered by the automobile battery. However, a power source is built-in the device as an emergency backup.

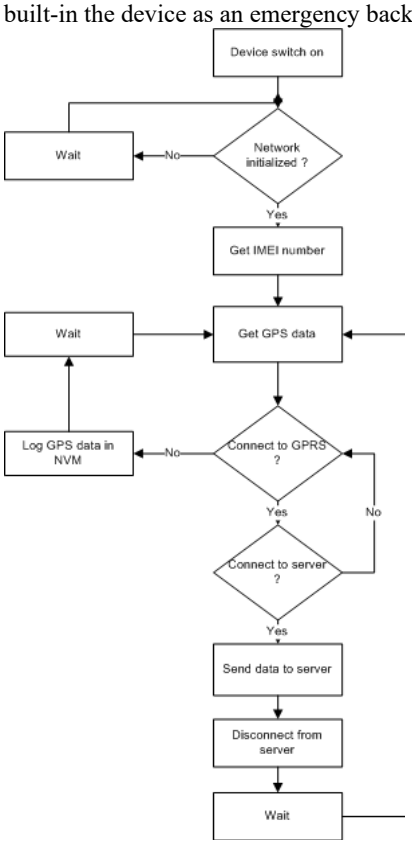


**Figure 5. Hardware Flowchart**

After turning on the device, it automatically initializes the network. Then it gets the GPS data in NMEA 0183 format and adds it with its own unique IMEI number [10], [11]. It then tries to connect to GPRS. If it fails due to GPRS unavailability then it logs the data in the non-volatile memory and waits for a certain fixed time period. After that it tries to connect to the GPRS again. After establishing the GPRS connection it tries to connect to the service provider's server using the HTTP protocol. After successful connection, the GPS data with IMEI number is sent to the server as a string. Then after a certain time period it checks the availability of GPRS and connects to the HTTP server. The current location of the device is sent. In this way the device communicates with the server and sends the location.

## 5. SOFTWARE SPECIFICATION

In this navigation & tracking system we used Google Earth software & Microsoft Visual Earth for tracking and viewing the status of the robot [14]. Google Earth currently supports most GPS devices. The engaged GPS Module has NMEA 0183 Protocol for transmitting GPS information to a PC. This protocol consists of several sentences, starting with the character $, with a maximum of 79 characters in length. The NMEA Message to read data with both position and time is: $GPRMC [14]. Therefore, only the $GPRMC information is used to determine the location of the automobile to reduce SMS text. The status of the automobile along with $GPRMC information is sent by the GSM modem of type MediaTek MT3329.

Consequently, the recipient GSM, also has NMEA 0183 protocol, receives the transmitted SMS to obtain GPS coordinates and status information of the system.

The transmitted GPS data is processed by a Visual Basic program using a Kalman filter to correct the current position. The resulted data of corrected position and automobile parameters is sorted in an Excel sheet. The Excel file is exported to a KML file that is compatible with Google Earth program. Hence, Google Earth will view the location and status of the automobile on the map by reading the KML file. Figure (6) illustrates the block diagram of the recipient module in the system.

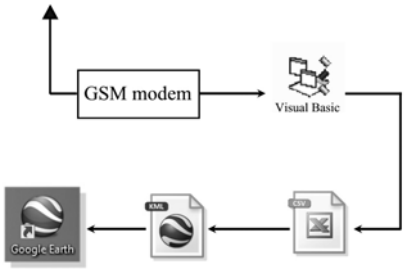


**Figure 6. Block Diagram of Monitoring System**

The KML file, developed for Google Earth, is used to save geographic data that includes navigation maps and other driving instructions. Figure (7) shows the live location of an robot in terms of latitude and longitude, and parameters retrieved by OBD-II: RPM, vehicle speed, acceleration etc.

**Figure 7. Google Earth Snapshot showing the live location and motor parameters of the robot**

**Figure 8. Google Earth Snapshot showing live tracking of robot.**

Furthermore, Google Earth provides the ability to track an object and view the related information at any position as shown in figure (8). The track shows the travel locations of the vehicle form the beginning of the route. All data is saved in a separate excel data sheets.

**Figure 9. Monitoring Side Flowchart**

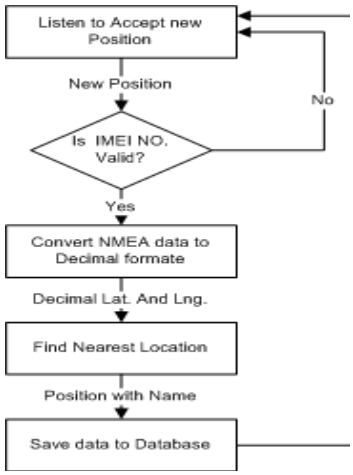

## 6. CONCLUSION

In this paper, a real-time automobile tracking system via Google Earth is presented. The system included two main components: a transmitting embedded module to interface in-vehicle GPS and GSM devices in order determine and navigate robot send & location and status information via SMS. The second stationary module is a receiving module to collect and process the transmitted information to a compatible format with Google Earth to remotely monitor the automobile location and status online.This system is used for tracking, positioning & navigating the system using the GPS signal & displaying the GPS navigation journey data & parameters on the LCD screen. The system is enabled with accelerometer, speedometer, odometer, navigation capabilities. The system is enabled with Line following & obstacle avoider capabilities. But the functionality of the system can be increased modularly by interfacing the microcontroller with sensors & modules like GSM & internet module to provide tracking & data transfer capabilities

The transmitted location of the vehicle has been filtered using Kalman filter to achieve accurate tracking. The 2DRMS accuracy of estimated vehicle coordinates has been enhanced. The accuracy of filtered coordinates was less than 15 meters compared to about 43 meters for transmitted coordinates received by in-vehicle GPS module.

## 8. REFERENCES:


[1] M. A. Al-Taee, O. B. Khader, and N. A. Al-Saber,“ Remote monitoring of Automobile diagnostics and location using a smart box with Global Positioning System and General Packet Radio Service,” in Proc. IEEE/ACS AICCSA, May 13–16, 2007, pp. 385–388.

[2] J. E.Marca, C. R. Rindt,M.Mcnally, and S. T. Doherty, “A GPS enhanced in-Automobile extensible data collection unit,” Inst. Transp. Studies, Univ.California, Irvine, CA, Uci-Its- As-Wp-00-9,2000.

[3] C. E. Lin, C.-W. Hsu, Y.-S. Lee, and C.C.Li, “Verification of unmanned air Automobile flight control and surveillance using mobile communication,”J. Aerosp. Comput. Inf. Commun., vol. 1, no. 4, pp. 189–197, Apr. 2004.

[4] Hapsari, A.T., E.Y. Syamsudin, and I. Pramana, “Design of Automobile Position Tracking System Using Short Message Services And Its Implementation on FPGA”, Proceedings of the Conference on Asia South Pacific Design Automation, Shanghai, China, 2005.

[5] Fan, X., W. Xu, H. Chen, and L. Liu, “CCSMOMS:A Composite Communication Scheme for Mobile Object Management System”, 20th International Conference on Advanced Information Networking and Applications, Volume 2, Issue 18-20, April 2006, pp. 235–239 .

[6] Hsiao, W.C.M., and S.K.J. Chang, “The Optimal Location Update Strategy of Cellular Network Based Traffic Information System”, Intelligent Transportation Systems Conference, 2006.

[7] Tamil, E.M., D.B. Saleh, and M.Y.I. Idris, “A Mobile Automobile Tracking System with GPS/GSM Technology”, Proceedings of the 5th Student Conference on Research and Development (SCORED), Permala Bangi, Malaysia, May 2007.

[8] Ioan Lita, Ion Bogdan Cioc and Daniel Alexandru Visan,“A New Approach of Automobile Localization System Using GPS and GSM/GPRS Transmission,” Proc. ISSE ' 06, pp. 115-119, 2006.

[9] T. Krishna Kishore,T.Sasi Vardhan, N.Lakshmi Narayana, ‘Automobile Tracking Using a Reliable Embedded Data Acquisition Sysytem With GPS and GSM’, International Journal of Computer Science and Network Security, VOL.10 No.2, 286-291, 2010.

[10] Wen Leng and Chuntao Shi, “The GPRS-based location system for the long-distance freight”, ChinaCom '06, pp1-5, Oct.2006.

[11] C. E. Lin, C. C. Li, S. H. Yang, S. H. Lin; C. Y. Lin, “Development of On-Line Diagnostics and Real Time Early Warning System for Automobiles,” in Proc. IEEE Sensors for Industry Conference, Houston, 2005, pp. 45-51.

[12] C. E. Lin and C. C. Li, “A Real Time GPRS Surveillance System using the Embedded System,” AIAA J. Aerosp. Comput., Inf. Commun., vol. 1, no.1, pp. 44-59, Jan. 2004.

[13] J. Lin, S. C. Chen, Y. T. Shin, and S. H. Chen, “A Study on Remote On-Line Diagnostic System for Automobiles by Integrating the Technology of OBD, GPS, and 3G,” in World Academy of Science, Engineering and Technology, 2009, aug. 2009, pp. 435–441.

[14] National Marine Electronics Association, “NMEA 0183 Standard For Interfacing Marine Electronic Devices,” Version 3.01, January 1, 2002.

# COMPUTATIONAL VISION AND ROBOTICS

**MAZIDUL AHMED, JAYACHOUDHARY**

IT Department, CMJ University, Shillong, Meghalaya

**Abstract-**The field of computer vision has been developed from the past several years. The applications of computer vision has been used in several years from medicine to robotics. Computational and robotic vision provides an overview of the latest research undergoing which been evaluated with robotic applications. Several new algorithms has been commonly developed for different applications in terms of computer vision. This computer vision is mainly seen as another sensory modality used in Robot. In terms of computer vision, used for Robots, there has always been requirement and comparision of methods in which very few methods are applied .But in realtime, the methods are strongly required in robotic applications.

## INTRODUCTION

Human being uses their eyes to observe the world and uses brain to analyse and interprete the data by interacting with an environment. So a new study has been developed that uses new computational method to act like human vision. This new research has been used in many applications like Robotics , industrial automation, smart vehicle biomedicine. But it is still a challenging research to compare computer vision with human vision. This paper presents the current development in the Robotic application in terms of computer vision.

Robotic vision is now a dayscommonly used in industries and agricultural field. It is a common replace for human beings to do several jobs like planting seeds and harvesting fruits/picking up of fruits.

This paper demonstrate the inclusion of methods for acquiring processing, analyzing and understanding images and high dimensional data from the real world for producing numerical or symbolic information. For image understanding it uses several models which isa enterprise of automating and integrating a wide range of processes. Computer vision covers the core technology of automated image analysis which is used in many fields. Machine vision usually refers to a process of combining automatic image analysis with other methods and technologies to provide automated inspection and robot guidance in industrial applications.

As a scientific discipline computer vision is concerned with the theory behind artificial system that extracts information from images. The image data can take many forms such as video sequence, views from multiple cameras or multidimensional data from a medical scanner. As a technological discipline , computer vision seeks to apply its theories and models to the construction of computer vision systems. Machine vision is the ability of a computer to “see”. A machine vision system employs one or more video cameras, analog to digital conversion(ADC) and digital signature(DSP). The resulting data goes to a computer or robot controller . Machine vision is similar to voice recognisation.

Two important specifications of any vision system are the sensitive and the resolution. Sensitivity is the ability of a machine to see in dim light or to detect weak impulses at invisible wavelengths. Resolution is the extent to which a machine can differentiate between objects. In general, the better the resolution ,the more confined the field of vision. Sensitivity and resolution are interdependent. All other factor held constant , increasing the sensitivity reduces the resolution and improving the resolution reduces access the sensitivity.

Human eyes are sensitive to electromagnetic wavelength ranging from 390 to 770 nanometers(*nm)*. Video cameras can be sensitive to a range of wavelengths much wider than this . Some machine vision systems function at infra red(R), ultraviolet(UV) or X-rays wavelengths.

Bonocular(*stereo*) machine vision requires a computer with an advanced processor. In addition , high resolution cameras, a large amount of random access memory and an artificial intelligence(AI) program are required for depth perception.

## LITERATURE REVIEW

From the past decade, survey has been done on computer vision for fruit harvesting robots. It review on harvesting robots based on three main criteria , the sensory configuration, visual cries and computational approaches. The authors summarise related literature from the last two decades ,identify the major limitations of the existing approaches and describe the main challenges with possible development directions.

A study on video based objects tracking has been done that aims to detect moving objects, filtering out noise and group motion vectors into a meaningful scene representation. A critical issues has been created for grouping or moving the object which size might change together. Under this issues, an estimation of approximate size of the moving object at different of the moving object at different distances has been recorded.

A study has been also done on multiresolution framework for multiobject tracking. They introduce

an adaptive moving object segmentation scheme and propose a multi-resolution tracking framework using Daubechies[1]complex wavelet transform. The framework consists of moving object detection and multi-object tracking modules. Several experiments were conducted on indoor and outdoor video sequences. The results illustrate the effectiveness and robustness of the proposed framework. Since gestures are a powerful means of communication in human life, gesture recognition is an active research domain in computer vision. The main problem was how to make computers understand gestures, thereby using human hand or body motions to replace an input device to perform human computer interaction. So, a proof of concept video game has been developed to demonstrate the validity of the proposed method .This video games was based on perceptual and recognition that proposes an approach to develop a 3D visual sensor based gesture control framework.

But there are different problems which rises in computer vision such as image segmentation, tracking, statistical shape modeling. To address these different problem, different set of level of methods has been designed to segment a complex scene into its parts and group these parts into different objects that produces meaningful descriptions of the scene. So different classification experiments were conducted with 400 image taken from four different angels of views. A survey had been conducted on medicinal plant images which has been identified and classified based on certain methods. The highest classification accuracies as reported were 98% ,97% and 94% for trees, herbs and shrubs respectively when using level set segmentation and SUM classifier. Biometric has been investigated for smart house applications. The potential application areas include resident access control, visitor registeration and public area surveillance. But the challenging is in with integrating biometric device with other security components to achieve a robost and accurate solution. Multi-functional intelligent access control system was designed based on hand vein. This control system describes a prototype of an access control system that unlocksa door either by the subject pressing an indoor button or performing hand vein verification on the subject. The major contribution of this work is in hardware design and system configuration in implementing hand vein access control system.

As the days are coming computer vision was growing. More and more sophisticated algorithm was developed and put into applications.

**Working Methodology**

Many tasks has been implemented on computer vision for image processing and machine vision . Several specialized tasks based on recognition exist was used like:-

1) Content based image retrieval:- Here all images was found in a larger set of images. The content can be specified in different ways like All the similar images relative a target image was taken.
2) Pose estimation:- Here technique had been used by assisting a robot arm in retrieving objects from a conveyor belt in an assembly line situation.
3) Optical Character Recognition(OCR):- Here characters in images of printed or handwritten text was identified with a view to encoding the text in a format.
4) 2D Code reading:- Here 2D codes were readed such as data matrix and (QR codes)[2].

**Motion analysis:-**

A motion analysis was done to estimate motion by processing image sequence to produce an estimate of the velocity either at each points in the image or in the 3D scene. During motion analysis several tasks was used such as:-

1) Egomotion:- It determines the 3D rigid motion of the camera from an image sequence produced by the camera.
2) Tracking: This task tracks the movements of a smaller set of objects.
3) Optical flow:- This task determine for each point in the image , explains how that point is moving relative to the image plane. This motion is a result of corresponding 3D point is moving in the scene and how the camera is moving relative to the scene.
4) Scene reconstruction:- By taking more images or a video of a scene , scene is reconstructed by using a 3D model of the scene to produce a complete 3D surface model.

**Image Restoration:-**

The purpose of image restoration is the removal of noise from images. Noise is removed from images by using various types of filters[3]such as low pass filters or median filters. Image data is first analysed in terms of the local image structure such as lines or edges and then controlling the filtering based on local information. Image restoration in computer vision system are highly application dependent. The implementation of computer vision system also depends on the functionality. Some of the functions found in computer vision systems are:-

a) Image Acquisition:- A digital image is produced by one or several image sensor, which besides various types of light sensitive camera include range sensors, tomography devices, radar, ultra-sonic camera etc. Depending on the type of sense the resulting image data is an ordinary 2D image, a 3D volume or an image sequence . The pixel values typically correspond to light intensity in one or several spectral bands but can also be related to various physical measures such as depth ,

absorption or reflectance of some or electromagnetic waves.

b) Pre-processing:- It is function for processing data before applying computer vision method to image data for extracting some specific piece of information so that it satisfies certain assumptions implied by the method.
   - Resampling to co-ordinate image system.
   - Noise reduction to assure that sensor noise doesn't introduce false information.
   - Contrast enhancement to assure that relevant information can be detected.
   - Scale- space representation to enhance image structure.

c) Feature extraction:- Various features at various levels are extracted from the image data which can include:-
   - Lines, edges and ridges.
   - Localized interest points such as corners, blobs or points.

**Detection/Segmentation**

During processing a decision,

a) Several image points or regions of the images are selected of a specific set of interest points.
b) Segmentation of one or multiple image region for a specific objects.

**High level processing**

In this step, a small set of input data is taken to contain a specific object. The other processing activities involves

a) Verification
b) Estimation of application specific parameter.
c) Image recognition- classifying a detected object into different categories.
d) Image registeration:- comparing and combining two different views of the same object.

**Decision Making**

Making the final decision required for application:-

a) Pass/fail on automatic inspection applications.
b) Match/No match in recognition applications.
c) Flag for further review in medical, military, security and recognition applications.

Robotics research covers areas as diverse as advanced mathematical theory through to the practical engineering applications of robots.

Robot autonomopara-monitorizationmedioambiental aims to develop an autonomous underwater robot along with software tools to build geo-referenced detailed photo-mosaics of the ocean floor and enable scientists to carry out repeated surveys to monitor its evolution over time.

**Mobile Robotic Lab**

In the mobile robotic lab there are two robotics platforms designed and built by different researcher working in the laboratory . These are used to carry out research in different fields of computer vision applied in the field of mobile robotics such as autonomous robot navigation, mapping local obstacles detection, fusion of sensory information visual localization and qualitative 3D reconstruction of the environment. The conducted research is also related to the identification, modeling the dynamic behavior of robots and control their movement using predictive control techniques. These robotic platforms are also used as a tool for final degree projects.

**Underwater Robotics Lab**

The underwater robotics laboratory is responsible for the study of control architectures for autonomous robots, the identification and modeling of underwater vehicle operating environment design and development of vehicle simulators, missions and environments. Underwater, the fusion of information from different sensors for navigation, location of vehicles, the construction of visual maps of submerged structure/ and or the sea bed and all involving the construction, development and commissioning of underwater robots.

**Video-based object tracking**

It is an object tracking tracking that aims to detect moving objects , filter out noise and group motion vectors into a meaningful scene representation. The critical issues are grouping the objects that move or change together and estimating the approximate size of the moving object at different distances. The third paper entitled deals ' A multi-resolution framework for multi-object tracking in Daubechies complex wavelet domain by jalal and singhdwavelet deals with multi-object tracking in complex wavelet domain. They introduce an adaptive moving object segmentation scheme and propose a multi-resolution tracking framework.

**Analysis of tracking robotic location**

The construction Robotics unit at city university, London is developing a building inspection robot called CURIO to carry out a number of tasks, one of there is visual inspection. By knowing the robotic's position with respect to the whole building face, the feature or window can

Identified , located and the absolute position of the defect calculated.

The vision system on CURIO is too close to the building(Fig-1) to be able to find its own position. It suffers from the human inspection . Thus an approach needs to be found for locating its position.

Fig-1 Image of a real building

The location of the robot is carried out made by Alastair M.Paterson[5]in two stages. The first is the coarse positioning that is identifying at which floor the robot is or between two windows it is located. The second stage to be covered by a different project is to refine its position. The main aim of this study was system to produce a low cost, easy to use location system. The system investigated used a single uncalibrated camera that could be placed at any convenient point such that it could view the building face and be connected to a computer. A typical configuration is shown in fig 2. Here task is performed by capturing a single image of building and match its face to the CAD diagram. When matched, it is then necessary to identify the robot on the building and use the mapping to indicate robot's position.

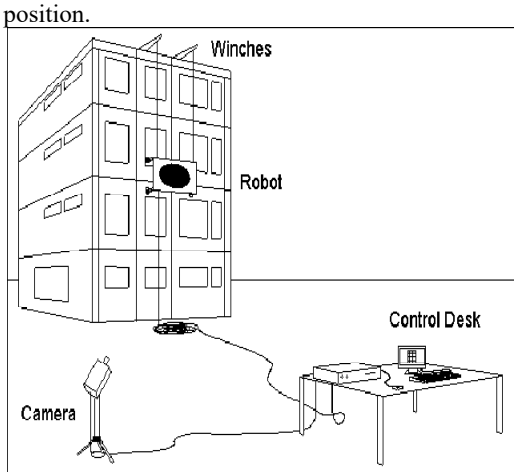


Fig-2- Typical Building inspection set-up

$X=(b_{1,1}x+b_{1,2}y+b_{1,3})(b_{3,1}x+b_{3,2}y+1)$

$Y=(b_{21}x+b_{2,2}y+b_{2,3})/(b_{3,1}x+b_{3,2}y+1)$

In physical terms, these equations state that if four points in the image can be identified on the diagram, then a mapping can be calculated such that any point in the image(x,y), say the centre of the robot target can be mapped onto a point(X,Y) on the CAD diagram . This point then corresponds to the true location of the robot.

**Algorithm Used**

The CAD diagram(Fig-3) of the building face is being inspected is used to generate map of features again with descriptions of neighboring position of Robot.

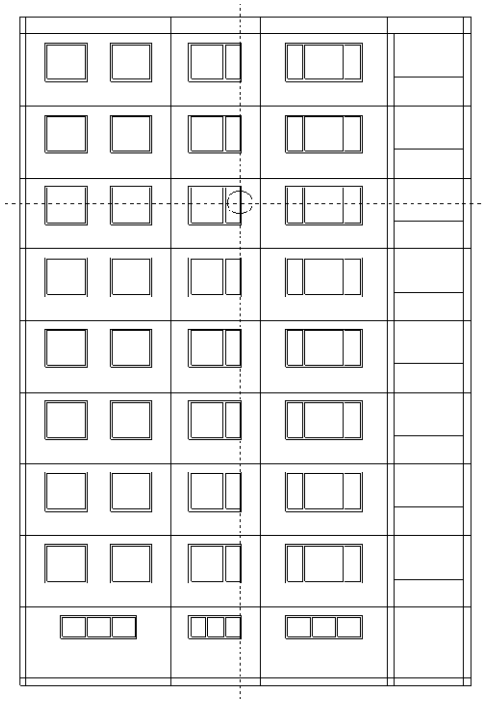

Fig-3 CAD diagram showing calculated robot target position

The algorithm[6] is implemented as :-

For each building new face,
do:
Load the CAD diagram and generate mapping lists.
For each new robot or camera position,
Do:
Grab and pre-process the image
Reduce the image to shape boundaries and classify them
Identify the robot target and remove it from the image
Identify feature types in the image
Map the features to their specific CAD counterparts
Choose a set of control points and calculate the image to CAD mappings.
Apply mapping function to robot target to obtain its true location.

**Experimental Results**

The performance of the algorithm was initially measured by applying to real buildings . Here measure of accuracy were found. The building has been viewed from a Fig-4 horizontal angle($30^0$), a vertical angle of $0^0$ and has a resolution of 640 X 540pixels. It shows that the algorithm worked successfully. Close inspection has been revealed that there were faints shadows in the upper corners of the window.

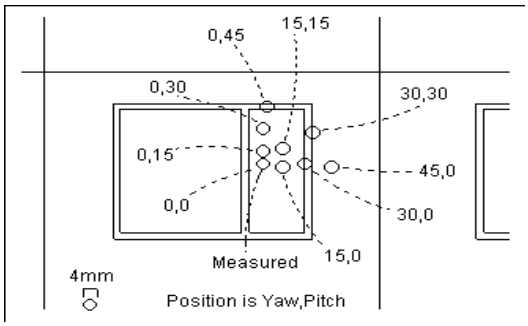


Fig-4 Calculated robot positions for different camera angles

## CONCLUSION

Thus it is concluded that as the field of computer vision grow , more and more sophisticated algorithm will be developed and put into new application. The work presented here has briefly shows how computer vision can help to keep track of object. It has potential and certainly produced good results that visualizes real . Computer vision can certainly help building inspection and should be researched further . The designed algorithm were proved to be useful with predictable errors so manual system is situated for immediate use.

## REFERENCES

1. [1] – Daubechies complex wavelet article by A. Khare-2007, Department of Electronic and communication.
2. [2] – QR codes by Jeff korhan
3. [3] – particle filtering by Eric Lehmann. Department of telecommunications engineering research school of information.
4. [4] – Biometric – Enrico Grosso computer vision laboratory university of Sassari, Italy. Anil K.Jain.
5. [5] – Alstair M. Paterson , Geoff R. Dowling, Denis A. chamberlain Building inspection:
   Can computer vision help? The city university, London, England ECIVO HB.
6. [6]- Building Inspection: Can computer vision help? Alstair M. Paterson , Geoff R. Dowling, Denis A. chamberlain, robotic unit The city university, London, England ECIVO HB.

# A SIMPLE AUTONOMOUS ROBOTIC MANIPULATOR FOR PLAYING CHESS AGAINST ANY OPPONENT IN REAL TIME

**NANDAN BANERJEE, DEBAL SAHA, ATIKANT SINGH, GAUTAM SANYAL**

Nandan Banerjee and Atikant Singh are undergraduate students with the Dept. of Computer Science and Engineering, Debal Saha is an undergraduate student with the Dept. of Mechanical Engineering and Dr.Gautam Sanyal is a professor with the Dept. of Computer Science and Engineering at the National Institute of Technology, Durgapur, INDIA. The project was funded by the Dept. of Computer Science and Engineering, National Institute of Technology, Durgapur, INDIA and manufacturing of the manipulator was done at Senco Engineering Works, Durgapur, INDIA.

**Abstract**— This paper presents a simple 3-DOF (degree of freedom) robotic serial manipulator which is capable of playing chess in real time against any opponent. This autonomous chess playing robot consists of a HD Logitech Webcam, a low cost custom made serial manipulator, algorithms for the efficient detection of the chess pieces on the chessboard and a robust control mechanism for the accurate movement of the manipulator

***Keywords***— *Human Robot Interaction, Chess playing robot*

## I. INTRODUCTION

This project introduces a 3 DOF robotic manipulator system that is designed to autonomously play the game of chess in real time against human or robotic opponents. The Chess Robot includes a Logitech HD webcam, a low cost custom made manipulator, algorithms for the efficient detection of the chess pieces on the chessboard and a robust control mechanism for the movement and control of the manipulator. Compared to prior work on robotic systems playing chess with specifically instrumented chess boards and/or pieces, our robot is not confined to just playing chess but it can also be used as a standard manipulator and can be controlled effectively using its own set of control commands.

## II. CHESS PIECE DETECTION

The chess pieces on the chessboard were detected using standard image processing techniques. A. Prerequisites For the image processing part in which the main objective was to find the current orientation of the board given the previous orientation, the following were used:

- openCV library (used along with qt, an open source C++ framework)
- Logitech C270 webcam
- Intel Core2Duo processor running at 1200 MHz

B. Methodology

A webcam was positioned directly over the chessboard and the resolution was set at 640 * 480. The openCV image processing library was used to capture the screenshots and apply the image processing procedures. Following factors were identified as having a major effect on the performance of the image processing techniques:

hess pieces on it. The most suitable light source was found to be a diffused light source on to the surface of the board. When a pointed light source from the side was found to have been used, shadows and glares thus created were sometimes misinterpreted as pieces.

C. Image processing algorithm

1) Set the Region of Interest: A screenshot is taken using the webcam and the region of interest is set manually. The region of interest is the part of the image where all the image processing procedures are to be applied.

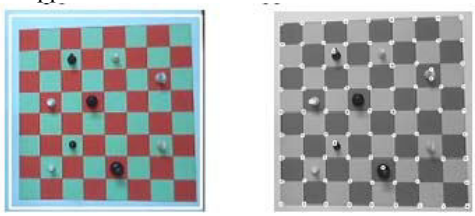

**Fig 1. (a) Region of Interest around a screenshot of the chessboard. (b) All probable corners detected using the Shi-Tomasi corner detection algorithm.**

2) Detect the corners and intersection points: Using the Shi-Tomasi corner detection algorithm, which is just a slight modification of the Harris corner detection algorithm, the corners of the chess squares are found out.

3) Find the top-leftmost, top-rightmost, bottom-leftmost and the bottom-rightmost corners: The four endmost corners of the chessboard are then determined using normal pixel position calculations.

4) Compare the probable and the actual corners: The probable corners are found out by dividing the difference of the corner points by eight, thereby finding out the corner points of all the chess squares. Then the probable corners are compared with the actual corners and if the difference between their values suggests that they are neighbouring points, then the probable corner is replaced by the actual corner. In this way, the corners for all the 81 chess squares are thus found out. This method is used to remove the corners thatare detected on the chess pieces. Also, because of bad ambient lighting conditions, sometimes a few of the corners are not

detected. In that case, the probable corner acts as the corner of the chess square. Therefore, to avoid these two errors, this comparison and assertion procedure is performed.

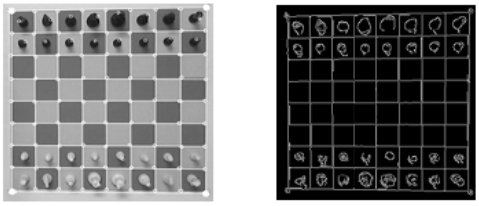

**Fig 2. (a) Showing all the chess squares with their corners detected. (b) After**

applying the Canny edge detection algorithm to detect all the chess pieces on the chessboard.

5) Check for the square occupancy using the Canny edge detection algorithm: The Canny edge detection algorithm is then used to detect the edges of the chess pieces on the chessboard. From the already found values for the four coordinates of all the 64 chess squares, all the chess squares are chosen. The dilation operation is then applied on the edge detected binary image on each of the chess squares, and the number of white pixels is then compared with a designated threshold value. If it exceeds the threshold value, then the chess square is occupied otherwise empty.

6) Determination of the colour of the chess piece: The image is thresholded. The threshold is chosen according to the ambient lighting conditions and the texture of the chessboard. After thresholding, the black pieces stay black whereas everything else becomes white. Then, the erosion operation is applied on the thresholded image on each of the chess squares, and the number of black pixels is then compared with a designated threshold value. If the value exceeds this threshold value, then the chess piece is black otherwise white if the square is not otherwise empty.

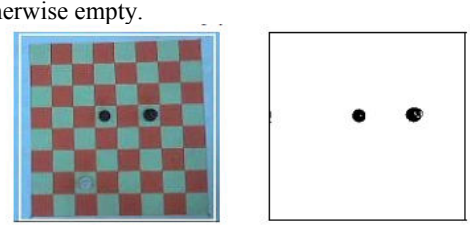

**Fig 3. (a) Showing a chessboard orientation with two black pieces and one white piece. (b) After thresholding, only the black pieces are deemed as objects and everything else is ignored.**

D. Chess Move Detection

After the orientation of the chessboard has been successfully detected, the individual identities of every chess square is known, i.e. if the chess square is empty or not, and if not empty, then the colour of the chess piece present in it. An eight by eight matrix is then constructed consisting of three values [0, 1 and 2]. '0' signifies that the square is empty. '1' signifies that the square has a white piece in it and a '2'signifies that the square has a black piece in it. The image processing algorithm described above is applied on the entire chessboard and all the 64 values of the squares are hence determined and stored in the matrix. Then the matrix is compared to a previously recorded matrix of a previous image and the changes are noted. From these changes, it can be ascertained as to what move has been given by the opponent. After this move is realized, it is then fed as the input to the GNU Chess engine described in the next segment. The vision system could be thwarted simply by swapping chessmen so it is being assumed that there won't be any foul play on the user's part.

## III. GNU CHESS INTERFACE

GNU Chess is a computer program which plays a full game of chess against a human or other computer program. The goal of GNU Chess is to serve as a basis for research. It has been used in numerous research contexts. It is free software, licensed under the terms of the GNU General Public License and is maintained by collaborating developers. It's one of the oldest computer chess programs for UNIX based computers and one of the earliest available with full source code. On basic, current computer chess architecture, GNU Chess plays at senior master/weak international master strength (2500+_ELO on simple hardware – Intel Core2Duo), without parallel processing, according to the IQ6 test suite. In this project, the GNU Chess version 6.0.1 has been used to determine the moves by the Chess Robot. The GNU Chess engine has been interfaced in "qt"` using the QProcess class. GNU Chess is started in the Xboard mode using the -x argument. The moves are sent to and received from the GNU Chess engine using standard coordinate algebraic notation through the standard input and output streams.

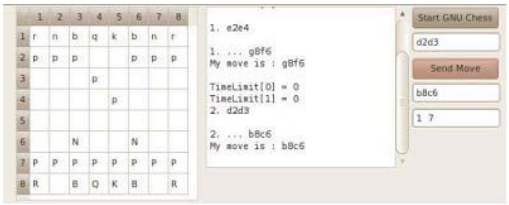


**Fig 4. GNU Chess Interface using QProcess in qt.**

As mentioned in the previous section, the move ascertained after applying the image processing techniques is fed into the input stream of the GNU Chess engine which is interfaced using the Process class as already mentioned. The GNU Chess engine then figures out the appropriate response and it is then relayed to the robot control module which then automates the robot.

## IV.MECHANICAL ASPECTS OF THE SERIAL MANIPULATOR

The various mechanical aspects of the serial manipulator
can be categorized as follows:

- Mechanism Development and Actuation
- Stress and Force Analysis and CAD modeling
- Material Selection
- Manufacturing of the Serial Manipulator

A. Mechanism Development and Actuation The manipulator is intended to perform a pick and place task. A simple model for a serial manipulator for this purpose is a 2PR (two prismatic and one rotary joint) serial manipulator. The base link carries the first link and there exists a rotary joint between them. Between the first and second and between the second and third link there are prismatic joints. While the prismatic joints help in easily locating the end-effector of the serial manipulator in the desired point in the work space, the rotary joint increase the total work space and provides more manoeuvrability. The rotary joint between the base and first link is established by fixing a high torque motor to the base and mounting the first link on the motor shaft. The actuation of the prismatic joints can be achieved by using linear motors. But due to its high cost, an efficient and comparatively cheaper screw joint mechanism actuated by a dc motor is used to achieve the linear motion.

B. Stress and Force Analysis and CAD Modelling
The arrangement of the last link makes it act like a cantilever beam. The forces acting on the last link are same as that on a cantilever beam. The length of the last link is decided by the farthest distance needed by the end effector to traverse (the distance to the farthest square on the board). The links are linearly actuated by the screw joint motion for which they need to be cylindrical and shape and should carry screw threads. The pitch of the screw thread is decided by the velocity of the actuating motor and the required linear velocity. This cantilever beam type link is mounted on another link which too carries another prismatic joint which is actuated by a dc motor using the screw mechanism. The diameter of this cylindrical link is decide by calculated the cumulative effect of the bending moment and torsion of the cantilever beam on it and also the torsion due to its own inertia. This cylindrical link which supports the cantilever
beam type link is mounted on a motor's shaft fixed to the base. The stress and force analysis helps to decide the actuation torque required for the motors to drive these joints. The cantilever beam type link required a motor with comparative larger shaft length. The base motor needed a high torque motor as it had to bear the weight of the links mounted on it. the problem of increased torque due to the inertia/weight of the links on the base is resolved by mounting the links via bearing on the base and then actuating the link from the top end instead of mounting the whole link arrangement on the shaft of the motor and revolving it on the shaft. The serial manipulator consists of various joints and links. The actuating joints need to be placed properly for dynamic balancing. The shape of thread, its position on the cylindrical links, the position of the motors, the mounting clamps, the alignment of the motor shaft etc. are some of the various points that are to be kept in mind while designing the manipulator. Most of the time the stress and force analysis is just not enough for obtaining the correct design which is free from all types of faults. Many decisions regarding alignments and positioning of various parts need to be decided in a heuristic manner. Computer aided designing packages help one to develop such designs. CATIA is one such package and it has been used to develop the design of this serial manipulator. The CAD designing approach helps us to perceive the implemented mechanisms in a better way. The probable areas of fault can be figured out while studying a CAD model and it aids in making fine changes in the intricate details of the model.

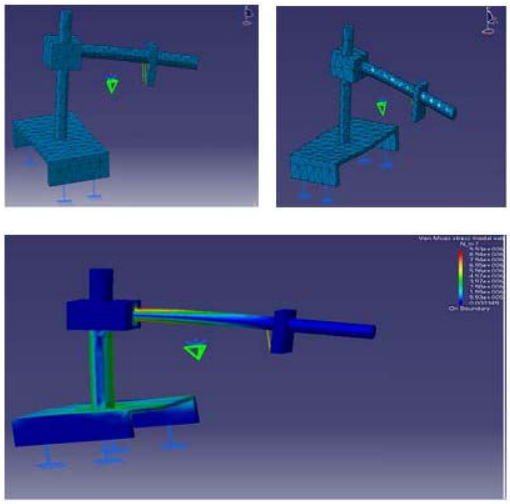

**Fig 5. In the above figures, a simple representative model for the manipulatoris used to analyse the stress distribution using the "Generative Structural Analysis" module of the CATIA software. In the clockwise direction, first the force applied and the mesh created for analysis is shown followed by the depiction of stress distribution with different colours representing various ranges of stress.**

C. Material Selection

Once the mechanism is decided and the resulting force and torques are determined, the materials are selected for individual links of the manipulator. The base has the support the whole weight the other links and the actuating joints. Cast iron suits the requirements for such a base. It is capable of absorbing shocks. The base made of cast iron reduces the vibration of the cantilever beam type link and thus helps in precise positioning of the end effector. The first link on the manipulator has to support the cantilever type link and thus have to act like a strong column. The hollow cylindrical shape

is suitable for this purpose. The thickness is limited by the machining stresses induced while making the threads on the column. Mild steel is suitable for making the column. The cantilever type link too is a hollow cylinder with low weight. Aluminium is a suitable material for manufacturing it to account for the low weight constraint .D. Manufacturing of the Serial Manipulator While manufacturing the manipulator certain issues were kept in mind. The selection of proper material is just not enough to dampen the inherent vibration produced in the links. The proper positioning of the actuating mechanism, the alignment of the links and mounting of the motors also play a crucial role in dampening this vibration and thus helps to attain dynamic stability and consequently better performance. The link which acts as the supporting beam for the cantilever beam type end link is mounted on a bearing on the base. The bearing is welded to the base and a protrusion from the supporting link is press fit in to the bearing. The cantilever type link has a cuboidal end with a cylindrical hole carrying inner groves matching the threads on the supporting beam. The cuboidal end has a protrusion which runs in a straight grove on a bar mounted on the base. This helps to attain a prismatic joint's to and fro motion with the help of the screw joint motion. Similarly the cantilever type link is fitted with a cuboidal block carrying a cylindrical hole with grooved inner threads that matches the threads on the cantilever type link and also possesses a protruded edge that runs on a grooved overhead bar. This cuboidal block that moves on the cantilever beam type link carries the end effector.

## V. GRIPPER, STRUCTURE AND MOVEMENT OF THE MANIPULATOR

The manipulator has three degrees of freedom. The manipulator consists of 4 links and 3 joints. There

are base linked can be termed as link 0 and the consecutive links can be numbered/named successively as link 1, 2 and 3. Joint 1 exists between link 0 and 1 and is a revolute joint. There exists two screw joints, one between link 1 and 2 and the other between link 2 and 3. The screw joints are good replacement for prismatic joints. The linear motors used for making a prismatic joint between to links is far more costly than the combined cost of machining threads (outer and inner) on links and that of a servo motor on which the links will be mounted after machining to form the screw joint.

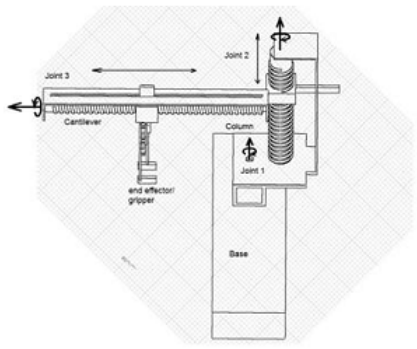


**Fig 6. A sketch of the serial manipulator showing all the joints and links.**

The linear motion achieved by the screw joint is also shown in the above diagram. The table/stand shows the base. Vertical column with the grooved mounting consists link one. The horizontal cantilever beam can be considered the link two. The end effector is the gripper which is in form of two spur gears with the gripping plates mounted on them. The revolute joint between the base and the first link is also shown. Thus, the joints and links are named as follows –

- Link 0 – Base
- Link 1 – Column
- Link 2 – Cantilever
- Link 3 – End effector/gripper
- Joint 1 – Revolute Joint
- Joint 2 – Screw (vertical) Joint
- Joint 3 – Screw (horizontal) Joint

Joint 2 is responsible for vertical lift necessary for picking up the chess piece and go for the necessary movement once of has been grabbed properly by the gripper. Once the image processing of the grabbed images of the board and chess pieces on it are done, a move for the serial manipulator is decide and the commands for the necessary movements of the joints for execution of the decision are transferred to the microcontroller. It thus drives the servo motors in compliance with the commands generated. The initial task for the manipulator is always to reach the desired coordinates where it has to pick up the desired chess piece. The picking up of the chess piece is the next task. Then it needs to take the chess piece to the destined position and then place it back on the board at the new position.

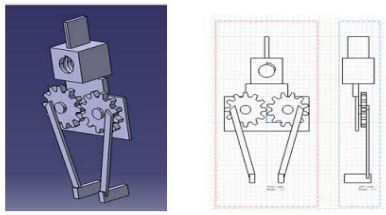

**Fig 7. (a) 3-D view of the gripper. (b) Front and side view of the gripper.**

Grabbing the chess piece, picking it up from the board and placing it back are similar kind of actions and can be grouped in a set. This set requires lowering of the gripper and holding the chess piece. Then it needs to be pulled up without disturbing the position of neighbouring chess pieces. This set of actions requires the movement of the grippers and point 2. The movement of joint 2 provides the lift necessary for picking and placing the pieces. The height of the lift should be such that while moving the grabbed pieces from one position to another, then it should be hit other pieces and thus should not disturb their position. This can be ensured by estimating the position from where the chess piece desired to be moved is grabbed by the gripper and the average height of the chess pieces above which this particular grabbed chess piece will pass during while traversing its path from its initial to the final position across the board. For gripping the chess pieces spur gears are used on which gripping jaws are mounted. Actuation of the gears leads to the gripping action. The angle to which this gripping jaws can spread is decided by the angle by which this actuating spur gears (and in turn the shaft of the motor driving the spur gear arrangement) turn which is constrained by the distance rL of the piece from the neighbouring chess pieces. Moving the gripper to the initial position of the chess piece and taking it to the desired destination is another set. This set of task requires knowledge of the coordinates of the place where the chess piece is positioned on the chess board in reference to suitable axes.

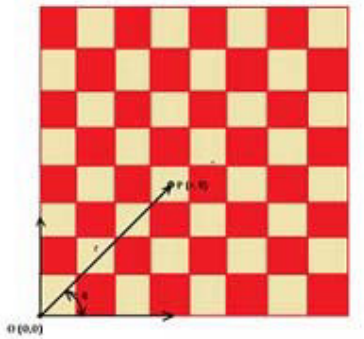

**Fig 8. The polar coordinate system which is used to determine the location of**

the chess squares.

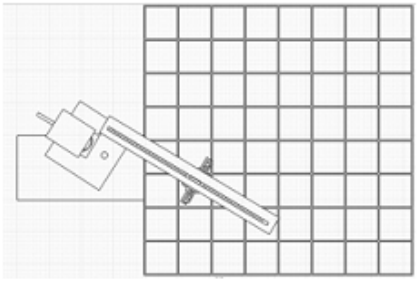

Fig 9. Movement of the manipulator over the chessboard (Not to scale). If the manipulator starts with the end effector located at O (0,0) for reaching destination with coordinates P(r, θ), then the Joint 1 will move by angle θ and then joint 3 will rotate by a certain degree so that the end effector travels the radial distance 'r'.

## VI. ROBOT FEEDBACK AND CONTROL

As the name suggests, robot feedback refers to the sensory data from every joint of the manipulator which is used to effectively control the movement and orientation of the manipulator. The interface between the robot and the computer is via a control circuit with an AVR microcontroller at its centre. The microcontroller connects to the computer using the serial port via an USB to serial port converter. The manipulator motors are driven using high power motor drivers.

### A. Sensory Data

Various sensors have been used to determine the instantaneous position of the manipulator. A 1 turn, 2 KΩ potentiometer was used to determine the angle of rotation of the manipulator about its base axis. It is referenced with a potential of 5 V and the value from the potentiometer is read in through the ADC with a resolution of 10 bits sampled at 172.8 kHz. Two optical encoder wheels with IR sensors were used to determine the linear movement of the vertical and the horizontal screw drive mechanisms. The optical encoder wheel has ten protruding teeth with an IR sensor placed around it. So, for a count of 10 by the IR sensor, the screw has a complete rotation about its axis and hence moves the distance equal to the pitch of the screw. The minimum distance that can be determined by this movement is 1/10th of the pitch of the screw.

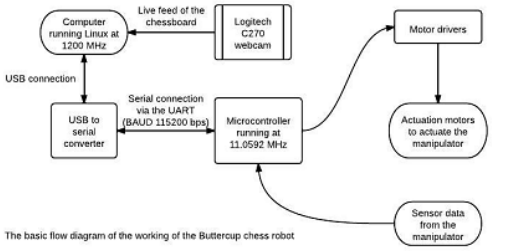


**Fig 10. Flow diagram of the working of the Chess Robot.**

### B. Control Circuit

The microcontroller, sensors, motor drivers and the serial port driver are the main elements of the control circuit. The microcontroller is an ATMEL ATMega32 microcontroller running at 11.0592 MHz. The output from the potentiometer (the rotation sensor) was input into the ADC2 pin and the output from the horizontal screw mechanism encoder was first compared using a comparator (LM324) and then input to the microcontroller. A 20 × 4 LCD (HD44780 driver) was connected to the microcontroller for debugging purposes. The

motor drivers were built using complementary MOSFET transistors (IRF540 and IRF9540) and controlled using the microcontroller pins. The serial port driver was made using Hex Schmitt inverters (74HCT14) for Rx and Tx (UART) and an USB to serial port adapter. Everything was soldered on Vero boards. A 220 V AC to 12 V 10 A DC SMPS was sed to effectively regulate the voltage output provided to the control circuit. The computer connects to the robot through a serial connection to the microcontroller. The serial connection has a baud rate of 115.2 kbps. The manipulator is controlled through a set of commands which controls all the movements of the actuation motors precisely. C. Chess Piece Movement using the Manipulator The locations of the various chess squares (in algebraic coordinate notation) on the chessboard are calculated, and then stored in a table in the program which communicates with the robot via the serial interface. When the output from the GNU Chess engine is directly fed to the program, it then sends a series of commands to the microcontroller specifying the angle of rotation and the position of the screws for the source and the destination. The manipulator then picks up the desired piece from the source location and then places it to its respective destination position.

## VII. EXPERIMENTAL EVALUATION

The detection of the corners of the chessboard was done effectively using image processing methods. Challenges were faced when there were bad lighting conditions and skewed orientation of the chessboard under the webcam. It was found that the best image processing results were attained when the chessboard was oriented in parallel to the viewing angle of the camera. Choosing a threshold value of 50 to identify the color of the piece seemed to work in almost 99% of the cases where the ambient light came from an overhead white fluorescent light. After every move the opponent makes, the program is able to determine the movement of the piece between the old and new position. Errors in detection occurred when the lighting conditions were changed without altering the computation values. In dark lighting conditions, the algorithm detected false chess pieces at the edges and certain other portions of the chessboard. The GNU Chess Interface odule sends and receives the moves by running GNU Chess in background and using its standard input and output stream to effectively communicate with it and extract the moves given by the engine. The engine returned „valid well thought out " moves in response to the user moves as determined by the image processing module. The interfacing and communication of the chess engine with the image processing module was perfect. The gripper slipped a few times while gripping the chess piece. More padding and provision of optimum curvature to the gripping claws reduces the slippage. A more articulate gripper can solve this issue efficiently. The overshoot of the end effector of the manipulator is observed while it is about to arrive at the destination. With a trial and error method it was found that when the manipulator stops after execution of the commands (rotation of the joints) to perform the decided move, the revolute joint should be rotated for a small angle (most of the times less than 2 degrees) in the opposite direction (to which it was initially moving) to arrive at the destination properly.

## VIII. REFERENCES


[1] G.D.Illeperuma, Unversity of Colombo. ”Using Image Processing Techniques to Automate Chess Game Recording” Proceedings, 27(2011) 76-83

[2] Cynthia Matuszek, Brain Mayton, Roberto Aimi, Marc Peter Deisenroth “Gambit : A Robust chess-Playing Robotics System", IEEE Int. Conf. on Robotics and Automation, May 2011, pp. 4291-4297

[3] Sokic E.; Ahic-Djokic M.; "Simple Computer Vision System for Chess Playing Robot Manipulator as a Project-based Learning Example", IEEE International Symposium on Signal Processing and Information Technology,Dec. 2008, pp. 75-79

[4] Learning Open CV Computer Vision with Open CV Library - Gary Bradski and Adrian Kaehler

[5] Rafael C. Gonzalez and Richard E. Woods, “Digital Image Processing”.

[6] Daniel Molkentin, “The book of QT4 : the art of building Qt applications”.

[7] “Designing Embedded Hardware” - John Catsoulis.


◈◈◈

# DESIGN AND DEVELOPMENT OF ACTIVE ENDOSCOPE USING SHAPE MEMORY ALLOY ACTUATORS

**AMAN ARORA & PARTHA BHATTACHARJEE**

[1]Cybernetics Department Central Mechanical Engineering Research Institute, CSIR. Durgapur, India.
[2]Scientist-F and HOD, Cybernetics Department, Central Mechanical Engineering Research Institute, CSIR. Durgapur, India.

**Abstract**— Minimally invasive surgery is well accepted in the society because it involves lesser operative trauma for a patient than an equivalent invasive procedure. It causes less pain and scarring, faster recovery, and reduces the incidence of post-surgical complications. An endoscope is considered as one of the most powerful diagnostic and therapeutic tool for dealing abnormalities inside the body. This article aims at deciphering a solution to the problem of passive bending of conventional endoscopes by introducing a concept of active bending by using Shape Memory Alloy (SMA) micro actuators. The developed prototype has many small segments connected to one another by a ball and socket joint, actuated independently, which gives rigidity and high degree of maneuverability to the scope. The article proposes an algorithm for traversing the scope inside the body and addresses a very important issue of taking it out without causing any damage to the track. A graphical interface gives the practitioner a number of options to orient the scope [on the basis of three dimensional (3-D) discrete points reached by the tip and segment orientations based on camera image] and simultaneously shows a 3-D view of orientation of the full scope.

**Keywords**-SMA; active endoscopy; active bending; actuated arm; complex trajectories.

## I. INTRODUCTION

### *A. Present Endoscopic Technology*

Endoscope widely used in clinical practice generally consists of a flexible shaft that contains channels for air, water, instruments and electric wires. At the distal end of the shaft is a 4- to 10-cm long steerable tip. At the tip, there are digital camera chips, light emitting diodes or glass fibers, and an exit for air water and instrument channel. At the proximal there is a grip with one or two control wheels or handles that are used to bend the tip in one or two directions [1]. Present endoscopic technology allows passive bending of the scope by one or more cables attached to the tip. Bending motions of the tip of a conventional endoscope are controlled from outside the body by wire traction.

Although flexible scopes are used because their flexibility enables traversing tortuous trajectories (though not very easily) and reaching many anatomical sites noninvasively, but this flexibility also causes difficulties that limit the functionality of the instrument. Thus, the stiffness of the flexible scope is designed as a compromise between being stiff enough to enable pushing the endoscope forward and being compliant enough to adapt to the curves of the complex path. This renders the scope too compliant to fully prevent it from undesired bending and buckling and too stiff to prevent it from pushing against and deforming the track. Therefore, precise operation of the endoscope is difficult, especially following complex trajectories such as that of the intestine. Furthermore, patients suffer pain during a procedure with an endoscope. For instance, if a conventional endoscope is being inserted into the colon [Fig. 1(a)] by simply pushing it forward and steering the tip (the only steerable part), the shaft pushes against the colonic wall until the colon and its surroundings provides sufficient counter pressure to force the shaft to bend [Fig. 1(b)]. In practice, this means that the colon is often stretched substantially. This frequently leads to formation of loops in the flexible endoscope shaft and colon, which can hinder further advancement of the tip [Fig. 1(c)] and can cause considerable patient discomfort.

Methods like computed tomography [2], magnetic resonance imaging, fecal occult blood testing [3], capsule endoscopy [4] and combination have been proposed as alternatives to screening and diagnostic procedures. However, these alternatives do not entirely replace conventional endoscopy as they lack the therapeutic means that a conventional scope provides. If abnormalities are diagnosed, conventional scopes are still required for biopsies or to treat abnormalities [1].

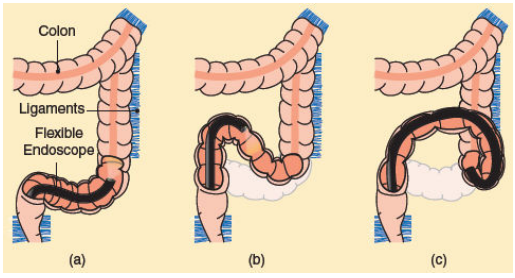


Figure 1. (a) Flexible endoscope following the curves of colon (b) The tip pushing against the colon and stretching it thus forcing the scope to bend (c) Typical loop shape (n-loop) that occurs during conventional colonoscopy

Some researchers reported on design of active endoscopes where the bending action was achieved by various smart materials like Shape memory alloy (SMA), ionic conductive polymer metal composites (IPMC) etc. Chang et al. [5] developed an

intravascular micro active catheter system for microsurgery in human vascular systems. The tube-like catheter had a pathway for the functional catheters, such as conventional guide wire, balloon catheter, etc. This active bending catheter was actuated by zigzag-type springs made of SMA. In 2005, Haga et al. [6] devised a long intestinal tube made of silicone, actuated by SMA micro-coil actuators. The scope was capable of bending two sides by wire actuation. The tube consisted of a bending tip and a 3-m long silicone rubber tube. The maximum bending angle possible was 110°. Ho et al. [7] developed an SMA-based miniature robot for neurosurgery. The robot consisted of nine revolute joints, actuated by 0.012 inch-diameter SMA wires. Two such wires were antagonistically used between the two connected segments of the robot, controlled independently. Revolute joints connected consecutive segments.

In 2007, Yoon et al. [8] initiated the development of a low-cost active tip bending system for a scanning fiber endoscope or catheterscope and conducted a proof-of-concept fabrication and testing. Actuator material chosen for the design was an IPMC type electro-active polymer. The generative force of the actuator was measured and demonstrated to be sufficient to lift the rigid tip of the scanning fiber endoscope.

In this work, effort has been made to bend each segment of the actuator and control their actuation independently. SMA wires were used as actuators, three between each segment. Consecutive segments were connected by a ball and socket joint that gives high maneuverability to the structure and also provide sufficient rigidity, to avoid buckling, when transmitting longitudinal compressive force for pushing.

*B. SMA as Actuator*

SMAs belong to special class of material called smart material that has an exceptional ability to memorize their shape at a low temperature, and recover large deformations on thermal activation. From macroscopic point of view the mechanical behavior of SMAs can be separated into two categories: the *shape-memory effect* (SME), where large residual (apparent plastic) strain can be fully recovered after raising the temperature through loading and unloading cycle; and *pseudoelasticity* or *superelasticity*, which fully recovers very large (apparently plastic) strain after loading and unloading at constant temperatures (above austenite finish) [9]. Both SME and pseudoelasticity are results of martensite-phase transformation as explained below.

In stress-free state, an SMA material at high temperatures exists in the parent phase (usually body centered cubic crystal structure), also known as austenite phase. Upon decreasing the material temperature, the crystal structure undergoes a self-accommodating crystal transformation into martensite phase (usually face-centered cubic structure). The phase change in the unstressed formation of martensite from austenite is referred to as 'self-accommodating' due to the formation of multiple martensitic variants and twins that prohibits the incurrence of transformation strain. The martensite variants are evenly distributed throughout the material and are all crystallographically equivalent, differing only by habit plane. The process of self-accommodation by twinning allows an SMA to exhibit large reversible strain with stress. However, the process of self-accommodation in ordinary materials like stainless steel takes place via a mechanism called slip as shown in Fig. 2. Since slip is a permanent or irreversible process, the SME cannot occur in these materials.

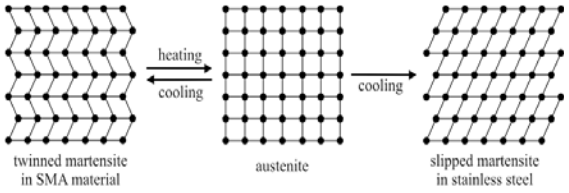


Figure 2. Phase transformations in SMA and steel.

The most common shape-memory material is an alloy of nickel and titanium in a ratio of 45% to 55%, respectively, called Nitinol (nickel titanium alloy developed for the first time at the U.S. Naval Ordnance Lab), which was discovered by Buehler and Wiley [10, 11]. This alloy has very good electrical and mechanical properties, long fatigue life, and high corrosion resistance. It also exhibits a much greater SME than any other materials. The recoverable strain up to a maximum of about 8% is achieved in this alloy. Another interesting feature is an over 200% increase in Young's modulus at a high-temperature phase as compared to low-temperature phase [7]. If the SMA encounters any external loads during the phase transformation, it can generate extremely large forces. This phenomenon provides a unique mechanism for actuation.

Figure 3 shows power density versus strain mapping of some conventional actuators and smart materials used as actuators [12].

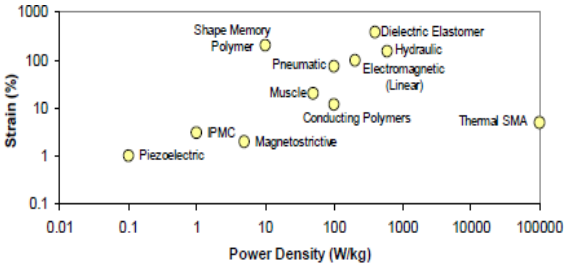


Figure 3. Power Density Vs Strain.

It is clearly visible that SMA actuators have an excellent 'power to mass ratio' making them ideal for

applications where power requirement is high but space is a constrain.

## II. PROTOTYPE DESIGN

A prototype was machined in Teflon to establish the concept. Teflon was selected as the material for the prototype as it was easy to machine, was lightweight, self-lubricating, cheap, and easily available. Fig. 4 shows one segment of SolidWorks (Dassault Systèmes) model for the prototype developed.

The ball and stem that connects two such Teflon segments was machined separately from aluminum block as Teflon with such narrow dimensions was difficult to machine and cannot take compressive loads. A hole was drilled at the bottom of the segment for inserting the stem where the ball was inserted in the top socket of the other similar block.

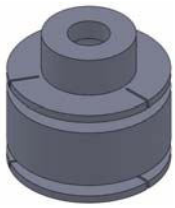

Figure 4. One segment of Solidworks model of the prototype.

Number of such segments (depends on application) was connected to one another with ball and socket joint as explained earlier. Ball and socket joint is a universal joint that gives high maneuverability to the structure and also provides sufficient rigidity, to avoid buckling, when transmitting longitudinal compressive force for pushing. Three SMA wires were attached between adjacent blocks at 120° angle from each other. The final prototype would have springs attached in parallel to the SMA wires that helps in restoring the straight position of the scope.

If the SMA encounters any resistance during its transformation from martensite phase to austenite phase, it can generate extremely large forces [13]. By using the SMA's increase in strength with temperature in a design, it can perform useful work. The attached wire, when heated, pulls the segment on top of it to produce a bending motion on that joint. The mechanical structure is made in a dimension that will arrest the bending of the upper segment at an angle of 30° with upright position. The SMA actuator works only in on-and-off mode and hence the joint switches between two discrete angles, that is, 0° and 30° as the SMA changes phase from martensite to austenite. The cumulative bending effect of all the segments renders the tip to reach discrete positions in 3D space and since each segment is independently actuated the scope can follow any complex trajectory and can negotiate tight bends. Fig. 5 shows a snapshot of 2D bending animation of the two segments when one wire is heated to temperature above austenite finish temperatures.

Figure 6 shows one segment of the actual prototype machined from Teflon rod.

The details of SMA actuation and scope modeling can be referred to in the previous published work by the authors [14].

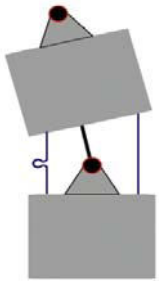

Figure 5. Snapshot of 2D bending animation when one wire is heated.

Figure 6. One segment of the protype.

## III. TRAVERSING ALGORITHM

The algorithm used for traversing the scope is very generic and addresses the issue of complications in maneuvering the scope through complex interior structures like that of an intestine and also a very important issue of navigating the scope out of human body.

The orientation of all the segments of the scope is classified into different states. Taking two segments into consideration, initial state A corresponds to no wire being triggered. Similarly state B corresponds to the triggering of wire 1 only, state C corresponds to the triggering of wire 2 only, state D corresponds to the triggering of wire 3 only, state E corresponds to the triggering of wire 1 and 2 simultaneously, state F corresponds to the triggering of wire 2 and 3 simultaneously and finally state G corresponds to the triggering of wire 1 and 3 simultaneously. Fig. 7 shows the same concept of changing states graphically by specific wire actuation.

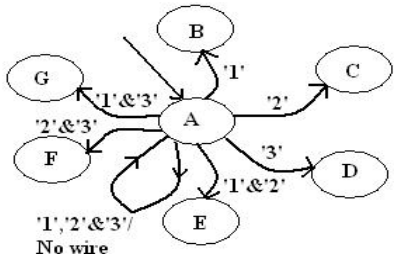


Figure 7. State diagram of the scope taking two segments into consideration

The algorithm works as; the practitioner guides the orientation of the first segment depending on the obstructions in the path (camera image) and the scope is pushed. The pushing and reorientation of the scope will take place simultaneously such that each segment takes the state of its preceding segment and the practitioner will orient the first segment.

The process will continue till the desired destination is reached. The orientation of the scope will be recorded and displayed graphically in 3D at each push.

This helps the practitioner to know the exact orientation of the scope in 3-D and solves a complicated issue of taking the scope out of the body without causing any damage to the track. Conventional endoscopes are pushed by orienting the tip of the scope but while taking out the scope is just pulled causing pain and discomfort to the patient. The scope developed will keep a track of all the bends and curves in the track and will orient itself along the track while pulling out thereby making the process easier both for patient and practitioner. Again while pulling out the pulling and reorientation of the scope will take place simultaneously such that the scope is always oriented as the curves in the track.

Fig. 8 shows how the scope changes its state as it is pushed inside the body. State 1 corresponds to 2-D orientation of the segment 1; state 2 corresponds to 2-D orientation of segments 1 and 2 such that segment 2 takes the orientation of 1 after one push and so on. At every state the software (explained in Results section) records the wire triggered by the practitioner for the first segment and displayed the orientation of the full scope in 3-D.

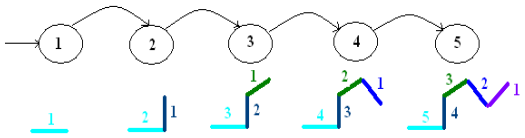


Figure 8. State diagram of the scope (while inserting the scope) taking orientation of all segments into consideration

Fig. 9 shows how the scope changes its state as it is pulled out form the body. The recorded orientation/states of the scope (while pushing) will now be used for guiding the scope out of the body. This way the doctor will have the track of orientation of all the segments of the scope at each instant.

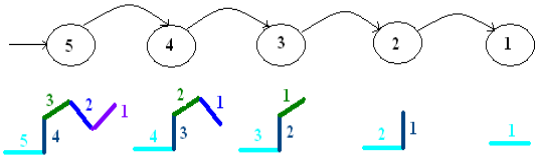


Figure 9. State diagram of the scope (while pulling out the scope) taking orientation of all segments into consideration

## IV. RESULTS

As discussed earlier a scaled up prototype was made with number of Teflon segments connected by ball and socket joint and actuated by three SMA actuators between the two consecutive blocks. Taking two segments into consideration the segments can be in any of the seven states, depending on the wires actuated. The number of discrete points reached by the tip of the scope is seven which increase geometrically with the increase in the number of segments; the number of states may be expressed as $7^{n-1}$, where $n$ is the number of segments including the base segment. The angle made by the top segment with *'z'* axis was calculated using an accelerometer and was found to be around 30° for the prototype and can vary depending on SMA actuation and application. The length of each segment in the prototype developed was 25mm; reduction of this length will give more flexibility to the scope.

Taking the angle made by each segment with *'z'* axis and length of each segment as variables and considering all segments to be identical, different software modules were written in MATLAB that simulates the discrete position reached by the tip of the scope with different number of segments.

Fig. 10 shows the discrete points reached by the tip of the scope and Fig. 11 shows the surface plot of those points in 3D space with six segments (including base), maximum bending angle of 15° with *'z'* axis and segment length of 25mm.

Another software module gives an option to simulate the orientation of the scope given the desired 3D position of the tip of the scope. The module finds all possible combinations of the number of segments to be used and orientations of each segments to reach the nearest discrete point in 3D space. The output shows the 3D orientation of the scope, number of segments required and the sequence of heating of each segment required reaching that specific point depending on the hurdles (space constraints), appropriate sequence of actuation may be chosen to reach in optimum time.

Fig.12 shows the output with desired position of the tip as $X$=5, $Y$=–8 and $Z$=115.

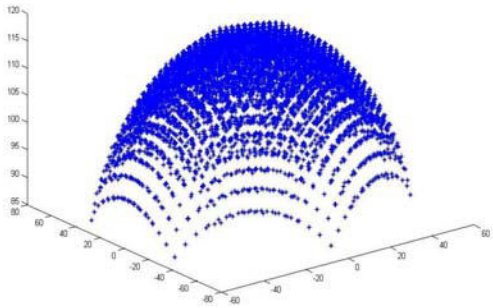

Figure 10. Discrete points reached by the tip of the scope with six segments.

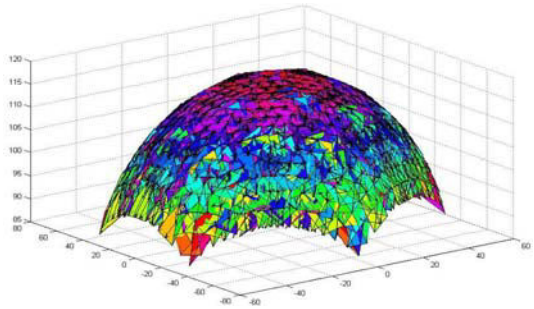

Figure 11: Surface plot of the discrete points with six segments.

The actual discrete point reached by tip would be $X$=4.8869, $Y$=–7.8265 and $Z$=115.2277 with six segments (including base) and heating sequence of wires 2 and 3 for the first segment, wires 2 and 3 for the second segment, wires 2 and 3 for the third segment, wires 1 and 3 for the fourth segment and wires 1 and 2 for the fifth segment as shown in Fig. 13.

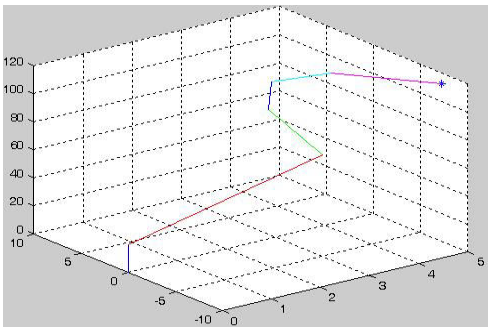

Figure 12. Orientation of the scope to reach $x$=5, $y$=–8 and $z$=115 as the position of tip of the scope.

```
Number of segments required are 6
nearest discrete position reached by tip is

ans =

    4.8869   -7.8265  115.2277
Sequence of wire heating is

seq =

     4     6     5     5     5
Distance between the required position and reached position is

min =

    0.3079
```

Figure 13. Matlab output as orientation of each segment to reach the desired position by the tip of the scope.

Another software module communicates to the microcontroller and gives an option to the user to use the scope with 3D points reached by tip or guide the scope-using algorithm discussed earlier.

The user gives the orientation of only the first segment of the scope by seeing the path in the camera image and the following segments takes the state of the preceding segment with some time delay (one push of segment). The module also stores and generates a 3D orientation of the scope after every push, making the job of practitioner easier and relieves patient of discomfort during procedure.

Fig. 14 shows the orientation of the scope with each push following the traversing algorithm as explained earlier. User enters the number of segments in the scope as six (including the base). Fig. 14(a) shows the orientation of scope with wire 1 being actuated for the top block. Fig. 14(b) shows the orientation of the scope with wire 2 being actuated for the top segment and wire 1 being actuated for the second segment from top (according to the algorithm).

Fig. 14(c) shows the orientation of the scope with wires 2 and 3 being actuated simultaneously for the top segment and wire 2 being actuated for the second segment from top and wire 1 being actuated for the third segment from top. Fig. 14 (d) shows the orientation of the scope with wires 1 and 3 being actuated simultaneously for the top segment, wires 2 and 3 being actuated simultaneously for the second segment from top, wire 2 being actuated for the third segment from top and wire 1 being actuated for the fourth segment from top. Fig. 14(e) shows the orientation of the scope with wire 1 being actuated for the top segment, wires 1 and 3 being actuated simultaneously for the second segment from top, wires 2 and 3 being actuated simultaneously for the third segment from top, wire 2 being actuated for the fourth segment from top and wire 1 being actuated for the fifth segment from top.

The user only needs to give orientation of the top block (according to obstacles as seen by the camera ahead of the tip) and the succeeding segments will follow the same set of state after some time duration required for one push operation of the scope.

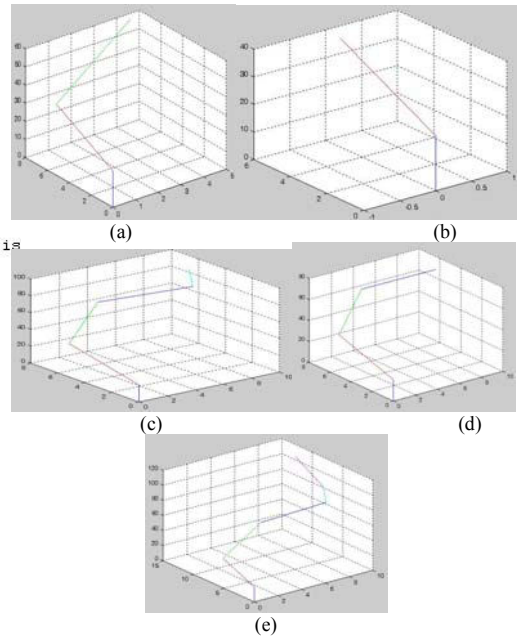

(a) (b) (c) (d) (e)

Figure 14. Orientation of the scope in 3d as it is pushed inside the body.

## V. CONCLUSION AND FUTURE WORK

A prototype of the scope capable of traversing areas of complex trajectories and negotiating tight bends was designed and developed in Teflon. The spherical joints used in between the segments gave high degree of maneuverability and rigidity (while pushing) to the scope. SMA wires were used for actuating each segment independently. Cumulative bending of all the segments renders the tip of the scope to reach huge set of discrete points in 3D space. Through holes were made in the structure for running control wires. The final scope would be kept inside a biocompatible silicone sheath to avoid any tissue contact and can be replaced after use. The algorithm developed for maneuvering the scope inside the body is very generic and can be used for any of such segmented structures (scope) having higher or lesser degrees of freedom. It also addresses a very important and complicated issue of traversing the scope out of human body without damaging the track and causing discomfort to the patient. The entire scope would be encapsulated inside a biocompatible silicon stealth, which can be replaced after every use.

MATLAB interface with the micro-controller makes the job of the practitioner a little easier. The practitioner can simultaneously actuate a particular segment and visualize the 3D orientation of the full scope. The software also remembers the orientation of the full scope at each instant, which helps the practitioner in further traversing, and retreating of the scope if required. Cooling SMA actuators in confined environments is an issue but since for medical devices like endoscope flexibility and accuracy is more important than speed, this issue is not taken into account in this work.

Future work should include calibrating the input current to the SMA actuation force that gives a better control and increases the workspace to a finer set of discrete points. Further analysis of hysteresis of the SMA-based actuation as well as heat loss calculations will help to improve the control bandwidth. Future work should also include the miniaturization of the presented structure with material other than Teflon to make finer endoscope.

## ACKNOWLEDGMENT

The authors thank Dean, School of Mechatronics, Shri S.N.Shome and Director, Central Mechanical Engineering Research Institute (CMERI), Durgapur, West Bengal, India for his support.

## REFERENCES

[1] A. Loeve, P.Breedveld, J.Dankelman, "Scopes Too Flexible...and Too Stiff", Pulse, IEEE, Vol. 1 Issue. 3, pp. 26 –41, Nov-Dec2010.

[2] G. Roseau, and J. A. Paolaggi, "Role of computed tomography, endoscopy and echoendoscopy in the management of alimentary tract lipomas", *An international journal of Gastroenterology and Hepatology,* volume 31 pp. 550.

[3] L. Paszat, L. Rabeneck, L. Kiefer, V. Mai, P. Ritvo, T. Sullivan, "Endoscopic follow-up of positive fecal occult blood testing in the Ontario FOBT Project", *The Canadian journal of Gastroenterology,* v.21(6); Jun 2007.

[4] "Sayaka, The next generation capsule endoscope" *http://www.rfamerica.com/sayaka/*.

[5] J.K Chang, et al. , "Intravascular micro active catheter for minimal invasive surgery" *1St Annual International IEEE-EMBS Special Topic Conference on Micro technologies in Medicine & Biology*, October 12-14,2000, Lyon, France.

[6] Y. Hagal , et al. , "Active Bending Ileus Tube Using Shape Memory Alloy for Treatment of Intestinal Obstruction", *Proceedings of the 3rd Annual International IEEE EMBS Special Topic Conference on Microtechnologies in Medicine and Biology*, Kahuku, Oahu, Hawaii, 12 -15 May 2005.

[7] Mingyen Ho, Jaydev P. Desai, "Characterization of SMA Actuator for Applications in Robotic Neurosurgery", *31st Annual International Conference of the IEEE EMBS Minneapolis*, Minnesota, USA, September 2-6, 2009.

[8] W. Jong Yoon, P. Reinhall, E. Seibel, "Analysis of electro-active polymer bending: A component in a low cost ultrathin scanning endoscope*", Sensors and Actuators A: Physical,*Volume 133, Issue 2, 12 February 2007, Pages 506-517.

[9] M. Brojan, D. Bombač, F. Kosel, T. Videnič, "Shape memory alloys in medicine", *RMZ – Materials and Geoenvironment*, Vol. 55, No. 2, pp. 173-189, 2008.

[10] J. Gilfrich, W. J. Buehler, R. Wiley, "Effect of low temperature phase changes on the mechanical properties of alloys near composition NiTi", *Journal of Applied Physics*, vol. 34, pp. 1475–1477, May 1963.

[11] W.J. Buehler, R.C. Wiley, F.E. Wang, "Nickel-based alloys", U.S. Patent 317485123, 1965.

[12] J. Madden, et al. "Data Table" based on "Artificial Muscle Technology: Physical Principles and Naval Prospects" in *IEEE J. of Oceanic Eng.*, Vol. 29, No. 3, p. 706, 2004

[13] William R.Fry, "Low-profile ,Shape memory alloy surgical occluder", US Patent No. 6746461B2,2004.

[14] A. Arora, P. Bhattacharjee, "Shape Memory Alloy Actuated Arm for Traversing ComplexTrajectories", *IEEE 2011 3rd International Conference on Electronics Computer Technology – ICECT, 2011*.

# MULTIPLIER BASED RECONFIGURABLE DESIGN OF PULSE SHAPING FILTER USING MAC ALGORITHM

**RAJESH MEHRA**

Associate Professor Department of Electronics & Communication Engineering,
National Institute of Technical Teachers' Training & Research Chandigarh, India-160019

**Abstract -**Pulse shaping for time as well as frequency selective channels is the need of hour for 3G and 4G wireless communication systems. The pulse shaping filter is a useful means to shape the signal spectrum and avoid Interferences. In this paper an FPGA implementation of RRC filter has been presented. The hardware implementation of RRC Filter has been performed using Direct form and a comparison in terms of hardware requirements and speed performance is made. The proposed design has been developed using MATLAB and simulated with Xilinx DSP Tools, synthesized with Xilinx synthesis Tool (XST) and implemented on Virtex2 Pro based FPGA device. The results show that developed RRC filter can work at a maximum frequency of 78.9 MHz by utilizing 13 multipliers and 577 LUT's of target FPGA device for direct form.

***Keywords****: FPGA, HDTV, ISI, MATLAB, RRC*

## 1. INTRODUCTION

Data communication using pulse shaping techniques has a critical role in a communication system. In wireless communication, pulse shaping is essential for making the signal fit in its frequency band. The analysis and simulation of transmit and receive pulse shaping filter is an important aspect of digital wireless communication since it has a direct effect on error probabilities. Pulse shaping is the process of changing the waveform of transmitted pulses to make the transmitted signal better suited to the communication channel by limiting the effective bandwidth of the transmission. By filtering the transmitted pulses this way, the intersymbol interference caused by the channel can be kept in control.

In a communication system, when the data is being transmitted in the form of pulses (i.e bits), the output produced at the receiver due to other bits or symbols interferes with the output produced by the desired bit. This is known as Inter symbol Interference (ISI).The Inter symbol Interference introduces errors in the detected signal. It is a form of distortion of a signal in which one symbol interferes with subsequent symbols. ISI is usually caused by multipath propagation or the inherent non-linear frequency response of a channel causing successive symbols to "blur" together.

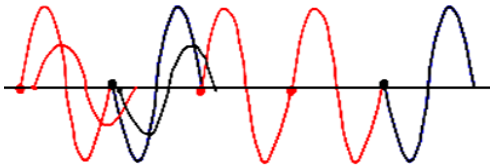

**Fig. 1 Inter symbol Interference**

Transmitting a signal at high modulation rate through a band-limited channel can create intersymbol interference. As the modulation rate increases, the signal's bandwidth increases. When the signal's bandwidth becomes larger than the channel bandwidth then signal occurs. This distortion is usually seen as inter symbol interference. The Inter symbol Interference ISI arises due to the imperfections in the overall frequency response of the system. When a short pulse of duration $T_b$ seconds is transmitted through a band limited system, then the frequency components contained in the input pulse are differentially attenuated and more importantly differentially delayed by the system. Due to this, the pulse appearing at the output of the system will be dispersed over an interval which is longer than $T_b$ seconds. Due to this dispersion, the symbols each of duration $T_b$ will interfere with each other when transmitted over the communication channel. This will result in the Inter symbol Interference (ISI).

In communications, the Nyquist ISI criterion describes the conditions which, when satisfied by

a communication channel, result in no intersymbol interference or ISI. It provides a method for constructing band-limited functions to overcome the effects of Intersymbol Interference. When consecutive symbols are transmitted over a channel by a linear modulation such as ASK and QAM, the impulse response of the channel causes a transmitted symbol to be spread in the time domain. This causes intersymbol interference because the previously transmitted symbols affect the currently received symbol, thus reducing tolerance for noise. In band limited channels, intersymbol interference (ISI) can be caused by multi-path fading as signals are transmitted over long distances and through various mediums. More specifically, this characteristic of the physical environment causes some symbols to be spread beyond their given time interval. As a result, they can interfere with the following or preceding transmitted symbols. One solution to this problem is the application of the pulse shaping filter.

## 2. PULSE SHAPING FILTERS

In communications systems, two important requirements of a wireless communications channel demand the use of a pulse shaping filter. These requirements are:

a) Generating band limited channels, and
b) Reducing Inter Symbol Interference (ISI) arising from multi-path signal reflections.

Both requirements can be accomplished by a pulse shaping filter which is applied to each symbol. Pulse shaping filters are used at the heart of many modern data transmission systems like mobile phones and HDTV to keep a signal in an allotted bandwidth, maximize its data transmission rate and minimize transmission errors. Pulse shaping filter are often used in communication transmitters for baseband processing in order to improve the transmission efficiency of a signal spectrum. The pulse shaping filters are widely used in Mobile Phones, HDTV, Space communication, Radar, Audio/data/CD/video system, Speech synthesis recognition, A/D and D/A conversion. The ideal pulse shaping filter has two properties. Firstly it should exhibit high stop band attenuation and secondly it should exhibit minimum inter symbol interferences (ISI) to achieve a bit error rate as low as possible. The pulses are sent by the transmitter and ultimately detected by the receiver in any data transmission system. At the receiver, the goal is to sample the received signal at an optimal point in the pulse interval to maximize the probability of an accurate binary decision [1]. Sender side pulse shaping is often combined with a receiver side matched filter to achieve optimum tolerance for noise in the system. In its simplest system configuration, a pulse shaping interpolator at the transmitter is associated with a simple down sampler at the receiver.

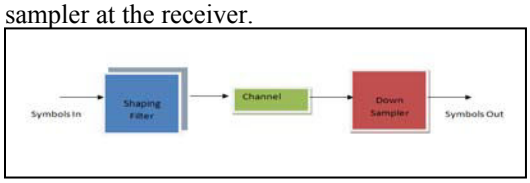


**Fig. 2 System Configuration**

Data transmission systems that must operate in a bandwidth-limited environment must contend with the fact that constraining the bandwidth of the transmitted signal necessarily increases the likelihood of a decoding error at the receiver. Bandwidth limited systems often employ pulse-shaping techniques that allow for bandwidth containment while minimizing the likelihood of errors at the receiver. Before digital filters were available, pulse shaping was accomplished with analog filters. Unfortunately, the response of an analog filter is affected by variations in component values due to specified tolerance ranges, temperature, and ageing. The response of a digital filter, by contrast, is solely dependent on the filter coefficients, which are invariant to both temperature and ageing. Therefore, digital pulse-shaping filters have become an integral part of many digital data transmission systems.

The fundamental shapes of the pulses be such that they do not interfere with one another at the optimal sampling point. The pulse shape exhibits a zero crossing at the sampling point of all pulse intervals except its own. Otherwise, the residual effect of other pulses will introduce errors into the decision making process. The shape of the pulses be such that the amplitude decays rapidly outside of the pulse interval. This is important because any real system will contain timing jitter, which means that the actual sampling point of the receiver will not always be optimal for each and every pulse. So, even if the pulse shape provides a zero crossing at the optimal sampling point of other pulse intervals, timing jitter in the receiver could cause the sampling instant to move, thereby missing the zero crossing point. This, too,

introduce error into the decision making process. Thus, the quicker a pulse decays outside of its pulse interval, the less likely it is to allow timing jitter to introduce errors when sampling adjacent pulses. In addition to the non interference criteria, there is the ever present need to limit the pulse bandwidth. A rectangular pulse is probably the most fundamental. It is easy to implement in a real-world system because it can be directly compared to opening and closing a switch, which is synonymous with the concept of binary information [1, 2]. The rectangular pulse is zero at all points outside of the present pulse interval. It clearly cannot cause interference during the sampling time of other pulses. The trouble with the rectangular pulse, however, is that it has significant energy over a fairly large bandwidth. In fact, because the spectrum of the pulse is given by the familiar sinc response, its bandwidth actually extends to infinity.

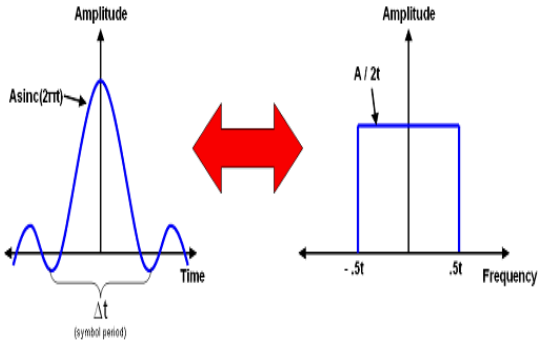


**Fig. 3 Sinc Pulse Time & Frequency Response**

The sinc pulse is periodic in nature and is has maximum amplitude in the middle of the symbol time. In addition, it appears as a square wave in the frequency domain and thus can effectively limit a communications channel to a specific frequency range. The unbounded frequency response of the rectangular pulse renders it unsuitable for modern transmission systems. This is where pulse shaping filters come into play. If the rectangular pulse is not the best choice for band-limited data transmission, then what pulse shape will limit bandwidth, decay quickly, and provide zero crossings at the pulse sampling times. The raised cosine pulse is used to solve this problem in a wide variety of modern data transmission systems.

## 3. ROOT RAISED COSINE FILTER

The RRC filters are required to avoid inter-symbol interference and constrain the amount of bandwidth required for transmission. Root Raised Cosine (RRC) is a favorable filter to do pulse shaping as its transition band is shaped like a cosine curve and the response meets the Nyquist Criteria. The first Nyquist criterion states that in order to achieve an ISI-free transmission, the impulse response of the shaping filter should have zero crossings at multiples of the symbol period. A time-domain sinc pulse meets these requirements since its frequency response is a brick wall but this filter is not realizable. It can be approximated by sampling the impulse response of the ideal continuous filter. The sampling rate must be atleast twice the symbol rate of the message to transmit. That is, the filter must interpolate the data by atleast a factor of two and often more to simplify the analog circuitry. The FIR structure with linear phase technique [3, 4] is efficient as it takes advantage of symmetrical coefficients and uses half the required multiplications and additions.

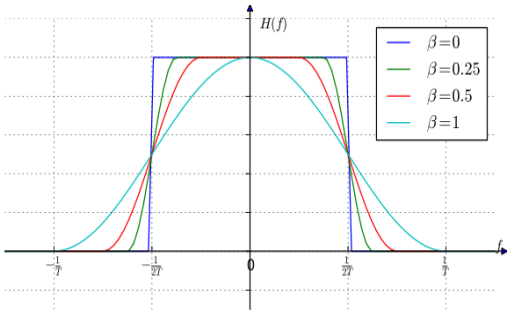


**Fig. 4 RRC Filter Response**

Raised-cosine filter is practical to implement and it is in wide use. It has a parametrisable excess bandwidth, so communication systems can choose a trade-off between a more complex filter and spectral efficiency. The raised-cosine filter is a filter frequently used for pulse-shaping in digital modulation due to its ability to minimize intersymbol interference (ISI). Its name stems from the fact that the non-zero portion of the frequency spectrum of its simplest form ($\beta = 1$) is a cosine function, 'raised' up to sit above the *f* (horizontal) axis.

The raised cosine filter is one of the most common pulse-shaping filters in communications systems. In addition, it is used to minimize intersymbol interference (ISI) by attenuating the starting and ending portions of the symbol period. Because these portions are most susceptible to creating interference from multi-path distortion, the shaping characteristics of the raised cosine filter helps reduce ISI [5]. This impulse response

for this filter is given by the equation shown below. It shows that the sinc pulse is implemented in the creation of this filter. The filter roll off parameter, alpha (α), can range between values of 0 and 1.

$$h_{RC}(n) = \frac{\pi}{4}\sin c(\frac{\pi n}{R}).[\sin c(\frac{\pi}{2} - \alpha\frac{\pi n}{R}) + \frac{\sin(\frac{\pi}{2} - \alpha\frac{\pi n}{R})}{(\frac{\pi}{2} - \alpha\frac{\pi n}{R})}] \quad (1)$$

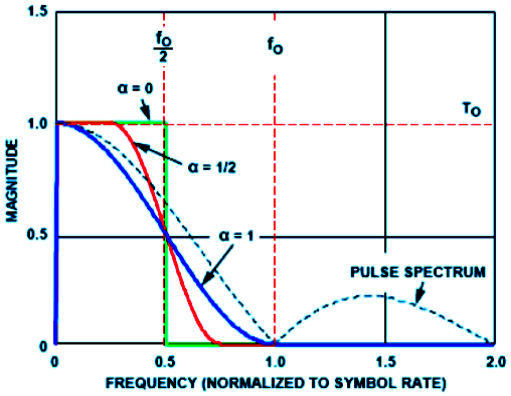


**Fig. 5 Raised Cosine Spectrum**

## 4. PROPOSED DESIGN SIMULATION

A raised cosine filter is typically used to shape and oversample a symbol stream before modulation/transmission. The roll off factor, (α), determines the width of the transition band. Practical digital communication systems use a roll off factor between 0.1 and 0.5. A minimum stop band attenuation of 60 to 80 dB is also desirable to suppress Inter channel Interference. In this paper a 25 tap RRC filter has been designed using roll off factor of 0.5 using MATLAB [6, 7] and simulated using Xilinx DSP Tool. First of all m-code for proposed RRC filter has been developed with required specifications using Matlab. The floating point output has been simulated which is then verified and analyzed. The next step is floating point to fixed point conversion and its output verification as shown in Fig.6. The purple plot shows the input to the filter and sky blue plot is the output from RRC filter.

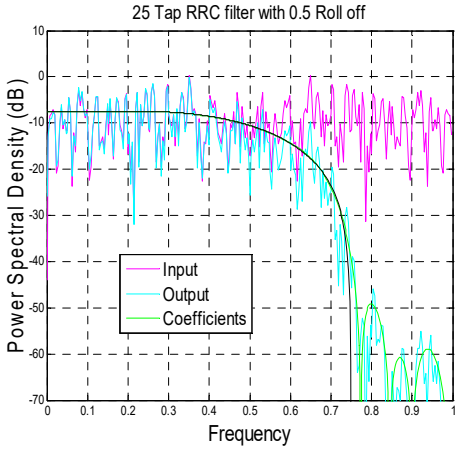


**Fig. 6 Fixed Point RRC Filter Responses**

The corresponding normalised error fixed point response after scaling and delay has been shown in Fig.7.

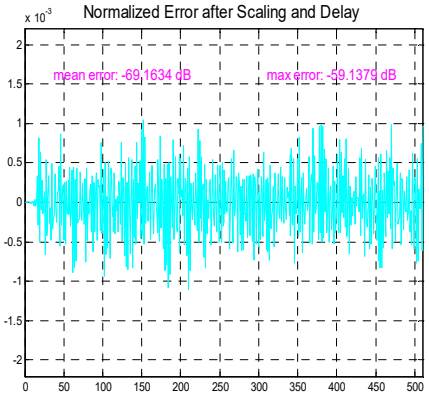


**Fig. 7 Fixed Point Normalized Error Response**

## 5. HARDWARE SYNTHESIS

The RRC filter has been developed by efficiently utilizing the LUTs and slices of target FPGA. The optimal number of embedded multipliers has been used to design the proposed RRC and implemented using MAC algorithm based transposed structure. The MAC based pulse shaping filter has been synthesized and implemented on Virtex II Pro based XC2vp30 device. The Virtex-II Pro FPGA slices contain a dedicated two-input multiplexer and a two-input OR gate to perform AND-OR gates operations. These combine the four-input LUT outputs. These gates have been cascaded in a chain to provide the wide AND functionality across slices. The output from the cascaded AND gates has been combined

with the dedicated OR gates to produce the Sum of Products (SOP).

The resource utilization and speed performance results have been shown in Table 1 and Table 2 respectively for direct form. The developed RRC can operate at a maximum operating frequency of 78.9 MHz with a minimum period of 12.6690 ns. The RRC design has consumed 480 slices, 671 slice flip flops and 577 LUTs and 13 multipliers available on target device for direct form implementation.

**Table 1. Direct Form Resource Utilization**

| Device Logic | Used | Available |
|---|---|---|
| **Slices** | **480** | **13696** |
| **Flip Flops** | **671** | **27392** |
| **LUTs** | **577** | **27392** |
| **Multipliers** | **13** | **136** |

**Table 2. Direct Form Speed Performance**

| Clock Name | Requested Frequency | Estimated Frequency | Estimated Period |
|---|---|---|---|
| Clock | 100.0 MHz | 78.9 MHz | 12.6690 ns |

The resource consumption and speed performance results of Optimized RRC design are compared with RRC design [1] as shown in Table 3.

**Table 3. Resource & Performance Comparison**

| Description | RRC Design [1] | Proposed Design |
|---|---|---|
| **Slices** | **450** | **480** |
| **Flip Flops** | **893** | **671** |
| **LUTs** | **544** | **577** |
| **Multipliers** | **-** | **13** |
| **DSP 48 E** | **13** | **-** |
| **Max. Frequency (MHz)** | **69.08** | **78.9** |

The proposed direct form and transposed RRC design can work at an estimated frequency of 78.9 as compared to 69.08 MHz in case of RRC design [1] by consuming almost same resources in terms of slices and embedded multipliers.

## 6. CONCLUSION

In this paper, a 25 Tap RRC Pulse Shaping filter has been presented with 0.5 roll off factor and error is normalized after scaling and delay. The developed filter has been implemented using MAC algorithm based transposed structure. The embedded multipliers and Look up Tables of target device have been optimally utilized to optimize area and speed simultaneously. The results have shown that proposed MAC based design can operate at an estimated frequency of 78.9 MHz by consuming 480 slices, 671 flip flops, 577 LUTs and 13 multipliers. The developed design has shown an improvement of 14% in speed by consuming almost same resources to provide cost effective solution of wireless communication systems.

## REFERENCES

[1] Rajesh Mehra, Dr. Swapna Devi, “FPGA Implementation of High Speed Pulse Shaping Filter for SDR Applications”, International Conference on Networks & Communications, CCIS 90, pp. 214–222, Springer-Verlag Berlin Heidelberg , 2010.

[2] Rajesh Mehra, Dr. Swapna Devi, “Area Efficient & Cost Effective Pulse Shaping Filter for Software Radios”, International Journal of Ad hoc, Sensor & Ubiquitous Computing (IJASUC), Vol.1, no.3, pp.85-91, 2010.

[3] Mohamed Almahdi Eshtawie , “FPGA Implementation of an Optimized Coefficients Pulse Shaping FIR Filters”, International Conference on Semiconductor Electronics (ICSE), pp. 454-458, Kuala Lumpur, Malaysia, IEEE, 2006.

[4] Rajesh Mehra, Swati Singh, “Design Of RRC Filter For ISI Removal In Software Defined Radios”, International Journal of VLSI and Signal Processing Applications, (IJVSPA) ,Vol.1, no.1, pp. 1-5, 2011.

[5] Rajesh Mehra, Swati Singh, “FPGA Based Gaussian Pulse Shaping Filter For Error Removal”, International Journal of Research and Innovation in Computer Engineering,(IJRICE) Vol.1, no.1, pp. 23-28, 2011.

[6] Kyung-Saeng Kim and Kwyro Lee, "Low-power and area efficient FIR filter implementation suitable for multiple taps", IEEE Transaction on Very Large Scale Integration, Vol. 11, no. 1, pp.150-153, 2003.

[7] Mathworks, “Users Guide Filter Design Toolbox 4”, 2007.

**ACKNOWLEDGEMENTS**

The author would like to thank Director and Head of Electronics and Communication Engineering Department, National Institute of Technical Teachers' Training & Research, Chandigarh, India and for their constant inspirations, support and helpful suggestions throughout this research work**.**

**AUTHORS PROFILE**

**Rajesh Mehra** received the Bachelors of Technology degree in Electronics and Communication Engineering from National Institute of Technology, Jalandhar, India in 1994, and the Masters of Engineering degree in Electronics and Communication Engineering from National Institute of Technical Teachers' Training & Research, Panjab Univsrsity, Chandigarh, India in 2008. He is pursuing Doctor of Philosophy degree in Electronics and Communication Engineering from National Institute of Technical Teachers' Training & Research, Panjab Univsrsity, Chandigarh, India.

He is an Associate Professor with the Department of Electronics & Communication Engineering, National Institute of Technical Teachers' Training & Research, Ministry of Human Resource Development, Chandigarh U.T. India. His current research and teaching interests are in Signal Processing, Very Large Scale Integration Design. He has more than 75 Journal and Conference publications.

Mr. Mehra is life member of ISTE.

# KINECT QUALITY ENHANCEMENT FOR TRIANGULAR MESH RECONSTRUCTION WITH A MEDICAL IMAGE APPLICATION

**AMORNRAT KHONGMA[1], RUCHANURUCKS[2], TEERA PHATRAPORNNANT[3], YASUHARU KOIKE[4], MITI PANJAWEE RAKPRAYOON[5]**

[1]TAIST Tokyo Tech, ICTES Program, Electrical Engineering, Kasetsart University, Bangkok, Thailand. National Electronics and Computer, Technology Center (NECTEC), Bangkok,
[3]Thailand.Kasetsart Signal and Image Processing Laboratory, Electrical Engineering, Kasetsart University, Bangkok,
[5]Thailand. Tokyo Institute of Technology,Yokohama, Japan.

**Abstract**— This paper presents a method to estimate proportion between skin burn area and body surface using computer vision techniques. The data are derived using Microsoft Kinect. We first show a comprehensive Kinect calibration method. Then the color image is segmented into 3 sections, background, burn area, and body area. The segmentation method developed is based on watershed algorithm and Chebyshev's inequality. The segmented color image is to be mapped with the depth image to generate triangular mesh. We discover that reconstructing the 3D mesh, using marching cube algorithm, directly from Kinect depth information is erroneous. Hence, we propose to filter the depth image first. After the enhanced mesh is derived, the proportion between 3D meshes of burn area and 3D meshes of body surface can be found using Heron's formula. Finally, our paradigm is tested on real burn patients.

***Keywords****-component; Microsoft Kinect; Burn Patient; Triangular mesh reconstruction;*

## I. INTRODUCTION

Currently, the technology of burn therapy is indispensible. "For patients with burns over 50% of the total body surface area, death rate is 52%", this statistic of burn patients is from Nopparat Rajathanee Hospital in Thailand [2].

The death rate will decrease, if a patient gets the correct treatment in primary period. One crucial treatment procedure is giving a correct does of water to the patient. The dose value can be computed by equation (1) :

$$Doses = (4cc)(\%Burn)(Body\ Weight) \quad (1)$$

As can be observed, to estimate the dose of water, physician must know the proportion between burn area and body surface. Nowadays, to measure the proportion, physician use an eye estimation with a body chart called ***rule of nine*** to determine the percentage of burn area for each major section of body [3]. However, the approximation of burn area is not accurate.

This research proposes a computer vision method to estimate such proportion between burn area and body surface. Our system composes of Kinect, computer, software application and user interface. First, a comprehensive Kinect calibration method is presented [4][10]. It consists of calibration between RGB and depth camera. Calibration parameters are then used to map depth information to color image [11]. The benefit of having color image is we can segment the scene into 3 categories, background, burn area, and body area based on edge and color information. More detail about the segmentation can be found from [9], in which the used of watershed algorithm and Chebyshev's inequality is shown.

After we map the depth information to color image, of only the burn area and the body surface, next step is triangular mesh reconstruction. The reconstruction algorithm used in this work is marching cube [13]. In doing experiment, we found that the triangular mesh contains more than one layer, despite the fact that the original surface has only one layer. This is because the depth information from Kinect has low accuracy as mentioned in [6]. We then propose to apply average filter to the depth information before the reconstruction [1]. The filtered depth image then results in one layer of triangular mesh correctly. Using Heron's formula [14], accuracy of triangular mesh is also compared to ground truth.

Finally, the proportion between burn area and body surface can be found by accumulating the size of triangular meshes of both area using Heron's formula.

This paper is organized as follow. Section 2 explains a comprehensive Kinect calibration method. Section 3 describes the tri-state segmentation. Section 4 shows the data normalization using average filter and the marching cube algorithm as well as Heron's formula. Section5 shows experimental result. Conclusion is in section 6.

## II. A COMPREHENSIVE KINECT CALIBRATION METHOD

With an active scanning technique, an inexpensive Kinect is used in order to acquire RGB and depth information (Figure 1a-b). Alignment and mapping between RGB and depth image is applied to calculate the burn surface area of patient. Prior to that, we must calibrate the equipment. The calibration consists of calibration of RGB camera (intrinsic parameters), calibration of depth camera (raw depth to real depth

conversion, intrinsic parameters), and calibration between RGB and depth camera (extrinsic parameters).

### A. Characteristics of Microsoft Kinect

Kinect is a alternative gaming device. It consists of RGB camera, 3D depth sensor: depth camera and IR projector, multi-array microphone, motorized tilt [12]. The RGB video stream uses 8-bit VGA resolution with a Bayer color filter, while the monochrome depth sensing video stream is in VGA resolution with 11-bit depth, which provides 2,048 levels of sensitivity [5]. The depth measurement process is based on triangulation [6], [15].

Technically, the depth sensor uses a static Laser pattern projector and a CMOS camera to triangulate a dense depth map. Illumination intensity, baseline, depth of field and speed are tuned to cover a depth range that depends on several open source. The sensor can be use in typical indoor environments for the purpose of segmenting and 3D motion recognition [8].

### B. Calibration of RGB/Depth Camera(sensor)

For considering the interested depth data, mapping between RGB and depth images must use intrinsic and extrinsic parameters of the two cameras. To calibrate depth and RGB cameras, a chessboard is a known object, is captured into depth and color images simultaneously. Then, coners of the chessboard in the depth and color images are detected to estimate the intrinsic and extrinsic parameters using a stereo cameras calibration with OpenCV functions.

Since, Kinect's depth camera returns the raw depth data. For acquiring real depth data, depth calibration is applied using line regression technique. Then, raw depth data must be transformed into the depth data (in centimeter) using equation (3) and (4):

$$Depth = \frac{1.0}{f(d)} \quad (2)$$

$$f(d) = -0.00307110156374373d + 3.33094951605675 \quad (3)$$

Where;

$d$ is the depth data which measure from depth sensor. $f(d)$ is a linear function which can be estimated from regression techniques [6].

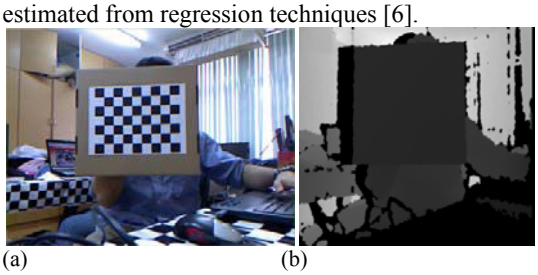

(a) (b)

Figure 1. the output of Kinect consists of RGB image (Left hand side) and depth image (Right hand side). a) Chessboard corners on color image are detected to find the intrinsic parameter. b) Red corners of the chessboard contain positions in depth image which are used to calibrate the depth sensor.

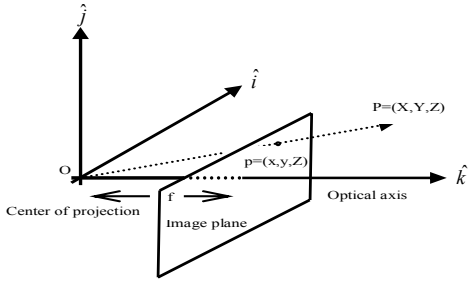


Using the intrinsic parameters of depth camera, the 3D point (XYZ) can be approximated from the depth image (xyZ) in equation (5) and (6).

$$X = \frac{Z(x - c_x)}{f_x} \quad (4)$$

$$Y = \frac{Z(y - c_y)}{f_y} \quad (5)$$

$$Z = depth \quad (6)$$

Where;

$x$ , $y$ are pixel of depth image.

$Z$ is a distance between object and Kinect.

$f_x, f_y, c_x, c_y$ are the elements of intrinsic parameter[M] of depth camera.

### C. Mapping between RGB and Depth Image

Using the extrinsic parameters [R|T], the equation (7) is used to project each 3D point (XYZ) in depth camera coordinate onto the RGB camera coordinate:

$$P3D' = R * P3D + T \quad (7)$$

$P3D$ is a matrix consists of $X, Y, Z$ in depth camera coordinate. The rotation and translation matrices are transferred in RGB camera coordinate ($P3D'$).

After that, the intrinsic parameters of RGB camera are processed with 3D point on the color image. We can then map the 3D depth images onto 2D color images using equation (8) and (9):

$$P2D.x = \left(\frac{P3D'.x * f_x}{P3D'.z}\right) + c_x \quad (8)$$

$$P2D.y = \left(\frac{P3D'.y * f_y}{P3D'.z}\right) + c_y \quad (9)$$

Where, $f_x, f_y, c_x, c_y$ are the elements of intrinsic parameter [M] of RGB camera. The $P2D$ is a position of 2D color image as shown Figure3a. Do not confuse the mapped image with the RGB image. The mapped image consists of RGB plus depth information, shown in 2D coordinate. In other words, we can also show the mapped image in 3D coordinate as well, as shown in Figure3b, using OpenGL.

## III. 3-STATE SEGMENTATION

To achieve our goal of burn area proportion estimation, we must divide the depth information into 3 areas, namely, the burn area, the body area and the background area. Luckily we already mapped the RGB image and depth image. Hence, the segmentation can be done based on color and edge

information in RGB image. Then the result can be reflected onto the same area in the depth image.

The segmentation program is based on a locally segmentation method called watershed algorithm and a statistical threshold called Chebyshev's inequality. The detail of algorithm can be found from [9]

In our implementation, to generate 3 areas, there are 2 steps. First, segment between the skin and the background (Figure 2b). Second, further segment the skin into normal skin and the burn areas (Figure 2c). Now we are ready to prepare image for reconstruction (Figure 2d/Figure 3a).

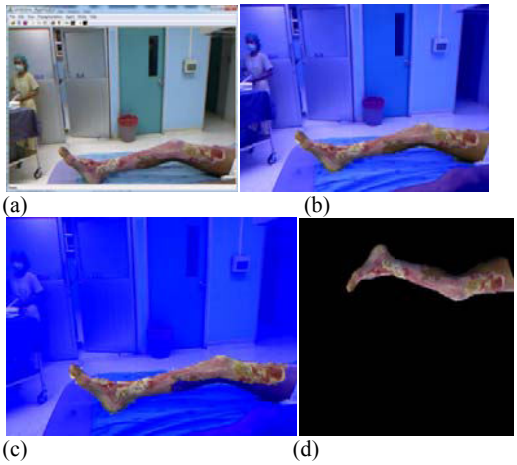

(a) (b) (c) (d)

Figure 2. shows the samples collected using segmentation program. (a) The original sample image. (b) The threshold image of skin area and background. (c) The threshold image of burn and skin area. (d) The skin area image is prepared to implementation.

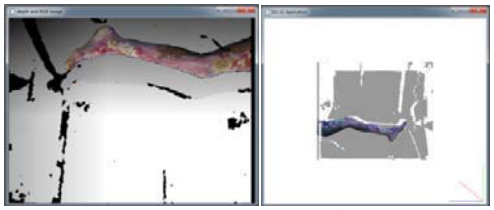

(a) (b)

Figure 3. (a) The depth coordinate (XYZ) is mapped to get position onto color image in 2D. (b) A combination of RGB image and depth coordinate is displayed on OpenGL scene.

## IV. TRIANGULARMESH ECONSTRUCTION

Next step is the triangular mesh reconstruction using a well known algorithm called marching cube. From experiment, if we use point cloud from Kinect directly for the mesh reconstruction, the resulting mesh contains a lot of error. Marching cube may generate two or more layers of mesh even the original data is one layer. The reason is Kinect's point cloud is quite unorganized [1]. Hence, we propose to smooth the point cloud from Kinect first using average filter. Then, we calculate the surface area of the mesh using Heron's formula.

### *A. Average Filter*

Average filter normalizes noisy surface into an enhanced one.

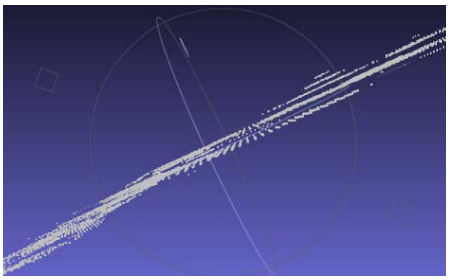

Figure 4. A sample point cloud of the planar object that is shown in top view.

Figure 4 shows a point cloud of a planar surface. One may notice that it is not in the same plane, even it should be so. This is due to the fact that Kinect's resolution is coarse. So we normalize it using the average filter only for depth information (Z axis) of 3D-world coordinate.

$$\bar{Z} = \frac{1}{n}\sum_{i=1}^{n} Z_i \qquad (10)$$

Where, $z_i$ is a raw depth data of each point cloud. $\bar{Z}$ is a normalize depth data of average values. $n$ is a number of average set.

### *B. Marching Cube*

For point cloud to 3D triangular mesh reconstruction, there are many methods, e.g. intrinsic property driven (IPD) method [7]. We will focus on marching cubes as it is a well-known technique and, currently, many variants of it are still being developed.

The marching cubes algorithm is a high resolution 3D surface construction algorithm [13]. This algorithm generates a triangular mesh estimates iso-surface. It calculates the normal vector of the surface at each vertex of the triangle.

The principle of marching cubes algorithm locates the surface of point cloud in a cube of eight vertexes. The surface intersects edge of this cube where one vertex is outside and the other inside the surface. There are 256 cases that the surface may intersect this cube. It reduced to 15 patterns using symmetries reduces. After that, it calculates normal vectors and marches to the next cube.

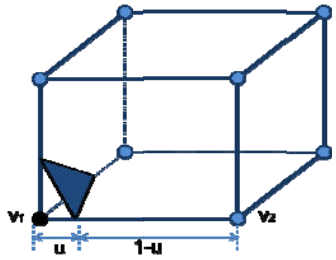


Figure 5. the cube of eight vertexes is represented with surface intersection by triangular mesh.

Interpolate surface intersection along each edge:

$$v_i = v_i + (1 - u) + v_2 \quad (10)$$

$$u = \frac{(v_1 - v_i)}{(v_1 - v_2)} \quad (11)$$

Calculate normal for each cube vertex:

$$G_x(i,j,k) = \frac{(D(i+1,j,k) - D(i-1,j,k))}{\Delta x} \quad (12)$$

$$G_y(i,j,k) = \frac{(D(i,j+1,k) - D(i.j-1,k))}{\Delta y} \quad (13)$$

$$G_z(i,j,k) = \frac{(D(i,j,k+1) - D(i,j,k-1))}{\Delta z} \quad (14)$$

The central differences with the three coordinate axes are used to estimate the gradient at cube vertex $(i, j, k)$.

Interpolate the normals at the vertices of the triangles:

$$\vec{n}_1 = u\vec{g}_2 + (1-u)(\vec{g}_1) \quad (15)$$

*C. Area Calculation*

From the triangular mesh, we use the Heron's formula to calculate each triangle's area [14].

$$T = \sqrt{(s(s-a)(s-b)(s-c))} \quad (16)$$

$$s = \frac{(a+b+c)}{2} \quad (17)$$

Where;

$T$ is a triangular area of each triangular mesh.

$s$ is the semiperimeter of the triangle.

$a, b, c$ are lengths of each sides.

## V. EXPERIMENTAL RESULT

Experiment is divided into two parts. First is the average filter's evaluation. Second is burn area estimation.

First, we compare the resulting area of our method with and without average filter. We calculate the resulting area of sample rectangular shapes between the ground truth and our program. In this experiment, a set of point cloud is captured in range between 0.5 m to 1m as shown in Figure 6.

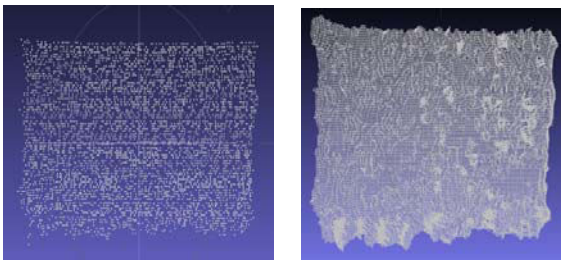

Figure 6. (a) Point cloud of sample object is normalized using average filter. (b) Triangular mesh area of planar object is generated using marching cubes algorithm.

| Surface Area Distances (in front of views) | | Result of Surface Area ($cm^2$) | | | %Error of Surface Area | |
|---|---|---|---|---|---|---|
| Width (cm) | Length (cm) | Actual Area | Marching Cubes | Marching Cubes (Normalized) | Marching Cubes | Marching Cubes (Normalized) |
| 5.11713 | 8.28747 | 42.40806136 | 68.1104 | 45.3756 | 60.6072002 | 6.997581459 |
| 4.66838 | 7.91935 | 36.97053515 | 60.3286 | 39.4187 | 63.1802184 | 6.621935108 |
| 4.76699 | 9.06871 | 43.23044988 | 52.9238 | 46.8473 | 22.4225058 | 8.366441078 |

Table.1 comparison results of ground truth and average filter techniques

The accuracy is shown in Table 1. It is clear that average filter (normalization) enhances the correctness of surfaces dramatically.

Second, we segment the burn area and the skin area as shown in Figure 7. An example of such area's point cloud is shown in Figure 8.

(a) (b)

Figure 7. (a-b) show the segmentation of burn area and the skin area.

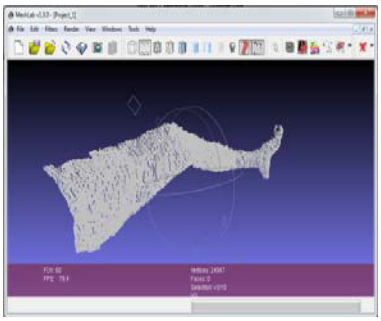

Figure 8. The rest point cloud is deleted that shows in MeshLab Program

## VII. CONCLUSION

Using marching cube algorithm to generate triangular mesh from Kinect data is erroneous. The error of Kinect increases in proportion with the distance from the device [6]. A simple method that can filter such point cloud to be more accurate is proposed. Experiment is done with the target objects in the range between 0.5 to 1 meters. Error rate of triangular mesh area reduces to a great deal. The remaining error, in Table 1, is assumed to be that due to inaccuracy of Kinect itself as mentioned in [6].

## ACKNOWLEDGMENT

This research is financially supported by Thailand Advanced Institute of Science and Technology (TAIST), National Science and Technology Development Agency (NSTDA), Tokyo Institute of

Technology, Kasetsart Signal and Image Processing Laboratory (KSIP), Kasetsart University (KU) and supported in part by Centre for Promoting Research.

**REFERENCES**

[1] Nopparat Rajathanee Hospital. [Online]. http://www.nopparat.go.th/

[2] MD, FAAEM Benjamin C. Wedro. Burn Percentage in Adults: Rule of Nines. [Online]. http://www.emedicinehealth.com/burn_percentage_in_adults_rule_of_nines/article_em.htm

[3] Bas des Bouvrie, "Improving RGBD Indoor Mapping," the Netherlands, 2011.

[4] Brett Jones Rajinder Sodhi, "Kinect-projector calibration," 2010.

[5] Marek Šolony, "Scene Reconstruction from Kinect Motion,".

[6] Koichi Ogawara, and Katsushi Ikeuchi Miti Ruchanurucks, "Integrating Region Growing and Classification for Segmentation and Matting," , Tokyo, 2008.

[7] Harvey E. Cline William E. Lorensen, "Marching cubes: a high resolution 3D surface construction algorithm," in *Proceeding SIGGRAPH '87 Proceedings of the 14th annual conference on Computer graphics and interactive techniques*, 1987.

[8] K. Khoshelham, "Accuracy analysis of kinect depth data," in *International Society for Photogrammetry and Remote Sensing*, 2011, p. 6.

[9] Miti Ruchanurucks, Teera Phatrapornnant, Yasuharu Koike, Panjawee Rakprayoon Amornrat Khongma, "Kinect Calibration and Quality Improvement for Triangular Mesh Reconstruction," , Bangkok, 2012.

[10] James W. Wilson, "PROBLEM SOLVING WITH HERON'S FORMULA," in *the Northwest Mathematics Conference*, 1986.

[11] Teardown. (2010, November) Microsoft Kinect Teardown. [Online]. http://www.ifixit.com/Teardown/Microsoft-Kinect-Teardown/4066/1

[12] K. Conley. (2011, May) Wikipedia. [Online]. http://www.ros.org/wiki/kinect_node

[13] M. Zlatka, "Triangulation methods," in *Triangulation Methods.*, 2009, pp. 9-10.

[14] M.Lenz, H. Bischof M.Ruther, "µNect: On using a gaming RGBD camera in micro-metrology applications," in *Computer Vision and Pattern Recognition Workshops* , 2011 , pp. 52 - 59.

[15] Z. Jianhui, Y. Zhiyong, D. Yihua, Z. Yuanyuan L. Chengjiang, "Improvements on IPD Algorithm for Triangular Mesh Reconstruction," in *International Conference on Multimedia Information Networking and Security*, 2009.

# 3D MODELLING AND DESIGNING OF DEXTO:EKA:

[1]SULABH KUMRA, [2]SHILPA MEHTA, [2]SHALIJA RAHEJA

[1]Department of Electronics and Instrumentation Engineering
[2]Department of Electronics and Communication Engineering
[1,2]ITM University, HUDA Sector 23-A, Gurgaon, Haryana, India

**Abstract**- The presented paper is concerned with designing of a low-cost, easy to use, intuitive interface for the control of a slave anthropomorphic teleo- operated robot. Tele-operator "masters", that operate in real-time with the robot, have ranged from simple motion capture devices, to more complex force reflective exoskeletal masters. Our general design approach has been to begin with the definition of desired objective behaviours, rather than the use of available components with their predefined technical specifications. With the technical specifications of the components necessary to achieve the desired behaviours defined, the components are either acquired, or in most cases, developed and built. The control system, which includes the operation of feedback approaches, acting in collaboration with physical machinery, is then defined and implemented.

***Keywords***- *humanoid, tele-operated, exoskeleton, robot, anthropomorphic*

## I. INTRODUCTION

In this paper we present "DEXTO:EKA: - the humanoid robot", which is a human-scale tele-operated self-balancing anthropomorphic robot. "Anthropomorphic" means having a shape like a human and "Tele-operated" means operated from a remote location. The humanoid is able to perform simultaneous mimicking motion of a person. The overall system is aimed at being able to yield complex meaningful interaction in a seamless and continuous manner. This humanoid will have torso with a head, two arms, face, eyes, mouth, ears and lots of sensors. Its upper body will resemble human while its lower body will be wheeled. Fig. 1 shows the block diagram of humanoid control system, in which the servos, sensors and all the peripherals are interfaced with the microcontroller unit. Audio and video are sent via Wi-Fi and all other data is sent to the other end via Xbee. Fig. 2 shows the block diagram of Man Machine nterface (MMI), which is used by the tele-operator to remotely control the robot. It consists of an Exoskeleton, joystick, display unit and an auditory system. The mode selection switch enables the tele-operator to select one of the three modes of operation. The three modes of operation are manual, semi-autonomous and autonomous. In manual mode, full control will be in the hands of the tele-operator and robot won't be able to perform any action on its own. In semi-autonomous mode, the control will be still in the hands of the tele-operator but the robot will reject the commands if they are dangerous for survival of the robot. In autonomous mode, the robot will be autonomous and will do live entertainment

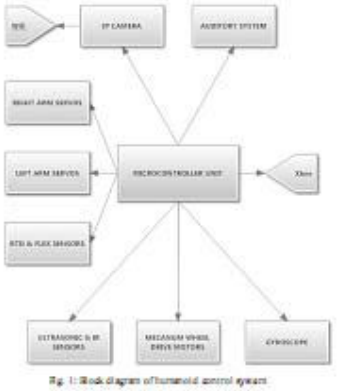

Fig. 1: Block diagram of humanoid control system

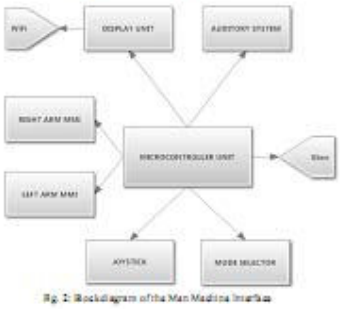

Fig. 2: Block diagram of the Man Machine Interface

## II. STRUCTURE

After conducting various tests on the mecanum drive developed, it was concluded that the weight of the complete robot can't be more than 20kg. Several computer based sketches were made to get a design which weighs less than 20kg and has a center of mass at the midpoint of the robot. Out of the 17 designs, the design in Fig. 3 was selected as it best suited our requirements. Most of the structure is made up of aluminium alloy to keep the robot lightweight nd compact. Aluminium has higher strength to weight ratio, compared to other metals. For both 1 kilogram of aluminium and steel material, aluminium is stronger. It's hard but easily shaped (bent) properties are ideal for this project. echanical

structure and motor brackets can be formed using aluminium. Main controller, batteries, servo controllers/drivers are located in chassis. The torso is a lightweight hollow structure, which has wires passing through the backbone. The backbone is a hollow Galvanised Iron pipe. The camera is placed at the top of the robot and is hidden in hair.\

Fig. 3: 3D computer generated sketch of the robot

## III. LOCOMOTION

A. Drive One of the common omni-directional wheel designs is Mecanum Wheel or Ilon wheel. Mecanum wheel is based on the principle of a central wheel with a number of rollers placed at an angle around the periphery of the wheel. The angled peripheral roller translates a portion of the force in the rotational direction of the wheel to force normal to the wheel directional. Depending on each individual wheel direction and speed, the resulting combination of all these forces produces a
total force vector in any desired direction thus allowing the platform to move freely in direction of resultant force vector, without changing the direction of the wheel. Fig. 4 shows Mecanum wheel design by Ilon with the peripheral roller with
45° degree slope held in place from the outside.

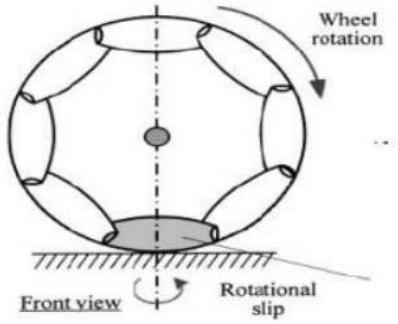


Fig. 4: Front view of Mecanum wheel

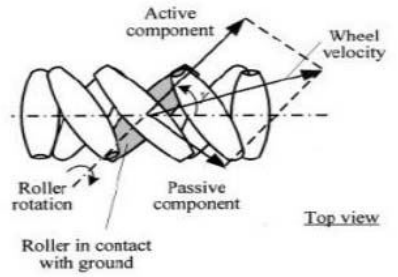


Fig. 5: Top view of Mecanum wheel

This design ensures that the rollers are always in contact with the work surface, thus allowing better performance on uneven surfaces. Using four of Mecanum wheels provides omni-directional movement for a vehicle without needing a conventional steering system. Positioning four Mecanum wheels, one at each corner of the chassis (two mirrored pairs), allows net forces to be formed in the x, y and rotational direction.

B. Navigation Depending on each individual wheel direction and velocity, the resulting combination of all these forces produce a total force vector in any desired direction thus allowing the platform to move freely in the direction of the resulting force vector, without changing of the wheels themselves. Fig. 6 shows the force vectors created by Mecanum wheels for each wheel. Summing these vectors we get a resultant vector in forward direction, thus giving us a forward motion

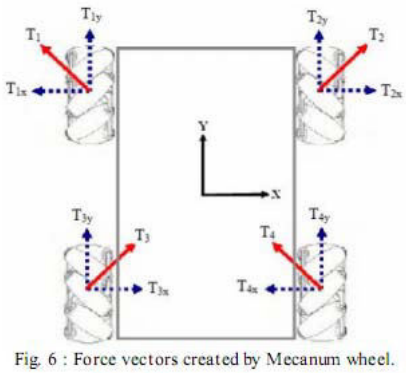


Fig. 6 : Force vectors created by Mecanum wheel.

Fig. 7 shows the robot motion according to the direction and angular speed of the wheels. Thus the

robot is able to translate on any direction, forward/backward but also sideways left/right and turning on the spot, thanks to its special wheels. This is especially helpful when having to manoeuvre in tight environments.

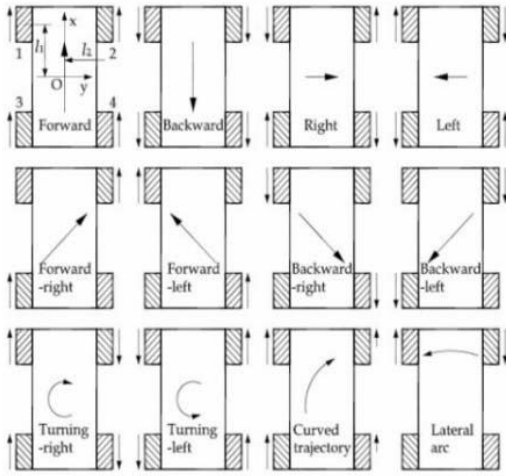


Fig. 7: Robot motion according to the direction and angular speed of the wheels

The navigation of a multi-sensor based mobile robot requires a good representation of the environment. An autonomous mobile robot should be able to construct a map of it senvironment based on the sensory information. Ultrasonic sensors have been widely used in mobile robots applications as they can produce good range information. Sharp IR sensors and Ultrasonic sensors are used for measuring distance of an object from the robot.

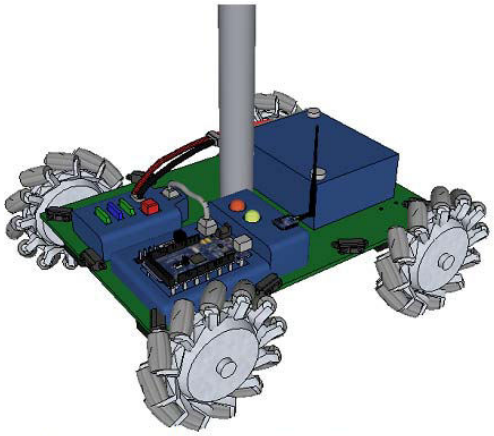

Fig. 8 : Design of Mecanum drive chassis with sensors

Ultrasonic sonar sensors actively transmit acoustic waves and receive them later. This is done by ultrasonic transducers, which transform an electrical signal into an ultrasonic wave and vice versa. Often it is possible to use the same transducer for both transmitting and receiving. On its path from the transmitter to the receiver, the wave becomes modified by the situation under investigation. The ultrasound signal carries the information about the variables to be measured. The task for the ultrasonic sensors is not merely to detect ultrasound. As intelligent sensors they have to extract the information carried by the ultrasonic signals efficiently and with high accuracy. To achieve this performance, the signals are processed,
demodulated and evaluated by dedicated hardware.

C. Self-balancing

The robot is capable of both balancing dynamically and has entirely holonomic ground movement. This is achieved using a gyroscope module, which is a low power 3-axis angular rate sensor. A rectangular arrangement of mecanum wheels gives it the load-lifting, performance, and manipulation benefits of a dynamically-balancing platform without the maneuvering difficulties. The arrangement is capable of holonomic motion, describe a controller that maintains dynamic balance during holonomic motion. Omnidirectional navigation is also clearly advantageous. The orientation of the humanoid can be found out with the help of the sensor data. The gyroscope is calibrated before using. The sensor is placed at the top of the robot, so that it is highly sensitive to change in orientation. If a situation rises,which causes the robot to incline in the forward direction, the gyroscope would send out the changed orientation data to the microcontroller which will interpret the data and respond accordingly, in this case it would make the robot move forward so that the head and the lower body of the robot are in the same plane perpendicular to the surface it is moving on. This would greatly increase the probability of the robot to remain stable in rough terrain and while moving on an inclined or rough surface.

## IV. ROBOTIC ARM

A. Design The main advantage of teleoperation is that human beings are adaptive and so are better able to deal with unstructuredwhich causes the robot to incline in the forward direction, the gyroscope would send out the changed orientation data to the microcontroller which will interpret the data and respond accordingly, in this case it would make the robot move forward so that the head and the lower body of the robot are in the same plane perpendicular to the surface it is moving on. This would greatly increase the probability of the robot to remain stable in rough terrain and while moving on an inclined or rough surface.

## IV. ROBOTIC ARM

A. Design The main advantage of teleoperation is that human beings are adaptive and so are better able to deal with unstructured nvironments. Specifically, this is an anthropomorphic robotic arm with 6-DOF (degree of freedom) as shown in Fig 1. The 6-DOF covers the major and most common arm movements to cover a large area, and it also makes the arm easy to maneuver to lift and move objects in any direction.It is very similar to a human arm with respect to the number and position of the joints. Of the six degrees of freedom, four are for positioning

(including the gripper) and two for orientation. If the joints are compared to their human equivalent, then the robotic arm can be said to have the following joints: abduction (shoulder rotation), shoulder back and forth, elbow, wrist up and down, pivot (wrist rotation), and gripper.

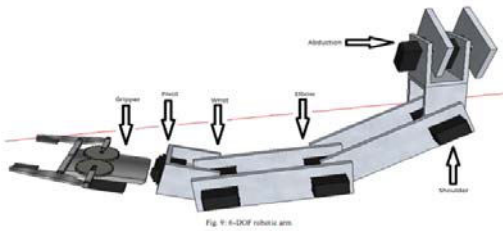

The actuators for all of these joints are servo otors. The gripper is a two-finger construction; each finger with two parallel links. Force sensors are mounted between the joints of the manipulator. These sensors measure the amount of strain placed on each of these joints: the higher the strain, the greater is the amount of force that the joint is exerting. The main advantages of this system are that it measures actual forces and that the measurement does not interfere with the operation of the joints themselves. It is appropriate, for the gripper joint, to use a force sensor to measure the amount of force the slave is exerting on an object in its grip.

TABLE 1
Joint ranges and joint torques

| S.NO. | JOINT | RANGE (degrees) | TORQUE (Kg-cm) |
|---|---|---|---|
| 1. | Abduction | 140 | 52.3 |
| 2. | Shoulder | 110 | 47.7 |
| 3. | Elbow | 125 | 32.6 |
| 4. | Wrist | 180 | 13.1 |
| 5. | Pivot | 180 | 8.4 |
| 6. | Gripper | NA | 3.2 |

To measure the force, a sensor is attached to the inside of one of the gripper prongs. When the gripper closes around the object, the sensor is compressed between the object and the gripper prong. From this the force can be measured.These sensors are mounted on a flexible circuit board and have a small circular dot of force-sensitive ink. The resistance of this ink increases as the force applied increases. By using a simple operational amplifier based circuit this force can be converted into an analog voltage that can be fed into one of the ADC inputs of the transducer interface.

B. Man-Machine Interface Special emphasis has been given to the ease of operation and some form of force sensation. The control rig is fitted to the user's arm. Use of a 'wearable' jig in a bilateral master slave control setup has been introduced to simplify the MMI (Man-Machine Interface).The prototype of the master unit, shown in Fig. 10 and Fig. 11, is aluminium frame which the user straps onto his arm.

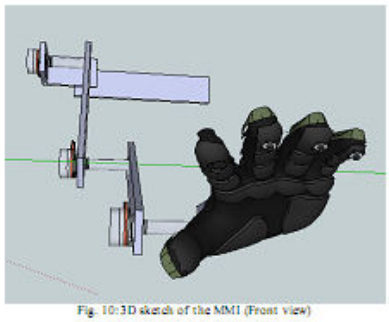

Fig. 10:3D sketch of the MMI (Front view)

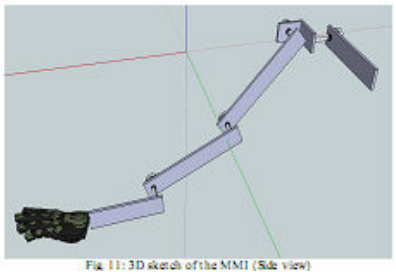

Fig. 11: 3D sketch of the MMI (Side view)

The proposed sensing mechanism is cost effective, accurate and can be easily implemented. In MMI, control methodology, which has been used in our work, the slave robot (teleoperator) exactly replicates the movements of the operator. Four potentiometers are placed on the slave robot, one each at the wrist, elbow, abduction and shoulder joints. The movements rotate the potentiometers' (relative to robot links) movements rotate the servo motors, by generating a variable analog voltage. The voltage signals from the potentiometers are fed to the transducer unit where their values are sampled and measured by an analog to-digital (ADC) converter. The voltage is thus a measure of the angular position of the robot joint. This arrangement is used to measure the positional error. A joint is commanded to move to a certain angle, and the voltage from the corresponding potentiometer is read.

## V. VISUAL & AUDITORY SYSTEM

An Internet Protocol (IP) camera is used as the visual system. It is a type of digital camera which can send and receive data via computer network and the internet. They can be moved around anywhere on an IP network (including wireless). e
have day and night vision with 11 IR LEDs (night visibility up to 10 metres). It allows remote viewing video and record from any internet connection and remote pan and tilt control, giving us 2-DOF. It has a higher image resolution of 640x480 and is Wi-Fi compliant with IEEE 802.11 b/g. Thus the teleoperator can view the live stream on a computer which is connected to internet. Fig. 12 shows the face with the IP camera, speaker and microphone

Fig. 12: 3D sketch of the face

mounted.Two- way build in audio via single network allows the teleoperator to communicate with what he is seeing. Thus we get the auditory system by installing a speaker and microphone to the IP camera and the teleoperator can communicate using headphones at tached to the same computer mentioned above.

VI. CONCLUSION This paper presented how we designed the humanoid robot Dexto: Eka:. Future work includes evaluating developed Dexto: Eka: through experiments. An improvement of Dexto: Eka:, which reflects user's feedback during experimental tests, is also our future work. Our desire is to put the Dexto: Eka: to practical use and creating a real market for enhanced versions of Dexto: Eka: such as Dexto: Dvitiya:, Dexto: Tritiya: etc. This also presented how we designed the 3D model of humanoid robotic platform for Dexto: Eka:, which has a ability to cope with rough terrain in the open air, to prevent tipping over, and mimic the movements of the tele-operator.

## ACKNOWLEDGMENT

We want to thank Dr Swaran Singh Ahuja and Prof. Ramandeep Singh for their guidance and all the team members for their support. We also thank ITM University for their financial support and providing labs with all the required tools and equipments.

## REFERENCES

[1] Thomas Braunl,2003 Embedded Robotics: Mobile Robot Design and Applications with Embedded Systems, First Edition. Springer-Verlag, Berlin.

[2] Anglees, J. (2005). An innovative Drive for Wheeled Mobile Robots, IEEE/ASME Tran. on Mechatronics, Vol. 10, No.1.

[3] J. W. Kang, H. S. Hong, B. S. Kim, and M. J. Chung, "Assistive Mobile Robot Systems helping the Disabled Workers in a Factory Environment," International Journal of Assistive Robotics and Mechatronics, Vol. 9, No. 2, pp. 42 – 52, June 2008.

[4] K. Kaneko, S. Kajita, F. Kanehiro, K. Yokoi, K. Fujiwara, H. Hirukawa, T. Kawasaki, M. Hirata, and T. Isozumi, , "Design of Advanced Leg Module for Humanoid Robotics Project of METI," Proc. IEEE Int. Conference on Robotics and Automation, (to be appeared), 2002.

[5] J.A Cooney, W.L. Xu, "Motion Control and Intelligent of an Mobile Robot", Massey University.

[6] K. Nagatani, S Tachibana, I Nagai and Y Tanaka, " Navigation of Omni-directional Vehicle wheel with Mecanum Wheels", Okayama University.

[7] Stephen L. Dickerson, Brett D. Lapin, "Control of An Omni-directional Robotic Vehicle with Mecanum Wheels", Georgia Institute of Technology.

[8] P. Viboonchaicheep, A. Shimada, Y. Kosaka, "Position Rectification Control for Mecanum Wheeled Omni-directional Vehicles", Hashimodotai Polytechnic University.

[9] I. W. Park, Y. Y. Kim, S. W. Park, and J. H. Oh, "Development of Humanoid Robot Platform KHR-2(KAIST Humanoid Robot - 2)", Int. Conf. on Humanoid 2004.

[10]J. Yamaguchi, and A. Takanishi, "Development of a Biped Walking Robot Having Antagonistic Driven Joints Using Nonlinear Spring Mechanism", in Proc. of IEEE Int. Conf. in Robotics and Automation, pp.14–21, 1997.

[11]Jung-Yup Kim, Ill-Woo Park, Jungho Lee, Min-Su Kim, Baek-Kyu Cho and Jun-Ho Oh, "System Design And Dynamic Walking Of Humanoid Robot KHR-2", IEEE International Conference on Robotics & Automation, 2005.

[12]J. J. Craig, Introduction to Robotics: Mechanics and Control, 2nd e. (Addison-Wesley Publishing Company 1989), p.129.

[13]M. Gienger, K. Loffler and F. Pfeiffer, "Walking Control of a Biped Robot based on Inertial Measurement", in Proc. Of Int. Workshop. on Humanoid and Human Friendly Robotics, pp.22–30, 2002.

[14] S. Kuindersma, E. Hannigan, D. Ruiken, and R. Grupen. Dexterous Mobility with the uBot-5 Mobile Manipulator. In 14th International Conference on Advanced Robotics (ICAR'09), 2009.

[15] T. Lauwers, G. Kantor, and R. Hollis. A dynamically stable singlewheeled mobile robot with inverse mouse-ball drive. In IEEE International Conference on Robotics and Automation (ICRA), 2006,pages 2884–2889, May 2006.

[16] Lauwers, T. and Kantor, G. and Hollis, R. One is enough! In Proceedings of the 12th International Symposium on Robotics Research, October 2005.

[17] K. M. Lynch and M. T. Mason. Stable pushing: Mechanics, controllability, and planning. Int. Journal of Robotics Research, 15(6):533–556, 1996.

[18] Franch J. Agrawal S. Pathak, K. Velocity and position control of a wheeled inverted pendulum by partial feedback linearization. IEEE Transactions on Robotics, 21, 2005.

[19] A. Salerno. Design, Dyamics, and Control of a Fast Two-Wheeled Quasiholonomic Robot. PhD thesis, 2006.

[20] E. Salih, J. Designing omni-directional mobile robot with mecanum wheel. American Journal of Applied Sciences, pages 1831–1835, 2006

◈◈◈

# SIMULATION OF OBSTACLE DETECTION AND SPEED CONTROL FOR AUTONOMOUS ROBOTIC VEHICLE

**VYAS SHAUNAK AGASTYA, LOVEKUMAR D THAKKER, AMIT PATWARDHAN**

School of Interdisciplinary Science and Technology
IGNOU-I$^2$IT Centre of Excellence for Advanced Education and Research
Pune, India

**Abstract**- This paper introduces a digital image processing algorithm to detect the obstacle in the path and according to the position of the obstacle, the speed of Autonomous Robotic Vehicle is controlled through PID based Speed control module. The camera mounted on Autonomous Robotic Vehicle captures image in such a way that the obstacle in image and actual vehicle position keep some distance to avoid collision. Based on the computed obstacle size, the vehicle actions are controlled. The streaming of the images of the path is done and each image is analysed through MATLAB Simulink based Video Processing Module. The control actions are taken based on the PID constants computed through MATLAB Simulink modules.

***Keywords***- *Autonomous Robotic Vehicle, Speed Control, PID Control, Simulation, MATLAB Simulink*

## I. INTRODUCTION

An Autonomous Robotic Vehicle (ARV) is designed as an automotive system that takes its own decision of Speed transition and Obstacle detection while driving itself from a source to a destination without human guidance.[1] It is considered that the path is single-colored and the obstacle on path is steady. ARV involves concepts of Sensors, Image Processing, Control Systems, Robotics, Engineering Mechanics and Electric Drives.

An image can be considered as an array of pixels that are separated through particular numbers of rows and columns. As shown in Figure 1, There are two regions named “TopLine” and “BottomLine” defined in the image. When ARV with a camera drives itself on a path, the camera continuously takes images of the path and sends them to the processing module for analysis. As the ARV drives, the obstacle on the path will be seen first in the TopLine region. At the point of Detection of obstacle in the TopLine region, the ARV will start decreasing its speed and will stop when the obstacle is in the BottomLine region.

## II. DIGITAL IMAGE PROCESSING IN ARV

An image may be defined as a two-dimensional function f(x,y), where x and y are spatial (plane) coordinates, and the amplitude of f at any pair of coordinates (x,y) is called the intensity or gray level of the image at that point. When x, y, and the amplitude values of y are all finite, discrete quantities, we call the image a digital image. The field of digital image processing refers to processing digital images by means of a digital processor. Note that a digital image is composed of a finite number of elements, each of which has a particular location and value. These elements are referred to as picture

elements, image elements, pels and pixels. Pixel is the term most widely used to denote the elements of a digital image.[4]

The roles of digital image processing in ARV are:

- Following the path
- Obstacle Detection
- Synchronization with PID Control for Motors

## III. ALGORITHM FOR OBSTACLE DETECTION

As the path is single-colored, all the TopLine region pixels have the same intensity level. There are two steps to be followed:

- Convert the path image to gray-scale.
- Threshold the image with a threshold value that is sufficient to distinguish the obstacle in the image.

The reason to convert the image to gray-scale is that it reduces the computation time of code, because if it is an 8 bit image there will be 256×256×256 RGB levels while here in this case, the gray-levels will be 256. This method of color conversion is very useful in obstacle detection.[6]

For getting the proper threshold value, the path color and all the possible gray-scaled shades of the obstacles are the deciding factors. One limitation of this method is that if the path color is same as the obstacle color (not even a single intensity level difference), then it will be difficult to recognize that obstacle.[2]

### *A. Thresholding and Region Growing based Image Segmentation*

Image Thresholding sets the pixels in the image to one or zero.

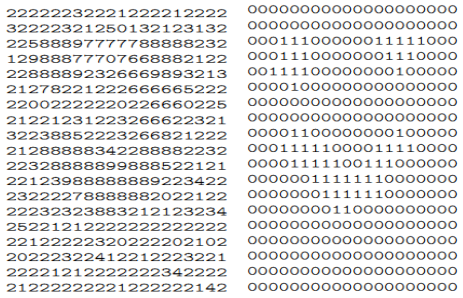

Figure 2 Image (Left) and the thresholded image (Right) [4]

Figure 2 shows an image in left and the thresholded image with Threshold value 8 in right. The TopLine and BottomLine of the path image are defined on this base.[5] As the path color is uniform, the TopLine and BottomLine regions can be defined on the same threshold value (the uniform intensity level of both the regions). When any obstacle enters the TopLine, the uniformity of intensity level gets disturbed. At this time the connectivity and neighborhood of TopLine pixels are continuously checked and if any disturbance-recognition is achieved, a "reduction-in-speed" signal is given to the PID Control Module of ARV immediately.

The number of rows between TopLine and BottomLine are known. The speed of the car is also known at the time of obstacle detection. Now the PID parameters are set in such a way that as soon as the obstacle is about to touch the bottommost row of the BottomLine, the ARV Stops.

Figure 3 shows the MATLAB Simulink Model for video processing. A video in "AVI" format is used as an input. This video contains the information of path of ARV. The video is converted to Gray scale through MATLAB Simulink block and saved. After that thresholding operation is applied to the video. As per shown in Figure 2, the obstacle is segmented through thresholding.

## IV. OVERVIEW OF PID CONTROLLER

PID stands for "proportional, integral, derivative." These three terms describe the basic elements of a PID controller. Each of these elements performs a different task and has a different effect on the functioning of a system.

In a typical PID controller these elements are driven by a combination of the system command and the feedback signal from the object that is being controlled (usually referred to as the "plant"). Their outputs are added together to form the system output.[3]

### *A. Proportional*

Proportional control is the easiest feedback control to implement, and simple proportional control is probably the most common kind of control loop. A proportional controller is just the error signal multiplied by a constant (proportional gain) and fed out to the drive. For small gains, the motor goes to the correct target but it does so quite slowly. Increasing the gain speeds up the response to a point. Beyond that point the motor starts out faster, but it overshoots the target. In the end the system doesn't settle out any quicker than it would have with lower gain, but there is more overshoot. If the gain is kept increasing, a point is reached where the system just oscillates around the target and never settles out- the system would be unstable. The motor starts to overshoot with high gains because of the delay in motor response.

### *B. Integral*

Integral control is used to add long term precision to a control loop. It is almost always used in conjunction with proportional control. Integral control by itself usually decreases stability or destroys it altogether. The integrator state 'remembers' all that has gone on before which is what allows the controller to cancel out any long term errors in the output. This same memory also contributes to instability- the controller is always responding too late, after the plant has gotten up speed. To stabilize the system, one needs a little bit of the plant's present value, which can be obtained from a proportional term. Error over time is added up in integral control, so the sampling time becomes important. Also an attention should be paid to the range of the integrator to avoid windup. The rate that the integrator state changes is equal to the average error multiplied by integrator gain multiplied by the sampling rate. If one has a controller that needs to push the plant hard, the controller output will spend significant amount of time outside the bounds of what the drive can actually accept. This condition is called saturation. If a PI controller is used then all the time spent in saturation can cause the integrator state to windup to very large values. When the plant reaches the target, the integrator value is still very large. So the plant drives beyond the target while the integrator unwinds and the process reverses. This situation can get so bad that the system never settles out, but slowly oscillates around the target position. The easiest and most direct way to deal with integrator windup is to limit the integrator state.

### *C. Differential (Derivative)*

If a plant can't be stabilized with proportional control, it can't be stabilized with PI control. Proportional control deals with the present behavior of the plant and integral control deals with the past behavior of the plant. If one has some element that predicts the plant behavior then this might be used to stabilize the plant. For this, a differentiator can be used. Differential control is very powerful but it is also the most problematic of all the three control types. The

three problems that one is most likely going to experience are sampling irregularities, noise and high frequency oscillations. The output of a differential element is proportional to the position change divided by the sample time. If the position is changing at a constant rate but the sample time varies from sample to sample, noise is generated on the differential term. So the sampling interval has to be consistent to within 1% of the total at all times. The rule of thumb for digital control systems is that the sample time should be between $1/10^{th}$ and $1/100^{th}$ of the desired system settling time.

## V. PID CONTROLLER BASED SPEED CONTROL OF PMDC MOTOR

Figure 4 shows the Simulink block for PID Control of PMDC Motor.

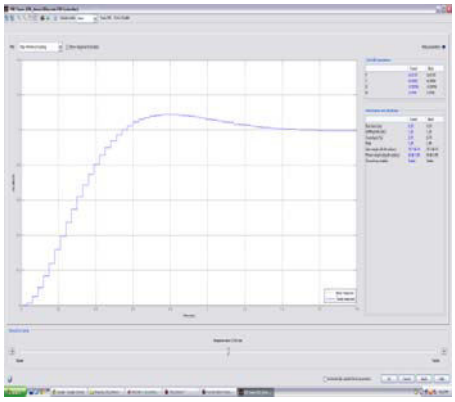

Figure 5 Tuning of PID Controller

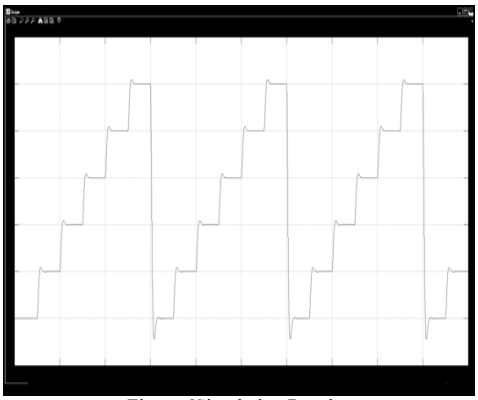

Figure 6Simulation Results

## VI. CONCLUSION

The design of ARV gives optimum results when the path is straight, single-colored and the obstacles are steady. The threshoding and region based image segmentation method gives proper obstacle detection required to drive ARV. The tuning of a PID Control for PMDC Motor is complex but it can be done very effectively with MATLAB Simulink if all the five required parameters of PMDC Motor named- Armature Resistance, Armature Inductance, Damping Ratio of Mechanical System, Electromotive Force Constant and Moment of Inertia are known.

## REFERENCES

[1] Martin Buehler, Karl Lagnemma, Sanjiv Singh- "The DARPA Urban Challenge- Autonomous Vehicles in City Traffic", Springer tracts in Advanced Robotics, Volume 56

[2] Sumit Badal, Srivinas Ravela, Bruce Draper, Allen Hanson, "A Practical Obstacle Detection and Avoidance System", IEEE, pp 97-104, 1994

[3] Su Whan Sung,Jietae Lee and In-Buem Lee - "Process Identification and PID Control", WILEY Publications, Pages 111-120

[4] Rafael C. Gonzalez, Richard E. Woods - "Digital Image Processing" Second Edition, Prentice Hall, Pages 64-66, 567-624

[5] E. R. Davies – "Machine Vision- Theory, Algorithms and Practicalities" Second Edition, Pages 79-85, 103-128, 437-440

[6] M. Anji Reddy, Y. Hari Shankar- "Textbook of Digital Image Processing", BS Publications, Pages 26-53

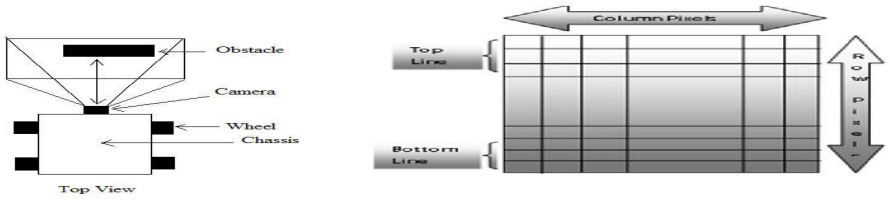


Figure 1 Top View of ARV (Left) and Captured Image Assumptions (Right)

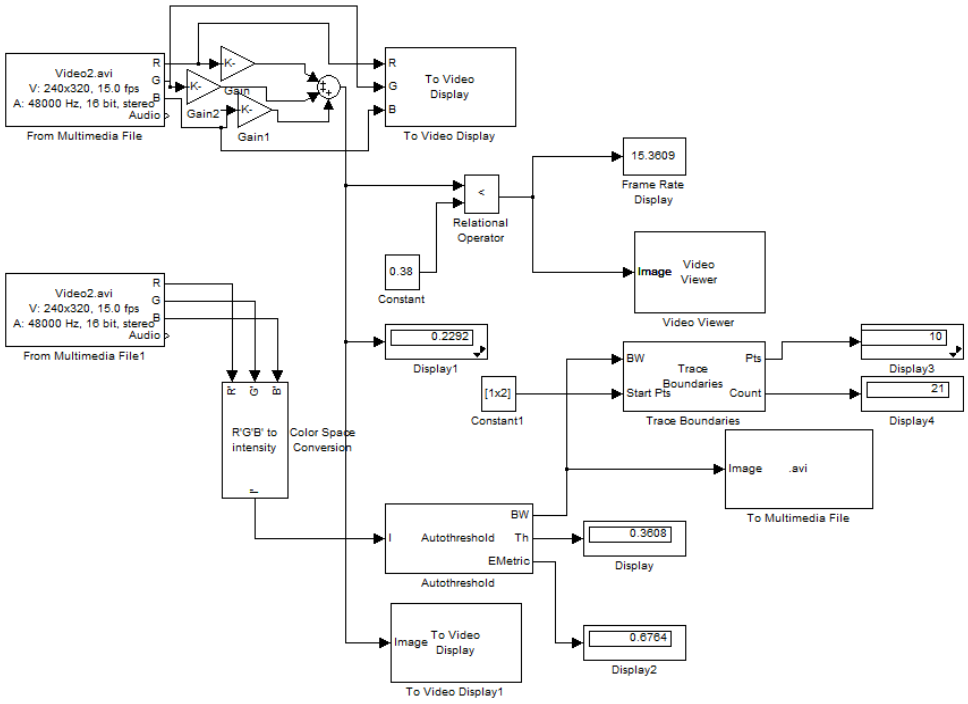


Figure 3 MATLAB Simulink Model for Video Processing based Obstacle Detection

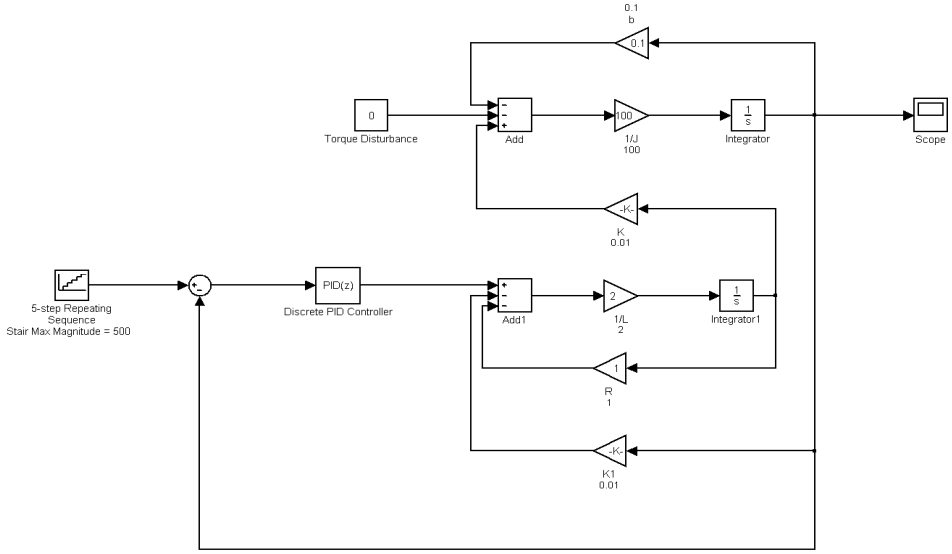


Figure 4 Simulink Block for PID Control of PMDC Motor

# EMBEDDED VISION FOR RETINAL IMPLANT

**N.SHARMILI, P.S. RAMAIAH & N.SWAPNA**

[1,2,]*Dept of CS and Systems Engg , Andhra University, Vishakhapatnam,India, ,*
[3]*Dept of CSE Andhra University, RIET Rajahmundry,India*

**Abstract-***Abstract*—Rapid advancements in Embedded technology in biomedical field shows great promise for the future is Retinal implants. *Retinitis Pigmentosa* (RP) and Age-related Macular Degeneration (AMD) are the two most common retinal diseases causing vision loss due to the degeneration of photoreceptors. Retinal implants are being developed around the world in hopes of restoring useful vision for patients suffering from certain types of diseases like AMD and RP. Photoreceptors are the key components in the retina that convert incoming light into neural signals which are then sent to the brain where the scene or image is interpreted. However, many of the inner retinal neurons such as ganglion cells and bipolar cells that transmit signals from the photoreceptors to the brain are preserved to a large extent for a prolonged period of time. Retinal prostheses are to replace the function of lost photoreceptors in these degenerative diseases. The Epi-Retinal prosthesis mimics the normal visual operation by stimulating the ganglion cells in the retina with an electric current. The Epi-retinal prosthesis system is composed of two units, extra ocular and intraocular. The two units are connected by a telemetric inductive link. The extra ocular system consists of CMOS image sensor and Microcontroller Based Image processing unit. Images are captured by an external camera and encoded into a 2 Mbps bit stream by an external signal processing unit. The bit stream is modulated on a 22 MHz carrier and then transmitted to the implant where every pixel can be independently programmed for pulse width, pulse amplitude, leading pulse polarity, etc. In this paper the related image processing on low cost, high performance, highly reliable MIPS-Based 32 bit PIC32 processor is discussed which will help for real time implementation of bionic eye.

***Keywords-****Epiretinal implant; AMD; RP; Extra ocular; Intraocular; PIC32 Microcontroller; Graphics Display controller; MPLAB;Graphics resource converter;CPLD*

## I. INTRODUCTION

After decades of development and years of clinical trials, an optical prosthesis capable of restoring at least partial vision to those suffering from retina-damaging diseases such as Age-related Macular Degeneration(AMD) and Retinitis Pigmentosa (RP). Age-related Macular Degeneration is a major cause of visual impairment among older adults which results in a loss of vision in the center of the visual field because of damage to the retina. AMD is the leading cause of blindness in individuals 60 years or older, with 200,000 eyes left legally blind each year. Retinitis Pigmentosa generally occurs in a younger age group. RP is a type of hereditary retinal dystrophy, a group of inherited disorders in which abnormalities of the photoreceptors or the retinal pigment epithelium of the retina lead to progressive visual loss. Affected individuals first experience defective dark adaptation or night blindness, followed by reduction of the peripheral visual field and, sometimes, loss of central vision late in the course of the disease. RP has an incidence of 1 in 4,000 and in the US alone afflicts 100,000 people. In both conditions patients are visually impaired due to loss of photoreceptors. But the inner remaining layers of retina such as ganglion cells and bipolar cells are still healthy. Different gene and drug therapies have been tried, but their ability to replace lost photosensitive tissue is limited. Researchers are therefore investigating the possibility of developing an effective visual prosthetic device to restore vision.

Vision begins as visual information from the retina's 130 million photoreceptors is compressed into electrical signals carried by 1.2 million highly specialized ganglion neurons, whose axons form the optic nerve. The optic nerve transmits visual information via the lateral geniculate nucleus to the primary visual cortex of the brain. Eye diseases cause vision loss due to degeneration of photoreceptors. Bypassing those photoreceptors and electrically stimulating the healthy layers of the retina has been able to restore partial vision in patients.

This research mainly focuses on design and development of prototype model for low cost, high performance, highly reliable Retinal Prosthesis. Electrical devices that can support or replace the function of defective organs are demonstrated in cochlear implants for the hearing impaired and pacemakers for individuals with heart disease [1]. This gives scientist's confidence to make a vision implant [2].

Retinal implant is a prosthetic device that maps visual images to control signals, based on which it stimulates the surviving retinal circuitry. In this regard we proposed to develop a system based on 80 MHz PIC32 microcontroller that implements edge detection of still images. Hardware-based signal

processors such as Texas Instrument DSP (Digital Signal Processing) or Field Gate Arrays (FPGA) are generally an expensive solution for image processing applications[3,4]. On the other hand a conventional 8-bit microcontroller doesn't have enough capability to handle memory intensive Image Processing algorithms. In this regard, Microchip offers a tradeoff between cost and performance. Our research presents a preliminary approach to perform any type of image processing task using microchip 32-bit Microcontrollers.

## II. EPIRETINAL APPROACH

An Epiretinal prosthesis system usually employs a multi electrode array implanted on the surface of the inner retina between the vitreous and internal limiting membrane. Epiretinal prosthesis pass signal to the ganglion cells. A data acquisition system located outside of the body captures images from the surroundings, and converts the information into patterns of electrical signals. Upon the reception of signals through data transmission and processing systems, the electrodes stimulate the remaining retinal ganglion cells and restore vision.

The Epiretinal prosthesis system(Epiretinal means the prosthesis is placed on the surface of a patient's damaged retina) is composed of two units, one extraocular and one intraocular [5]. The two units are connected by a telemetric inductive link, allowing the intraocular unit to derive both power and a data signal from the extraocular unit.
The extraocular unit includes a video camera and video processing board, a telemetry protocol encoder chip, and an RF amplifier and primary coil. At the extraocular unit side, a digital camera captures the image which is then preprocessed as defined in sec(III). The data is further processed by a pulse width modulation circuit and subsequently modulated onto an RF carrier using amplitude shift keying . The transmitters generate radio frequency electromagnetic fields containing both energy and the encoded image data for the implant. The device requires a wireless data link to provide captured image data to stimulate ganglion cells via electrodes array.

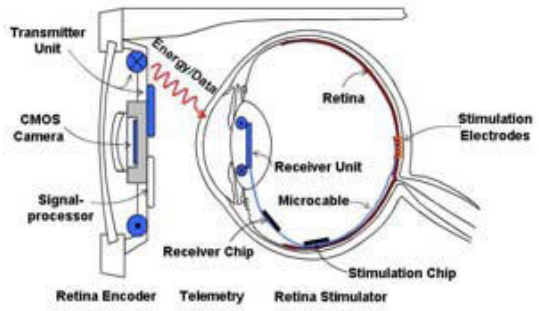


**Fig 1: Epiretinal implant architecture**

The symbol is encoded as a pulse width modulated signal, a 50-50% duty cycle encodes a 0 and 30-70% duty cycle encodes a 1.The modulated carrier is then inductively transmitted to the intraocular unit.

The intraocular unit consists of a secondary coil, a rectifier and regulator, a retinal stimulator with a telemetry protocol decoder and stimulus signal generator, and an electrode array.In intraocular unit the ASK demodulator receives the power-carrier envelope from the rectifier output and generates the digital PWM signal for the clock and data recovery block. Data and clock signals are then recovered by a delay-locked loop (DLL) and a decoder circuit. After decoding the image information the timing generator circuit is programmed to produce the timing of the stimulus waveforms, including the anodic/cathodic pulse widths, the interphase delay, and the biphasic pulse period [6]. The current control circuit specifies the full-scale amplitude of biphasic current pulses. The biphasic current waveform could be either an anodic pulse first followed by a cathodic pulse or vice versa only if an equal amount of charge is provided by both anodic and cathodic pulses in order to obtain a balanced charge [7]. These pulses will
stimulate the electrodes which are present on the implant to perceive the visual information by the patient. Based on received image information, the timing generation and current controlling is done by microcontroller.

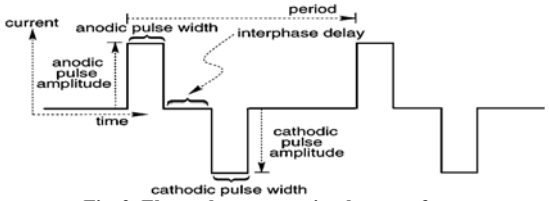


**Fig. 2. Electrode current stimulus waveform.**

Upto 1000 electrodes are suggested for retinal implant to perceive basic vision such as reading large-sized text, navigating a room unaided, and recognizing faces [5].Building an implant chip to drive 1000 electrodes is challenging and requires complicated control circuitry with potentially high power consumption, high data rate for realtime image updating, and compact size for fitting on the limited retina surface. The main objective of this research is to design a prototype implantable retinal prosthesis model with low power consumption, high datarate and high integration.

## III. IMAGE PROCESSING IN EXTRAOCULAR PART

The current camera captures images having a resolution of 480x640 at a rate of 30 frames/sec. For retinal implant the image processing on these frames consists of edge detection, edge enhancement, decimation and low-pass filtering. Due to limited electrodes fits in an eye the decimated output image

will be a 32 x 32 image thus decimating the original image by a factor of 7.5 x 10[9].

The images tend to be corrupted by noise when some operations are applied on them. So, it is highly recommended to filter the noise before performing further operations on them. The grayscale image is filtered by an averaging filter (low pass filter), which is defined as

$$\frac{1}{25}\begin{bmatrix}1&1&1&1&1\\1&1&1&1&1\\1&1&1&1&1\\1&1&1&1&1\\1&1&1&1&1\end{bmatrix}$$

Averaging Filter Mask [10]

Edges in images are the areas with strong intensity contrasts – a jump in intensity from one pixel to the next. Edge detecting an image significantly reduces the amount of data and filters out useless information, while preserving the important structural properties in an image. Edge detection is a fundamental tool in image processing and computer vision, particularly in the areas of feature detection and feature extraction, which aim at identifying points in a digital image at which the image brightness changes sharply or more formally has discontinuities. We have implemented a very sensitive edge detection algorithm which gives the better results than Sobel's and Canny's Edge detection algorithms [1].The algorithm is as follows:

1. Get the negative value of the second derivative of the current pixel.
2. Remove the center pixel value.
3. Subtract the four diagonal pixels values.

The operator equation is: **$F(x,y) = -\Delta 2\ f(x,y) - 4f(x,y)-f(x-1,y-1)-f(x-1,y+1)-f(x+1,y-1)-f(x+1,y+1)$**

The following operator mask represents the above equation:

$$\begin{bmatrix}-1&1&-1\\1&0&1\\-1&1&-1\end{bmatrix}$$

Adding diagonal values and remove the center value gives us the necessary balancing for edge detection and removes undesired noise. The operator employs the differences between neighboring pixels with respect to the current pixel to become the new value of the current center pixel. The operator removes undesired data (colors and noise) and only holds the edges. The simplicity of the algorithm makes it possible to be implemented by hardware which is suitable for high resolution and large size images.

Edge enhancement algorithm sharpens the edges in the image frame before decimating the image in order to preserve more edges. The edge image obtained as above is scaled and added to the original image to enhance the edges (i.e. convolution on original and filtered images).

Filtering and decimation will done after the convolution stage. One of the algorithms implements decimation and low-pass filtering using averaging and bi-cubic filter masks on every frame. The grayscale image is filtered by an averaging filter (low pass filter), which is defined as:

$$\frac{1}{25}\begin{bmatrix}1&1&1&1&1\\1&1&1&1&1\\1&1&1&1&1\\1&1&1&1&1\\1&1&1&1&1\end{bmatrix}$$

Averaging Filter Mask [10]

The bi-cubic algorithm is frequently used for scaling images and video for display. We adopt it here because it is able to preserve fine details more effectively compared with bilinear interpolation and nearest interpolation. The bicubic filter mask is given as:

$$\frac{1}{256}\begin{bmatrix}1&4&6&4&1\\4&16&24&16&4\\6&24&36&24&6\\4&16&24&16&4\\1&4&6&4&1\end{bmatrix}$$

Bi-cubic Filter Mask [10]

Decimation is implemented to output a final image of 32x32 dimensions in order to stimulate the 32x32 grid of electrodes. The results of implementation in matlab are shown in Figure 3. This 32x32 image is applied for binarization (by thresholding techniques) to generate the digital data. Now the digital data is encoded as a pulse width modulated signal.

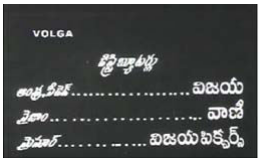


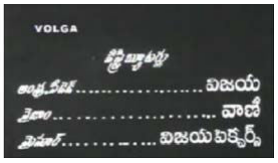


**Fig 3(a) Original image** **Fig 3(b) Filtered image**

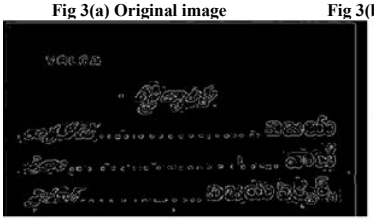

**Fig 3(c) Edge detected image** **Fig3(d) Decimatedimage**

## IV. IMAGE PROCESSING ON PIC32 MICRO-CONTROLLER

PIC32 microcontroller is configured to run computation intensive tasks like image analysis, or encoding calculation, etc. [9] which are involved in the epi-retinal prosthesis. This research mainly focuses on the development of a low cost prototype hardware based platform to perform image processing for extraocular part and it is demonstrated on PIC32

starter kit and Multimedia Expansion board. One common factor that lies with most of the signal and image processing algorithms is that it is highly computationally memory intensive. Specifically for image processing, the memory is the key requirement. Embedded hardware always faces memory limitations.

Although 16 bit microchip PIC24 and digital signal controller dsPIC [11] is fully capable of implementing most signal processing tasks. But PIC32 is having much better interrupts handling (32 vectors instead of 2, shadow registers) and much more superior ALU (32 register, memory and data cache, pipeline execution) than PIC24 and dsPIC. It means that it can execute twice the number of instructions per second that a 16 bit PIC24, dsPIC30 or dsPIC33 would, given the same clock [12]. MIPS core based PIC32, on the other hand, offers more RAM, more peripherals and more raw processing power.

To incorporate a camera and an LCD for capturing image and display it, the microcontroller is interfaced with a special coprocessor Solomon Systech Graphics Controller SSD1926 [4]. By handling all graphical transactions memory limitation also avoided.

A. *Hardware Considerations*

In hardware (Microchip PIC32) the pixels of QVGA image (320x240) are stored in continuous memory locations and are not similar to the matrix structure of Matlab. In Microchip PIC32, each memory location is identified by a unique address [12].

The hardware Development Environment used in this research is: Microchip MPLAB version 8.10 or later, C32 compiler version 1.05 or later and Microchip Graphics Library version 2.00.

To develop the application after installing MPLAB, download the latest version of the Microchip Graphics Library. Install the library with the default installation directory will place the library files and demos under the ”Microchip Solutions” directory. From Microchip Solutions v2011-12-05\ Microchip\ Graphics\bin location, the Graphics Resource Converter (grc.jar) is executed for converting the input images, bitmaps (BMP extension) and JPEG (JPG or JPEG extension) into formats to be used with Microchip Graphics Library . This conversion creates a new C file and a header file for that image with same resolution and color depth as input. The C file contains color palette and pixel information of the image. These details are used in image processing. To configure the pic32 hardware in software, edit the header file HardwareProfile.h and select the relevant pic32 hardware by uncommenting the relevant include statement.

Microchip Graphics Library has been chosen because it is free as long as the library will be embedded in Microchip products. The library was created to work with a number of Microchip graphics development boards (i.e. PIC24, dsPIC, and PIC32 devices). The Microchip Graphics Library is highly modular and is optimized for Microchip’s 16- and 32-bit microcontrollers. It is compatible with almost all well-known image coprocessors and can also be used in any image co-processor with slight modifications. The Microchip graphics library supports [13] Graphics, Fonts, User interface for Touch sensing, Image and animation.

*B. Image Processor*

The main image processor in the research is Microchip’s PIC32. SSD1926 co-processor [13] is sharing load from the main processor [12]. To drive SSD1926, PIC32 generates the required control signals (CS#, DC, RD#, WR#, and D[23:0]) [7]. SSD1926 is an image processor designed for image capture and process features with low power consumption. This co-processor takes the load off the main processor so that it can fully utilize its resources on image processing algorithm implementation. It also support 8080 indirect addressing mode which can minimize the pin count of control signals. Internal PLLs is built such that only single clock is required for SSD1926 to generate clocks for blocks with various clock speed requirement. The SSD1926 is available in 128 pin LQFP package. It has built-in Hardware decoder to decode JPEG image with variable size up to 1280 x 1024 [13] .

For viewing JPEG image on LCD panel, the JPEG decoder can decimate and crop the image such that the length is in multiple of 8. Block transfer from/to external host and Embedded 256K bytes SRAM takes place.

Here CPLD (complex programmable logic device) is provided on multimedia expansion board to configure the graphics controller bus interface, SPI channel and Chip Selects used for SPI Flash. SSD1926 may be configured to use an 8-bit or 16-bit bus interface.

The Multimedia Expansion Board provides two different on-board storage mediums, an 128 byte EEPROM and 2MB serial NOR Flash [13].The PIC32 microcontroller uses an I2C bus interface to communicate to the EEPROM. The PIC32 microcontroller uses a SPI bus interface to communicate to the NOR Flash. The CPLD needs to be properly configured for the PIC32 microcontroller to be able to access the NOR Flash.

*C. Implementation in MPlab*

Tasks assigned to main processor PIC32

1. Configure co-processor for the operations / tasks by initializing multimedia expansion board. In this CPLD is initialized to configure graphics controller bus interface, SPI channel and Chip Selects used for SPI Flash. Parallel mater port also initialized. Then the interrupts are disabled shortly, the DMA is suspended and the system is unlocked while performing the operation. Upon return the previous status of the interrupts and the DMA are restored. The system is re-locked. Reset the display device controller, move the cursor position to (0,0) and initialize the display to all black [14].

2. Taking data from image buffer of co-processor by using GetPixel(i,j) function (i.e.this function returns the color value at i,j position ) and performing image processing on that, then storing the processed image back to image buffer to show it on LCD by using SetColor(x); PutPixel(i,j).( the color of value x is written on LCD display at i,j position ) or By using JPEGPutImage(0, 0, &imagename) we are able to write the image information from internal flash memory to LCD display [13]. Figures 4(a)and 4(b) depict the results of his image processing.

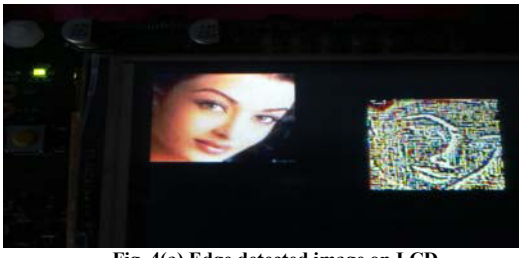

**Fig. 4(a) Edge detected image on LCD**

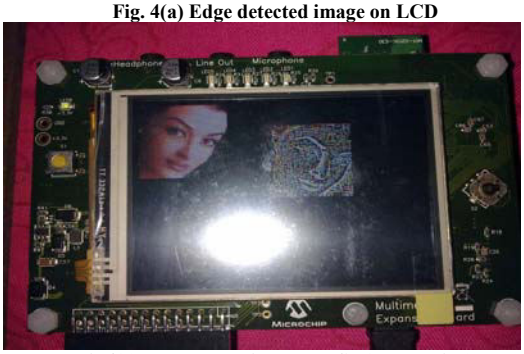

**Fig.4(b) Edge detected image on LCD (another view)**

## V. STIMULATOR IN INTRAOCULAR PART

In Retinal prosthesis, the Extraocular part uses wireless data link for transferring processed image data to stimulate ganglion cells via an electrodes array in Intraocular implant. For 32 by 32 pixel array, each pixel in this array corresponds to one electrode and is independently programmable. To drive these electrodes 1024-channel stimulator is composed. We have binary images and just the electrodes in the places of pixels related to edges of image should be stimulated, and all of these pixels have the same value, so we don't need different stimulation parameters for them. So we set the stimulator with these parameters and don't need to send them in data packets. We just transfer the information about addresses and values of image pixels. Using PIC32 micro controller every pixel can be independently programmed for frequency, pulse width, pulse amplitude, leading pulse polarity, etc. A delay timer in each pixel generates a programmable delay of the stimulation pulses. In such a waveform the first pulse causes activation, followed by a second one with opposite polarity to balance the charge delivered by the first. The Stimulation pulse should be a biphasic cathodic-first charge-balanced square wave pulse. Perceived light brightness is determined by the amount of charge delivered to the ganglion cells, and may be represented by stimulus current amplitude [7] or possibly by rate of stimulation [16] .In this regard any high performance circuit is proposed for extra ocular unit but for stimulating implant high speed 80MHz PIC32 microcontroller is advantageous.

## VI. CONCLUSION

Epi-retinal implant architecture and high-Performance 80 MHz 32-bit Microchip PIC32 microcontroller based image processing and are presented. To be able to meet the real-time requirements of a retinal prosthesis system some strategy for developing inexpensive image processing on high speed embedded hardware is presented. It enables easy to develop and modify different image processing strategies and evaluate their operational performance in software & hardware. The implant requirements have been outlined and the hardware programming is explained in detail. A major emphasis has been laid on the design for intraocular part —this makes the stimulator ready for production and implantation.

## VII.REFERENCES


[1] House W F. Cochlear implants. Ann Otol Rhinol Laryngol, 1976, 85(Suppl. 27, Pt. 2): 1—93

[2] Zrenner E. Will retinal implants restore vision? Science, 2002, 295(5557): 1022—25

[3] J. Hamon, V. Fristot and R. Rolland,"FPGA implementation of a real time multi-resolution edge detection video filter" *8th European Workshop on Microelectronics Education*, 2010.

[4] H. S. Neoh, A. Hazanchu. "Adaptive Edge Detection for Real-Time Video Processing using FPGAs" Available http://www.uweb.ucsb.edu/~shahnam/AEDfRTVPUF.pdf

[5] N. Tran, E. Skafidas, J. Yang, S. Bai, M. Fu, D. Ng, M. Halpern, and I. Mareels," A Prototype 64-Electrode Stimulator in 65 nm CMOS Process towards a High density Epi-retinal Prosthesi" in IEEE EMBS, pp. 6729-6732, 2011

[6] 2008;1: JinHai NIU, YiFei LIU, QiuShi REN, Yang ZHOU, Ye ZHOU & Shuai NIU :"Vision implants: An electrical device will bring light to the blind". Science in China Series

[7] M. Humayun , E. de Juan Jr., J. Weiland, G. Dagnelie , S. Katona , R.Greenberg, and S. Suzuki , "Pattern electrical

stimulation of the human retina," *Vision Res.*, vol. 39, pp. 2569–2576, 1999.

[8] Azzam Sleit, Abdel latif Abu Dalhoum, Ibraheem Al-Dhamari, Afaf Tareef "An Edge Detection Algorithm for Online Image Analysis " King Abdulla II School for Information Technology,University of Jordan, Amman, Jordan

[9] Yuexian ZQU*, Guangyi SHI, Yufeng JIN, and Yali ZHENG, "Extraocular Image Processing for Retinal Prosthesis Based on DSP," Proceedings of 2009 4th IEEE International Conference of the IEEE on Nano/Micro engineered and Molecular systems.

[10] W. Pratt, Digital Image Processing, 3rd Edition, Wiley 2001.

[11] dsPIC® Digital Signal Controllers, http://ww1.microchip.com/downloads/en/DeviceDoc/DS-70095K.pdf

[12] PIC32 microcontrollers datasheet: Available at www.microchip.com/downloads/en/DeviceDoc/61143E.pdf

[13] Multimedia Expansion Board User's Manual" (DS61160) available at ]www.microchip.com/downloads/en/AppNotes/ DS61160A.pdf

[14]www.microchip.com/downloads/en/AppNotes/01246b.pdf

[15] D. K. Warland, P. Reinagel, and M. Meister,"Decoding Visual Information From a Population of Retinal Ganglion Cells," *J Neurophysiol,* vol. 78, pp. 2336- 2350, November 1, 1997 1997

# THE SAFETY ASSESSMENT OF SAFETY CRITICAL PPLICATIONS

[1]ESTHER SUNANDA BANDARU & [2]P. SEETHARAMAIAH,

[1,2]Dept. of CS & SE, AU College of Engineering, Visakhapatnam, India

**Abstract**-Software safety involves ensuring that software will execute within a system context without resulting in unacceptable risk. Building safety-critical software requires special procedures to be used in all phases of the software development process. The Safety-Critical Systems have become more important as computers are increasingly used to monitor and control critical devices. The safety-critical systems should have safety issues included in the software development. Several Design Methods and Metrics have been developed for the safety and security of the Safety-Critical Systems. Modern electronic systems increasingly make use of embedded computer systems to add functionality, increase flexibility, controllability and performance. However, the increased use of embedded software to control systems brings with it certain risks. The increased flexibility and complexity can lead to new and different failure modes which cannot be addressed with traditional fault tolerance techniques.

**Keywords**- Software Safety, Safety Critical Systems, Safer Software Development, Software Safety metrics, Microcontroller based F our Finger Robotic Hand Controller.

## I. INTRODUCTION

[8]Safety-critical computing deals with the computations that may affect people's lives, health or properties, such as computing in nuclear power plants, aviation, and medical application domains. The progress of the computerization process in these safety-critical areas is relatively slow, compared with that of non-safety related applications. Moreover, this situation has not been improved much even after researchers have gone through many failed experiences, and devoted great efforts to these areas. The problem is that

Safety-related computerized systems have difficulty in providing convincing safety evidence to pass the safety review for an operational license. We believe this is due to the fact that the software developed by current methodology lacks some ingredients required for forming safety evidence.

[3]General guidance for developing safety-critical processor-based systems consists of the following:

- Avoid complexity in the design. Simplicity allows a more complete understanding of the system operation minimizing the chances for error, and makes the designs easier to test. Drastically reducing the number of functions performed by the safety-critical system (and enforcing this reduction) also keeps function creep under control and allows future changes to be made and verified. A good criteria to keep in mind is "Just because you can doesn't mean you should".
- Use deterministic design techniques. It is necessary for the processor-based system to operate the same way every time a critical function is performed. This is necessary to allow comprehensive testing of the system. If different timing or alternative paths through the logic due to multi-tasking, dynamic memory allocation, or other characteristics exist, all possible execution paths cannot be adequately tested.
- Separate safety-critical from non-safety-critical portions of the system. This allows simplicity to be maintained in the safety-critical portion of the system so that it can be adequately tested and maintained.

This paper is aimed at considering the analysis of a safety-critical systems and an approach to avoid the accidents that are frequently occurring. In the second section of the paper how safety analysis in safety-critical systems is done with methods is considered. In the third section of the paper, a case study of robot hand is taken into consideration for the safety analysis. In the final section of the paper it explains how the non-inclusion of safe-code causes problems and how the inclusion of safe-code helps avoid the accidents.

## II. SAFETY ANALYSIS IN SAFETY-CRITICAL SYSTEMS

[9]Failure analysis is the process of collecting and analyzing data to determine the cause of a failure and how to prevent it from recurring. It is an important discipline in many branches of manufacturing industry, such as the electronics industry, where it is a vital tool used in the development of new products and for the improvement of existing products. It is especially important in manufacturing and field use of safety-critical and mission-critical equipment. Failure analysis may be applied to both products and processes. Failure analysis may be conducted on the design stage and on field use stage of the product life cycle. Failure analysis of safety-critical and mission-critical equipment on the field use stage requires failure data collection and statistical analysis.

Over the years the occurrences of accidents have not stopped and for example let us consider the accidents that occurred in the field of robots.

Some of the accidents that occurred due to robots [2]:

- The first robot-induced fatal accident occurred in Japan in 1978.
- For the period 1978-1984, there were at least five fatal accidents involving robots: four in Japan and one in the United States.
- The first fatal robot-related accident occurred in 1984 in the United States.
- For the period 1978-1987, there were a total of ten robot-related fatal accidents in Japan
- In 1987, a study of 32 robot-related accidents in Japan, the United States, West Germany, and Sweden revealed that line workers were at the greatest risk of the injury followed by maintenance personnel
- A study reported that around 12-17% of the accidents in industries using advanced manufacturing technology were related to automated production equipment
- A material handling robot was operating in its automatic mode and a worker violated safety devices to enter robot work cell. The worker got trapped between the robot and a post anchored to the floor. Consequently, the worker was injured and died a few days later
- A maintenance person climbed over a safety fence without turning off robot power and performed tasks in robot work zone while it was temporarily stopped. When the robot recommenced operation, it pushed the person into a grinding machine and the person died, subsequently

Some of the methods used to analyze the safety, reliability and ability of the safety-critical systems are:

*A. Failure Mode and Effect Analysis (FMEA)*

[1]FEMA is an important tool to evaluate system design from the reliability and safety angle. Originally, the method was developed in the early 1950s to evaluate the design of flight control systems [14]. The FMEA approach demands listing potential failure modes of each and every component on paper and their effects on the listed subsystems, system, and the surroundings.

*B. Hazard and Operability Analysis (HAZOP)*

[1]HAZOP helps to identify problems prior to availability of full data concerning a product/system. The approach calls for the formation of a team made up of knowledgeable members with varying backgrounds, and in turn, the team brainstorms about potential hazards. An experienced individual chairs the team and serves as a facilitator during brainstorming sessions. One major drawback of the HAZOP approach is that it does not take into consideration human error in the final equation.

*C. Technic of Operations Review (TOR)*

[1]Just like in the case of HAZOP, TOR seeks to identify systemic causes rather than assigning blames. TOR allows management and workers to work jointly to perform analysis of workplace accidents, incidents, and failures [13]. TOR, basically, is a hands-on analytical methodology developed to determine the root system/product causes of an operation malfunction. The technique makes use of a worksheet containing simple terms requiring yes/no decisions. The basis for activating TOR is an incident occurring at a certain time and place involving certain individuals. The strength of the technique comes from involving line personnel in the analysis, and its weakness stems from the fact that it is designed as an after-the-fact process.

*D. Nuclear Safety Cross-Check Analysis (NSCCA)*

[1]The method consists of an adversarial approach with the objective of showing a high degree of confidence that the software will not cause an undesirable event. The NSCCA is composed of two main components: technical and procedural. The purpose of the technical component is to ensure that system safety-related requirements are fully satisfied. Similarly, the purpose of the procedural component is to provide effective protection and security for critical software elements.

*E. Probability Tree Analysis*

[1]This is one of the main techniques for human reliability analysis. Success or failure of each critical human action or associated event is assigned a conditional probability. The outcome of each event is represented by the branching limbs of the probability tree. The total probability of success for a particular operation is obtained by summing up the associated probabilities with the end point of the success path through the probability tree diagram. This technique, with some refinement, can include factors such as time stress, emotional stress, interaction stress, interaction effects, and equipment failures. [13]

*F. Fault Tree Analysis (FTA)*

[1]FTA may be described as an analytical methodology that uses graphic symbols to visually display the analysis process. Fault tree analysis begins by identifying an undesirable event, known as the top event, associated with a system. The events that could cause the occurrence of the top event are generated and connected by logic operators such as AND and OR. Thus, the fault tree itself is the logic structure relating the top event to the basic or the primary events.

## III. CASE STUDY: SAFETY ANALYSIS OF ROBOT HAND

Safety-critical systems, by definition those systems whose failure can cause [8]catastrophic results for people, the environment, and the economy, are becoming increasingly complex both in their functionality and their interactions with the environment. Unfortunately, safety assessments are still largely done manually, a time-consuming and

error-prone process. Here the safety-analysis of robot hand is examined and an approach to avoid the accidents is specified.

[12]The FFRH system as shown in fig1 has three main parts namely Robot Hand, Controller and Sensor Feedback unit. The Robot Hand consists of three fingers and an opposing thumb and is connected internally to the geared DC motors, for their movement. The FFRH controller is based on embedded processor, relay-based geared dc-motor drivers, LCD display for messages and debugging, an in-system programming (ISP) port for downloading programs from a PC to embedded processor's flash memory, data from IR sensors and limit sensors of hand via another embedded processor based encoder to control the limits of movement of hand, 5x5 key matrix interface using parallel port for hand's control commands.

All the joints of the hand including the base are controlled by geared DC motors using strong gut type wires wound from the shaft to the finger joint pulleys and idlers and relay drivers interfaced to parallel port bits of embedded processor. Base motor is used to move hand in 360 degrees in either direction programmed by key commands (base-cw, base-ccw). Four fingers use four geared DC motors/drivers with relays, for motion control of finger joints with pitch of 45 degrees maximum. Wrist geared DC motor drives the wrist with roll and pitch of maximum 180 degrees. The input from finger limit sensors placed on palm is used to control the free rotation of the finger. IR sensor placed at the center of the Palm is used to sense the presence of an object. All operations of embedded computer-based robot hand are achieved through control program.

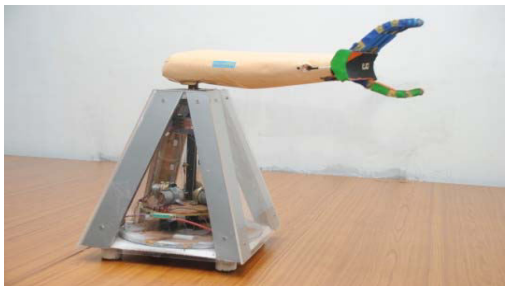

Figure1: AU HAND

*A. Insertion of Safety Code*

[12]In the design phase of the Four Fingered AU Hand some safety issues need to be included so that correct results may be got and the occurrence of accidents may be avoided.

The safety issues need to be included in the design phase of the Four fingered Robot which is not included in the actual design. The inclusion of the Safety Issues in the design phase should be present as without it accidents occur in the safety critical system of the Four Fingered Robot Hand.

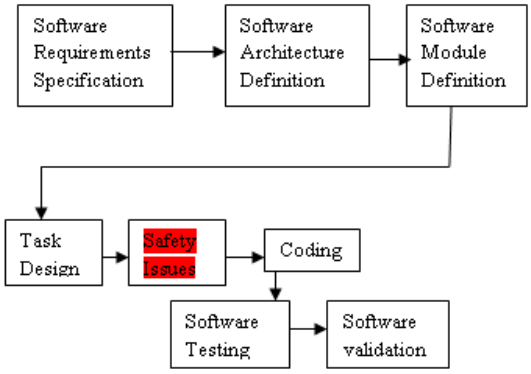


Figure 2: Insertion of Safety Issues in the Design Phase

*B. Software Verification*

[12]Here the software of the Four Fingered Robot is verified. The sensors used in the development of the Four Fingered Robot are taken into account. The sensors in the Four Fingered Robot are four individual sensors for each figure to move to and fro, three sensors in the wrist to move it and a sensor in the base which is used for the purpose of keeping the base in the home position. When the figure of the robot moves up the sensor present at the back of the finger detects its position i.e. finger is not holding any objects and is present in its actual position. At the wrist there are three sensors which specify that the wrist is in the correct position i.e. not holding any object. There is a sensor at the base which specifies that the Four Fingered Hand is in its home position.

There may be a case when the sensors in the above cases may not work properly, then the hand will not properly work. The objects that are to be hold by the hand many falls off or other damages may occur. Therefore, the software of the Four Fingered Hand must include a check case which checks the code used for the sensors to work properly. The actual flow chart of the Four Fingered robot Hand is shown below which do not include the safety issues of the sensors Figure 3.

The operations of the wrist, fingers and the base need to be monitered with the safety code and if the sensors present there work correctly then the opretions in the software can be done or else the works comes to halt. Some modifications are done for the flowchart of the Four Fingered Hand which is shown in the fig 4.

## IV. SOFTWARE MODIFIED WITH INCLUSION OF SAFE CODE

*A. Without Safe Code*

[12]The software code before the inclusion of safe code of the Four Fingered Robot Hand for a single finger to operate in the OPEN phase is:

```
nxtkey3: cjne a, #3eh, nxtkey4
         mov dptr, #0fe00h
         movx a,@dptr
         jnb acc.0,fok
```

```
acall f1open
mov a,#80h
acall command
mov dptr,#fng1
acall showmsg
mov a,#0c0h
acall command
mov dptr,#open

acall showmsg

acall stop

ajmp start

fok: mov a,#80h

acall command

mov dptr,#fng1

 acall showmsg

mov a,#0c0h

acall command

mov dptr,#crosslimit

acall showmsg

ajmp start
```

Here in the above code, if the sensor behind the finger is not in the condition of working then it may not proceed with the next operation of CLOSE and the code moves to an undefined loop. So, there must be a safe code which must be included so that the non-working condition of the OPEN state of the Four Fingered Robot when the sensor is in the non-working condition can be done without any interruption.

*B. With the Inclusion of Safe Code*

A loop must be included into the code so that the checking of the sensor's working condition may be checked. Here a variable "counter" is taken and is incremented and checked for condition. If the sensor is not in the contact of the finger then the operation will not be further done but halts as shown in the fig. 4. The modified code will be:

```
nxtkey3: cjne a, #3eh, nxtkey4

                mov dptr, #0fe00h

                movx a,@dptr

                jnb acc.0,fok

                cjne counter, #0fh, J1

acall stop

ajump start

J1:          acall f1open

                mov a,#80h

acall command
mov dptr,#fng1
acall showmsg
acall command
mov dptr,#open
```

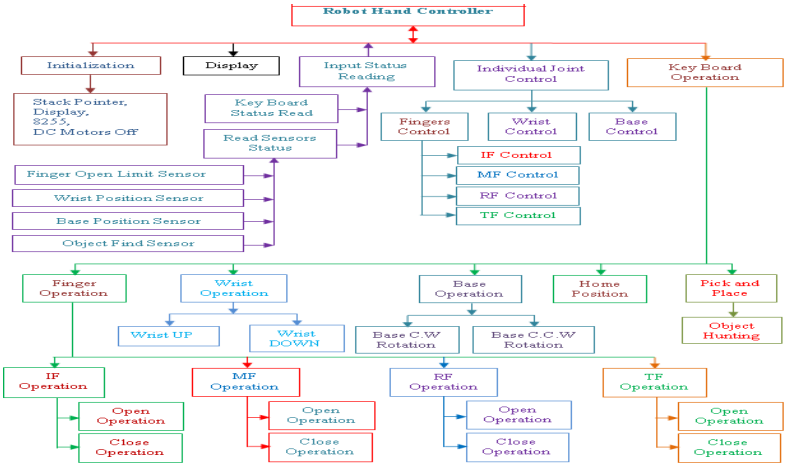

*Figure 3: Robot Hand Flow Chart Without Safety Issues*

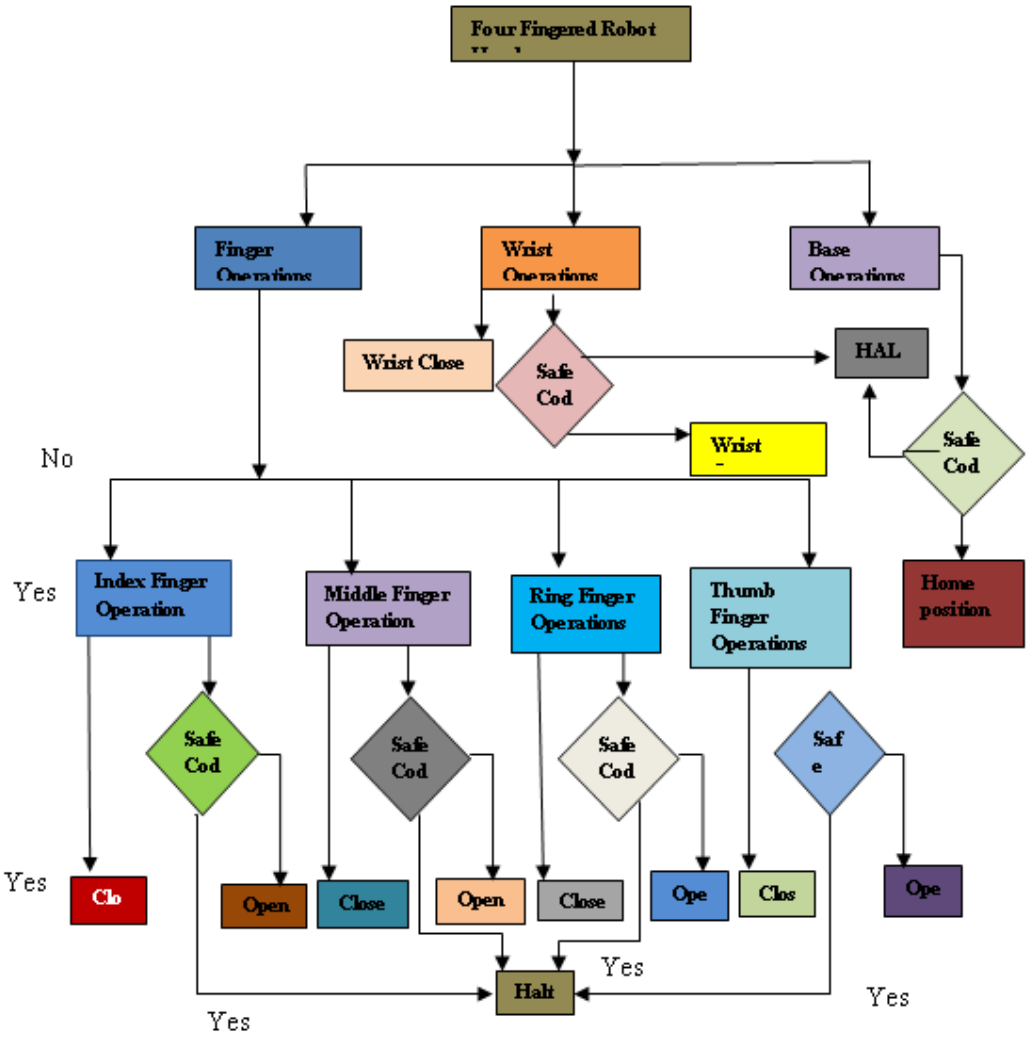


Figure 4: Inclusion of Safe Code before the operations

```
acall showmsg
                                    inc counter
                    acall stop
                    ajmp start
                    fok: mov a,#80h
                    acall command
                    mov dptr,#fng1
                     acall showmsg
                    mov a,#0c0h
                    acall command
                    mov dptr, #crosslimit
                    acall showmsg
                    ajmp start
```

These lines of code need to be included so that safety may be provided to the Robot Hand while the sensors are not in the working condition. The above code is for one finger only but there are 8 sensors in the Robot Hand which need to be checked. So the above code needs to be applied for the checking operation of every sensor i.e. for the 4 sensors of fingers, the 3 sensors of the wrist and the one at the base.

## V. CONCLUSION

Software safety involves ensuring that software will execute within a system context without resulting in unacceptable risk. Building safety-critical software requires special procedures to be used in all phases of the software development process. The Safety-Critical Systems have become more important as

computers are increasingly used to monitor and control critical devices. So, the code of the safety-critical system must include the safety issues and make the system to be executed in a proper manner so that accidents may be avoided.

**REFERENCES:**


1. Metrics and Models in software Quality Engineering by Stephen H. Kan Second Edition, Pearson Education India, 01-Sep-2003.
2. Zeldwan, M. I., What Every Engineer should know About Robots, Marcel De New York, 1984. An Interpretation of the Technical Guidance on Safety Standards in the Industrial Robots, Japanese Industrial Safety and Health Association, Tokyo, 1985.
3. Developing Safety-Critical Systems by Bill Petit *This article was printed in the 2006 Railway Age C&S Buyers Guide.*
4. "SAFETY ISSUES OF COMPUTER FAILURE", Dr. Sami M. Halawani, 30th March 2005.
5. Jones, James V., *Integrated Logistics Support Handbook*, McGraw–Hill Professional, 3rd edition (June 8, 2006).
6. SYSTEMSPECIFICATION",http://www.cs.umd.edu/~mvz/cmsc435-s09/pdf/slides6.pdf.
7. http://en.wikipedia.org/wiki/Life-critical_system
8. John C. Knight, "Safety Critical Systems: Challenges and Directions*" Proceedings of the 24th International Conference on Software Engineering (ICSE),* Orlando, Florida, 2002.
9. Debra S. Herman, "Software Safety and Reliability Basics:", (ch.2), *Software Safety and Reliability:Techniques, Approaches, and Standards of Key Industrial Sectors* Wiley-IEEE Computer Society Press.
10. N. Leveson, *Safeware: System Safety and Computers*, Addison-Wesley Publishing Company, Reading,Massachusetts, 1995.
11. Raghu Singh, "A Systematic Approach to Software Safety". *Proceedings of Sixth Asia Pacific Software Engineering Conference* (APSEC), Takamatsu, Japan ,1999
12. AN Embedded Computer Controlled Four Fingered Robot Hand Based On Anthropomorphic Model By Mandapati Venkateswara Rao